PHOTOSENSITIZERS FOR PHOTODYNAMIC ACTION AND SYNTHESIS OF MODULES FOR A MOLECULAR DEMULTIPLEXER

A THESIS

SUBMITTED TO DEPARTMENT OF CHEMISTRY

AND THE GRADUATE SCHOOL OF ENGINEERING AND SCIENCE

OF BILKENT UNIVERSITY

IN PARTIAL FULFILLMENT OF THE REQUIREMENTS

FOR THE DEGREE OF

MASTER OF SCIENCE

By

Tuğçe Durgut

August, 2014

I certify that I have read this thesis and that in my opinion it is fully adequate, in scope and in quality, as a thesis of the degree of Master of Science.

…….

Prof. Dr. Engin U. Akkaya (Advisor)

I certify that I have read this thesis and that in my opinion it is fully adequate, in scope and in quality, as a thesis of the degree of Doctor of Philosophy.

…….

Assoc. Prof. Dr. Dönüş Tuncel

I certify that I have read this thesis and that in my opinion it is fully adequate, in scope and in quality, as a thesis of the degree of Doctor of Philosophy.

…….

Assist. Prof. Dr. Murat Işık

Approved for the Graduate School of Engineering and Science:

…….

Prof. Dr. Levent Onural

Director of the Graduate School

ABSTRACT

PHOTOSENSITIZERS FOR PHOTODYNAMIC ACTION AND SYNTHESIS OF MODULES FOR A MOLECULAR DEMULTIPLEXER

Tuğçe Durgut

M.S. in Department of Chemistry

Supervisor: Prof. Dr. Engin Umut Akkaya

August, 2014

Photodynamic therapy (PDT) is a new therapeutic methodology that uses light as a distinguishing tool for the treatment of diseased cells. In recent years PDT has become one of the most preferred therapies because it is innocent for the healthy cells and tissues while diagnosing and curing the malignant cells and tissues. Bodipy is one of the most favorite fluorophore in this field due to its excellent chemical and physical properties. Logic gates are widely used in modern technology as the fundamentals of logical operations for the development of science. The progressive advances leads to the emergence and growth of molecular logic gates. Molecular logic gates can be used for the diagnosis and therapies of disease which are originated from the heredity. In addition, they occupy an important place in the theoretical and practical use of photodynamic therapy.

In the first part of my thesis, we designed and synthesized a calix[4]arene-Bodipy conjugate molecule as a carrier for the photodynamic therapy agents. It is an amphiphilic delivery molecule that is utilized for the curing of tumor tissues. In the second part, we synthesized modules for molecular logic gate function, DEMUX (demultiplexer), serving as a theranostic device which selects either singlet oxygen channel or energy transfer between the modules depending on the inputs. The superiority of the project is that it serves a realistic pathway for the PDT.

Keywords: Calixarenes, Logic gates, photodynamic therapy, demultiplexer

ÖZET

FOTODİNAMİK AKSİYON İÇİN FOTODUYARLAŞTIRICILAR VE MOLEKÜLER DEMULTİPLEKSER MODÜLLERİNİN SENTEZİ

Tuğçe Durgut

Kimya Bölümü, Yüksek Lisans

Tez Yöneticisi: Prof. Dr. Engin Umut Akkaya

Ağustos, 2014

Fotodinamik terapi (PDT), ışığı hasta hücrelerin tedavisinde ayırt edici etken olarak kullanan bir tanı ve tedavi yöntemidir. Kötücül hücre ve dokuların tanı ve tedavi işlemleri süresince sağlıklı hücre ve dokulara zararsız olması sebebiyle son yıllarda en çok tercih edilen terapi yöntemi fotodinamik terapi olmuştur. Bodipy, üstün kimyasal ve fiziksel öellikleri sayesinde bu alandaki en gözde floroforlardan biridir. Mantık işlemlerinin temelinde yatan mantık kapıları, bilimin ilerleyebilmesi için modern teknolojide sıkça kullanılır. Bilimde ilerleyen gelişmeler moleküler mantık kapılarının ortaya çıkıp gelişmesine öncülük etmiştir. Moleküler mantık kapıları kalıtsal olan hastalıkların tanı ve tedavisinde kullanılabilir. Ayrıca, fotodinamik terapinin teoritiksel ve pratik kullanmında önemli bir etki alanına sahiplerdir.

Tezimde, ilk bölümde fotodinamik terapi ajanslarını taşıyacak olan kaliks[4]aren-bodipy türevini ve sentezledik. Bu molekül, ampifilik özellik göstermekte ve tümörlü dokular için çalışmaktadır. Ikinci bölümde ise, bir moleküler mantık kapısı olan, teranostik cihaz vazifesi görerek glutatiyon ve asit girdileri ile singlet oksijen üretimini ya da ışımayı tercih eden DEMUX modüllerinin sentezi ile çalıştık. Bu projenin üstünlüğü ise, PDT için gerçekçi bir yol sağlamasıdır.

Anahtar sözcükler: Kaliksarenler, Mantık kapıları, fotodinamik terapi, Demultiplekser

Dedicated to my family…

Acknowledgement

I would like to express my sincere thanks to my research supervisor Prof. Dr. Engin U. Akkaya for his invaluable guidance, support, and patience during the course of this research. Excellent five years of my life has passed under his guidance in his group where I have met the most beautiful friends in my life. I will never forget the experiences that I have benefited from him throughout my life.

I owe a special thank to Sündüs Çakmak and Yusuf Çakmak for their everlasting help, support, invaluable guidance and friendship during these years. I would like to thank Tuğrul Nalbantoğlu for his kind collaboration during the project in which we worked together.

I am sincerely grateful to my close friends Ruslan Guliyev, Yiğit Altay, Hale Atılgan, Gözde Barım, Elif Başak, Melek Baydar, Jose Bila, Onur Büyükçakır, Muhammed Büyüktemiz, Merve Camcı, Ceren Çamur, Feyza Çangal, Gülizar Çangal, Şeyma Ekiz, Gamze Erdem, Tuğçe Karataş, Bilal Kılıç, Menekşe Koca, Tuğba Özdemir Kütük, Darika Okeeva, İlayda Ölmez, Seda Selçuk, Özlem Ünal and Tuba Yaşar for their invaluable friendship, necessary help, understanding and the wonderful memories we had together. Ankara can be a great city to live in with these people.

I would like to thank all past and present members of EUA Lab. for their friendship; Murat Işık, Serdar Atılgan, Ahmet Atılgan, Hande Boyacı, Özgür Altan Bozdemir, Seda Demirel, Murat Işık, Cansu Kaya, Safacan Kölemen, Ziya Köstereli, Şeyma Öztürk, Sencer Selçuk, Fazlı Sözmen, Esra Tanrıverdi, Taha Bilal Uyar, Nisa Yeşilgül, Deniz Yıldız, and the rest of the SCL group. It was a great experience for me to work with them.

I want to express my gratitude to Dielse Inroga for his love, invaluable friendship, support, patient and for always being there for me.

I am grateful that I have such a beautiful family that they support me in all situations. I want to express my gratitude to my parents, my sister Burçin, my brother Serdar,

my cousin İrem for their love and trust. I also want to thank my little nephew Toprak whose smile encouraged me to finish this thesis. I owe them a lot.

I would like to thank to TÜBİTAK (The Scientific and Technological Research Council of Turkey) for financial support.

LIST OF ABBREVIATIONS

AcOH	:	Acetic Acid
Bodipy	:	Boradiazaindacene
$CHCl_3$	:	Chloroform
ET	:	Energy Transfer
FRET	:	Förster Resonance Energy Transfer
HOMO	:	Highest Occupied Molecular Orbital
ICT	:	Internal Charge Transfer
LUMO	:	Lowest Unoccupied Molecular Orbital
MS	:	Mass Spectroscopy
NMR	:	Nuclear Magnetic Resonance
PDT	:	Photodynamic Therapy
PET	:	Photoinduced Electron Transfer
TFA	:	Trifluoroacetic Acid
TLC	:	Thin Layer Chromotography
DEMUX	:	Demuktiplexer

CONTENTS

LIST OF FIGURES

LIST OF TABLES

CHAPTER 1

1 INTRODUCTION

As the space need is getting bigger in the world everything in life has to be smaller and smaller. Molecular logic gates are the protagonists of this necessity. These small smart molecules can do everything one can imagine; from simple theoretical Boolean algebra to photodynamic therapy. This thesis includes the project that is about the molecular logic gates and their applications in photodynamic therapy.

Logic gates are designed to produce integrated circuits. They are small devices that carry out logical operations via Boolean function systematic. They can be applied to the electronics, molecules and so biological research and applications. When a molecule serves as a logic gate it can called as molecular logic gate.

The working principle of the molecular logic gates is as simple as the algebraic logic gates; there is one or more inputs which can be here physical or chemical and they give a response to that inputs as an output that can be measurable by analytical techniques such as intensity of emission. The combination of logic gates and their chemical applications was first represented by de Silva *et al.*[1] After that time the importance of molecules that can perform as logic gates has been covered in the molecular information processing era.

Cancer is accepted as one of the most vital disease in the last century. It is described as the abnormal growth of the malignant cells because of the damaged DNA. As its name implies, it sticks like a crab and it is hard to get rid of it. Although the certain reasons of cancer are not known well, there are some suspicious causes such as environmental effects, heredity, diet, smoking, sun exposure, radiation and hormones. Today, the medical treatment area of cancer is extended. The most common curing methods are medication, surgery, chemotherapy, immunotherapy, stem cell transplant and photodynamic therapy. Most of these techniques includes painful application to the diseased person who is quite demoralized. Also, the age, when surgery and radiation therapy were the only therapy, has ended as the knowledge of fundamental reasons of cancer lay on the molecular characteristics has

been covered.[2] In addition, most of them are not targeted treatments so they may harm the healthy cells, as well. The important issue here is that the therapeutic agents should be selective to the diseased cells.

Photodynamic therapy (PDT) is a developing treatment for carcinoma and other malignant cell diseases.[3] As it is known, light was used for treatment of some diseases in ancient times. PDT also uses light as a cornerstone for the course of treatment. The working principle of the PDT depends on the generation of singlet oxygen which is toxic to the living cells via excitation of a photosensitizer (PS) at an appropriate wavelength. Controlling its action in the body assures that it can find the diseased cells and cure them without damaging any other healthy cells.[4] This control can be done by using molecular logic gate methodology.

In the first project of this thesis, we designed a photosensitizer that includes a calix[4]arene scaffold as a carrier. This heavy atom bounded calix[4]arene-bodipy complex molecule might lead further studies in which it can also target a malignant tissue due its superior design and novel synthesis.

In the second project, modules for the molecular demultiplexer logic gate are synthesized. This theranostic system is designed as that it might selects between the emission at near-IR region and singlet oxygen creation for PDT by the pH control and glutathione switch. The advantage of this PDT agent is that, it is designed to work in aqueous medium that is necessary for in vivo applications for further therapeutic research.

CHAPTER 2

2 BACKGROUND INFORMATION

2.1 Photoluminescence Phenomenon

Photoluminescence phenomenon is about the emission of light in multifarious forms due to the absorption of photons that have appropriate energy. Atoms and molecules are in their ground state at room temperature according to the Boltzmann distribution.[5] When an atom or a molecule is exposed to electromagnetic irradiation there exists an electronic transition from ground state to the excited state that has higher energy and then the excess energy is emitted in different forms. This optical property is known as photoluminescence.

2.1.1 Physical Basis of Absorption of Light

There is a reason why some substances absorbs lights whereas the others do not; molecules that absorbs light has chromophores and its electron in the highest occupied molecular orbital (HOMO) is excited to the high energy level that is lowest unoccupied molecular orbital (LUMO) when an appropriate electromagnetic radiation is applied. In this process, energy of photon is joined to the energy of the molecule that absorbs light. For this electronically excited state process, the wavelength of the photon should be in the range of visible and ultraviolet radiation region.

There are two strict rules for the electron transition in energy levels of the molecule may take place. First of them, the spin selection rule implies that an electronic transition occurs only when there is no change in the total electron spin. It means that if the transitions require total electron spin to be changed, such as singlet to triplet or triplet to singlet state transitions, then the transition is defined as to be forbidden. However, as the spin orbit coupling phenomenon indicates, there is an interaction between the electrons with each other and also with the nucleus, and these interactions ensure that a singlet state has also some triplet character and vice versa. [6]

Spin orbit coupling can be enhanced via heavy atom substitution in organic molecules. Especially in singlet to triplet state electronic transition rate of the intersystem crossing is increased with the heavy atom substitution.[7] Enhancement of the rate of intersystem crossing due to spin orbit coupling via heavy atom substitution can be done in two ways; one is the internal heavy atom effect in which the heavy atom is incorporated to the molecule under interest, the other is the external heavy atom effect in which the heavy atom is placed in a solvent of the molecule.[8]

The second rule for the electronic transition is known as orbital symmetry selection rule. When the wavefunctions of initial state and final state are closer to each other then one can say that rate of absorption is greatest because the molar absorption coefficient, which can be defined as the measurement of the electronic transition at a given wavelength, will be greatest. As it is seen in Figure 1, there are six types of electronic transitions. Between these transitions π- π^* and n- π^* transitions require the lower energy such that π- π^* transition has ε values between 10^3 and 10^5 l mol cm^{-1} which is in the range of partially allowed transition. This property is due to the orbital symmetry selection rule, it is spin allowed but not symmetry allowed. In general, the transition is mentioned as fully allowed when the molar absorption coefficient value is above the 10^5 l mol $cm^{-1}$and it is spin forbidden but symmetry allowed when the molar absorption coefficient value is above the 10^2 l mol cm^{-1} such as n- π^* transition.

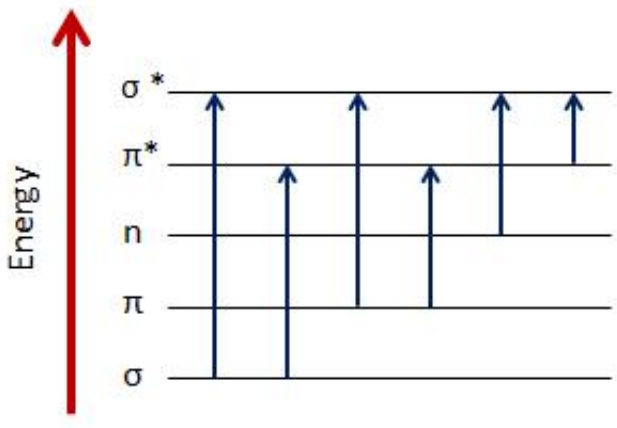

Figure 1. Molecular Orbital Energies and Electronic Transitions in Organic Molecules.

Absorption of light changes due to the variety of the substance that absorbs light. Molar absorption coefficient, being the probability of absorption, has an effect on the relationship between the intensity of light, concentration and the path length. As it is stated in the Beer-Lambert Law, there is a linear relationship between the absorbance, concentration and path length;

$$\mathbf{A=\log(I_{in}/I_{out})=\varepsilon cl}$$

where A is absorbance, I_{in} is the intensity of light that enters, I_{out} is the intensity of light that is released, c is the concentration of the absorbing species and l is length of path.

2.1.2 Physical Basis of Deactivation of Excited State

The molecule that is irradiated with a photon, that has proper energy in the range of UV-Vis wavelength, elevates its electron to the higher energy excited state. However, this excitation process is such a short living process that the physical deactivation takes place immediately to give away that extra energy. There are two main classes of this physical relaxation; intermolecular relaxation and intramolecular relaxation.

Intermolecular relaxation processes includes vibrational relaxation, energy transfer and electron transfer. Due to absorption of light molecules that have extra vibrational energy will undergo a relaxation to the lowest vibrational level of the energy level that is under interest, and this is named as the vibrational relaxation. The time scale for a typical vibrational relaxation is between 10^{-13}-10^{-9} s^{9}. Energy transfer occurs when the excited molecule transfer its energy to an acceptor group and electron transfer occurs when the excited molecule interacts with the ground state acceptor molecule and an ion pair is transferred. Electron transfer and energy transfer concepts are going to be presented in the later subsections.

Intramolecular relaxation processes are classified as radiative transitions that include fluorescence and phosphorescence and non-radiative transitions that include internal conversion and intersystem crossing. There is an emission as the relaxation takes place in the radiative transitions. If there is no emission during the relaxation then it

is called non-radiative transition. Fluorescence, an example of radiative transition, takes place when there is a photon emission between the spin allowed states. Phosphorescence is also a radiative transition between the spin forbidden states. Fluorescence exists from the lowest vibrational level of the excited singlet state, whereas phosphorescence exists from the lowest vibrational level of the excited triplet state.

Internal conversion is a non-radiative relaxation between the excited electronic states that have the same multiplicity. It is known that the energies of higher states are close to each other. To give an example, the lowest vibration level of S_3 state is close to the highest vibrational level of the S_2 state, so it there may exist a rapid energy transfer between them. As the Kasha rule implies, because the relaxation to the excited state with the same multiplicity is a very rapid process, dissipation of the energy with luminescence emission are originated from the S_1 at v=0[10].

Intersystem crossing occurs as a spin-forbidden transition between the vibrational states that have the same total energy with different multiplicity. For example, transition from S_1 at v=0 to T_1 at v=n where n is the highest vibrational level is an intersystem crossing. There is an illustration of these relaxation processes in Figure 2.

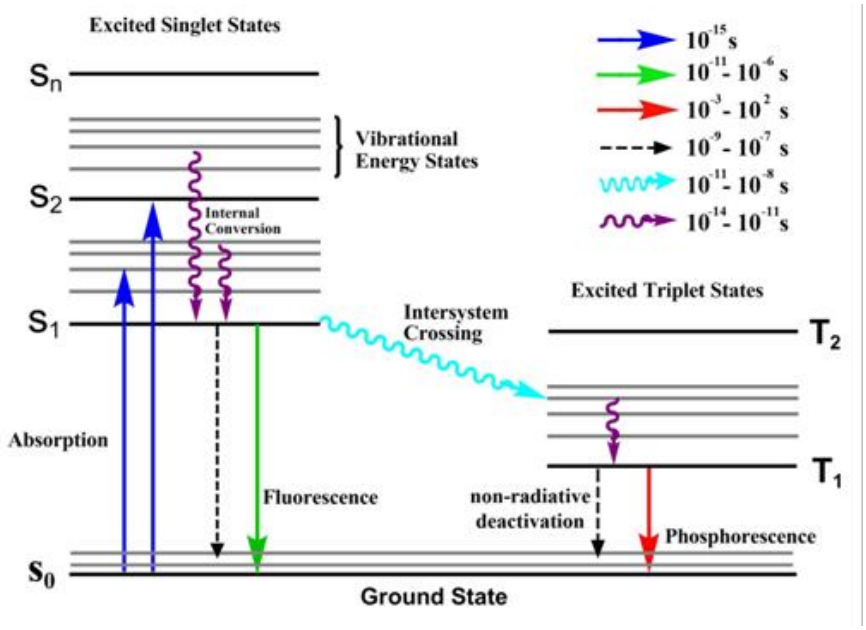

Figure 2. Jablonski Diagram.

It is seen that the energy of the absorbed light is higher than energy of the emitted light because of the energy loss of molecule before the emission. The difference between these energy is called as Stokes shift.[11] To be clear, it can be defined as the difference between the band maximum of the absorption and the band maximum of the emission of the same transition as it is seen in Figure 3.

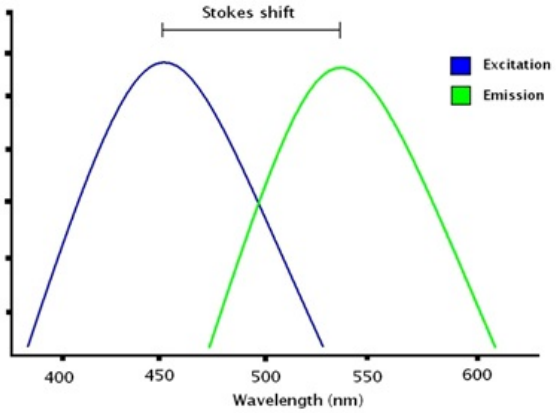

Figure 3. Stokes' shift.

2.1.2.1 Photoinduced Electron Transfer (PET)

The system that have photoinduced electron transfer (a.k.a. PET) has two main components; one of them is known as fluorophore, the other one is known as receptor. As its name implies fluoro means luminescence and phore means the one that carries fluoro/light/luminescence and the fluorophore can be used as a dye that has a property of re-emitting light due to the excitation. The receptor here is the component that transfer its electron to the fluorophore or accepts an electron from the fluorophore. These two components are separated from each other by an inert spacer which breaks down the conjugation between them, but holds them together for the chemical processes to be involved. Therefore, for a molecule to be a PET based sensor, there should be a fluorophore, a spacer and a receptor. Because the electron transfer occurs after the light absorption this mechanism is called as photoinduced electron transfer. If the energy levels of the highest occupied molecular orbital (HOMO) of the receptor and the lowest unoccupied molecular orbital (LUMO) of the fluorophore are at the convenient energy then there is an option for the PET mechanism to be materialize. PET occurs when the fluorophore that is excited has a

vacancy for an electron in its ground state. This vacancy in ground state can be filled by the electron transferred from the receptor if the HOMO of the receptor has higher energy than the HOMO of the fluorophore, or the excited fluorophore can transfer its electron to the LUMO of the receptor where the LUMO of the receptor has lower energy than the LUMO of the fluorophore.

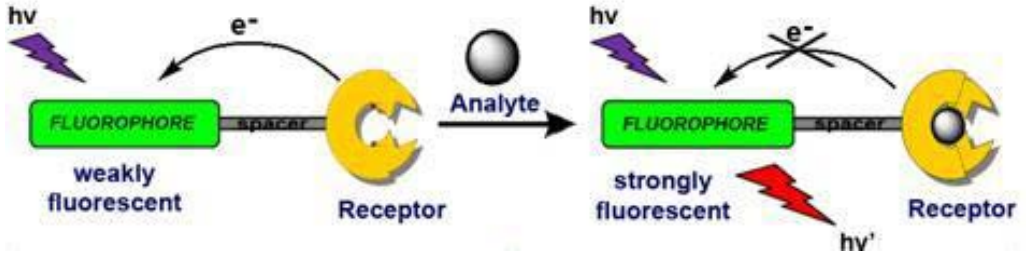

Figure 4. Schematic PET mechanism.

As Figure 4 shows PET mechanism is a way of blocking the ordinary relaxation and so quenching the emission. In this figure, receptor acts as an electron donor and transfers its electron to the fluorophore and quenches emission. It is also shown that the PET mechanism can be controlled by an analyte which prevents the receptor to transfer its electron to the fluorophore. By this way controlled PET mechanisms which can be on “on” or “off” state are emerged. It is clear on the left side of the Figure 4 that when the receptor is free to transfer its HOMO electron to the vacant HOMO of the fluorophore, the electron in the LUMO of the fluorophore cannot turn back to its original position so emission is quenched and no fluorescence is observed. On the right side of the Figure 4, it is seen that the receptor is bounded to a analyte, so its HOMO energy is lower than HOMO energy of the fluorophore. Therefore, it is not possible for receptor to transfer its electron to the fluorophore and the electron in LUMO of the fluorophore turns back to vacant HOMO of fluorophore. Because of this, there is fluorescence.

The natural and known example of PET mechanism is seen in photosynthesis.[12] In this process the sun pioneers the transfer of electrons which then causes charge separation. The emerging free energy from these steps is used for the generation of adenosine triphosphate. This example shows that oxidation-reduction processes of molecules are related to the light absorption.

PET type sensors are widely used in supramolecular chemistry and become an important research area for the molecular devices. [13,14]. In this step, the diversity of the molecular receptors becomes a necessary tool for a correct match between the analyte and receptor, because a rapid PET is depended on the fluorophore-receptor pair and the length of the spacer between them. [15] There are some molecules which are developed for being PET sensors; for example crown ethers are modified for being receptors for the alkali metal cations. The size of the crown ether determines the cation selectivity; as the ring becomes bigger, the cation that will be selected gets bigger.

1 2

Figure 5. Examples of PET sensors.

Simple PET sensors are shown in the Figure 5. The crown ether **1** that is modified with an amine group and an anthracene is a simple PET sensor used for the metal ions such as K^+ and it is observed that its quantum yield increases with K^+ ion in methanol solution.[16] Also some anthrylmethylamines like 11 are used as pH based PET sensors. [17] In addition to these simple examples there are molecules which are used as PET sensors such as calixarenes, cryptands and etc.

2.1.2.2 Intramolecular Charge Transfer (ICT)

The most important difference of intramolecular charge transfer (ICT) based signaling systems from the PET systems is that there is no linker between the fluorophore and the receptor, which means a direct integration of fluorophore and receptor and so the receptor becomes a part of the π system of the fluorophore. Because of this the orbitals of the chemical units overlapped well and this results in one terminal to act as electron donor whereas the other terminal to act as electron

acceptor. When such a molecule is excited at a suitable wavelength the electron density is redistributed which then results in a serious dipole in the molecule. There exists an intramolecular charge transfer from electron donor to electron acceptor. When an analyte binds to the receptor molecule in question there is an interaction with the dipole of the excited state and this interaction can be observed with a change in absorbance and emission spectra. [18]

ICT is such a signaling mechanism that there is a blue shift or red shift according to the properties of the molecules that plays a role in the formation of this process. If there exists an electron donating group like amino group or hydroxy group onto the receptor part that is directly conjugated to the fluorophore part, the interaction between the receptor and a cation will cause a decrease in the electron donating property of the receptor to the fluorophore which means also a decrease in the conjugation. Therefore a blue shift in the absorption spectrum will be observed due to the destabilization of the ICT system. In contrary, if the receptor unit has an electron withdrawing group such as carbonyl group the interaction between the receptor and a cation will increase its electron withdrawing property so a red shift will be observed in the absorption spectrum due to the stabilization of the ICT system [19] as it is represented in Figure 6.

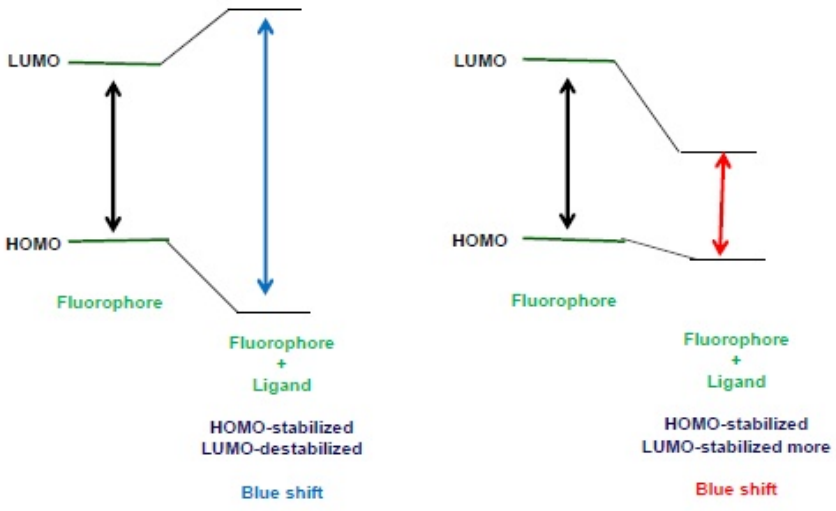

Figure 6. Spectral changes in ICT based sensor

The essential reason behind the changes in emission and absorption spectra lies on the charge dipole interactions. [20] When the molecule is excited, if it contains an electron donating group this part will partially charged positively and this positive charge will interact with the cation and so there will be a destabilization of the excited state which means excited state will be more destabilized than the ground state. In this situation, the gap between the excited state and the ground state increases so there will be a blue shift in the emission and absorption spectra. Oppositely, the reason of the red shift in the emission and absorption spectra is that there is a decrease in the gap that is between the excited state and the ground state due to the interaction between the fluorophore where the cation will stabilize the excited state more than the ground state.[15]

It is known that when the receptor and the fluorophore are integrated there exists a charge separation in the excited state. When the analyte is added, its π electron system will be perturbed.

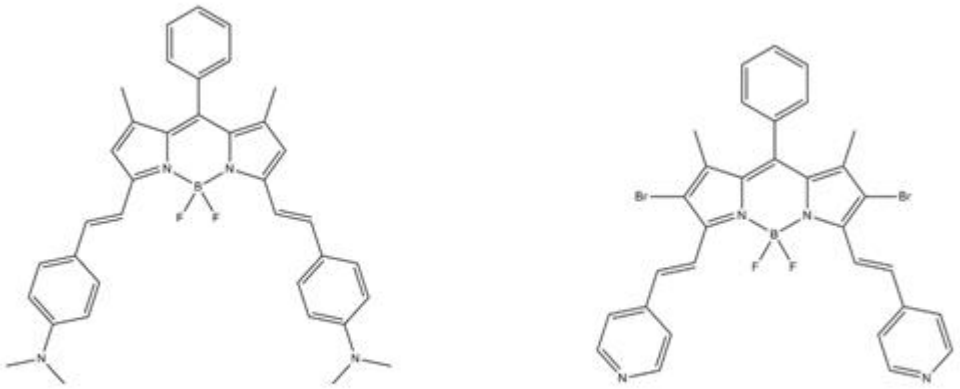

3 4

Figure 7. BODIPY dyes for ICT

Bodipy dyes are commonly used for the design of ICT based sensors. Modification of Bodipy with different groups may cause different results in spectral properties. For example, 3 given above gives blue shift upon protonation due to the aniline which has an electron donating property, whereas 4 gives red shift upon protonation due to the pyridine which acts as an electron accepting moiety.[21] By this way it can be said that it is possible to obtain different spectral properties with similar structures.

2.1.2.3 Energy Transfer (ET)

When the existing energy is transferred to the ground state of a chromophore from the excited state of another chromophore it is called as energy transfer.[22] It is represented in Figure 8. Here, the consignee of energy can be called as acceptor which is then excited to its first singlet excited state, and the consignor of the energy can be called as donor which transfers its excited state energy. Energy transfer is also known as electron energy transfer (EET) and fluorescence resonance energy transfer (FRET).

Because energy transfer is a kind of deactivation of excited state, it is effected by the rate of the other deactivation ways and so the choice of an energy transfer system should have meet properties to overcome the other patways.[23] In addition, life time of the excited state of donor should be longer than the time which is necessary for the energy transfer. Here the most important thing that determines the mechanism of energy transfer is the distance between the so called donor and the acceptor moieties. Mainly according to this distance there exists two energy transfer systems; Dexter type energy transfer system and Förster type energy transfer system.

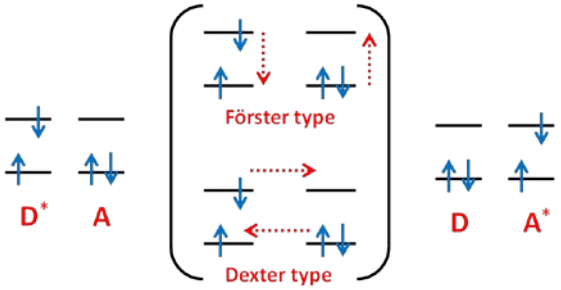

Figure 8. Schematic representation of energy transfer systems.

For a Dexter type energy transfer to take place the distance between the donor and the acceptor should be less than 10 Å and for a Förster type energy transfer to take place this distance should be in the range of 10 to 100 Å. [23] There are some ways to characterize the energy transfer such as comparison of quantum yields, relative lifetimes, emission of acceptor increase, emission of donor decrease, etc.

2.1.2.3.1 Dexter Type Energy Transfer

The orbital interaction between the donor and acceptor moieties is the decisive fact in Dexter type energy transfer. [24] There should be a conjugated linker between the donor and the acceptor to supply an exchange of electrons between the HOMOs and LUMOs of the donor and acceptor. As it is implied a short distance between the donor and the acceptor such as 10 Å is necessary for the orbital interactions. As the distance between increases the rate constant of energy transfer decreases exponentially;

$$\mathbf{k_{ET} = K\ J\ \exp(-2R_{DA} / L)}$$

Here, k_{ET} represents rate constant of energy transfer, K stands for orbital interaction, J symbolizes overlap integral between donor emission and acceptor absorbance, R_{DA} represents the separation between the donor and acceptor and L stands for the van der Waals radius. [23]

In other words, Dexter type energy transfer is depended on the interaction between the orbitals of donor and acceptor that leads to electron exchange from HOMO of the donor to LUMO of the acceptor. [25]

A variety of molecules that can be used as a Dexter type energy transfer system are synthesized. When these systems are excited at absorbance wavelength of donor they achieve energy transfer. One of them is shown below in Figure 9. In this system there are four terminal porphyrins that have zinc in the central are coordinated to the interjacent prophyrin. There occurs energy transfer from terminal porphyrins to the center through ethynyl bridge.

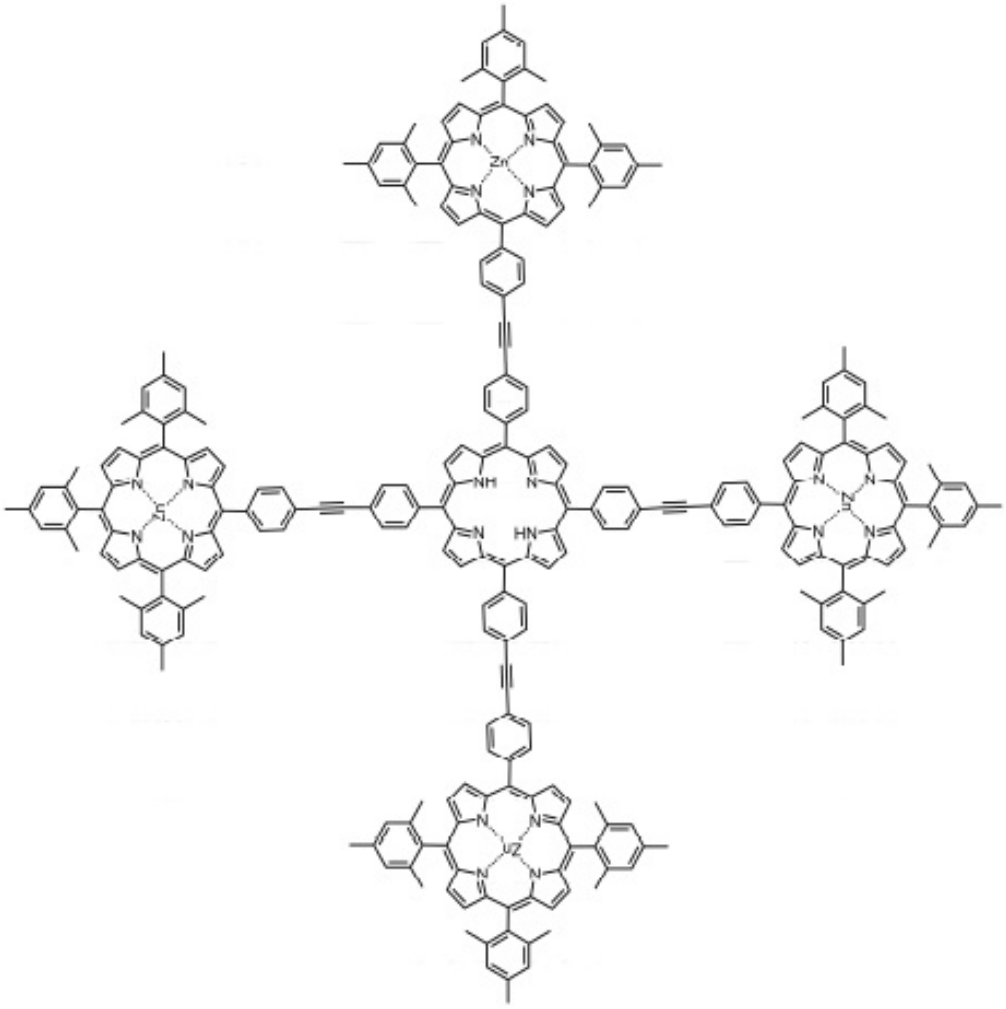

Figure 9. Dexter type energy transfer system 1[26] (Copyright ©, 1993, Elsevier. Reprinted with permission from Ref. 26)

Figure 10 shows another example for Dexter type energy transfer system which is composed of an anthracene moiety and a Bodipy. Here, energy is transferred from anthracene to Bodipy when the anthracene is excited. The reason depends on the parallel alignment of S_1 dipole moment of the donor and the S_0 dipole moment of the acceptor. [27]

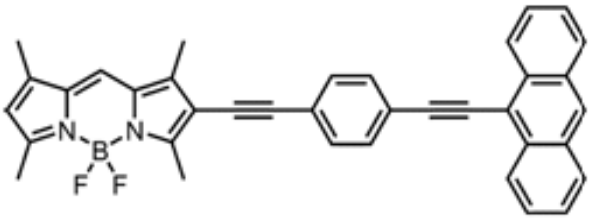

Figure 10. Dexter type energy transfer system 2[28] (Copyright ©, 2006, Elsevier. Reprinted with permission from Ref. 28)

2.1.2.3.2 Förster Type Energy Transfer

Förster type energy transfer is known as Förster resonance energy transfer (FRET) and also as electronic energy transfer (EET). There is a non-conjugated linker between the donor and the acceptor. In contrast to Dexter type energy transfer orbital interaction between the donor and the acceptor is not a remarkable property because the distance between them is large. There are three important parameters for FRET; one of them is the distance between donor and acceptor moieties, the second one is the spectral overlap between the emission of donor and the absorption of acceptor, and the third one is the relative orientation of the transition dipoles of these moieties. [29, 30, 31] They have an important role in the occurance of energy transfer, rate of energy transfer and the efficiency of the energy transfer.

In FRET mechanism, the energy released by the relaxation of the donor's electron from its LUMO to HOMO is used for the excitation of the acceptor's electron from HOMO to LUMO. The emission wavelength of the donor moiety should match with energy absorbed by the acceptor moiety for the existence of spectral overlap. The equations below shows the dependence of FRET on distance and overlap integral;

$$E_{FRET} = [1 + (R/R_o)^6]^{-1}$$

$$R_o^6 = [9\, Q_o\, (\ln 10)\, \kappa^2\, J] / [128\, \pi^5\, n^4\, N_A]$$

where R_o refers to the distance between the donor and acceptor moieties and called as Förster radius, R is the separation between the FRET moieties. Here, the quantum

yield of FRET donor is represented as Q_o, the orientation factor of dipole is □□□ the overlap integral is J, the refractive index of the medium is n, and the Avagadro's number is N_A. It is clear that as the spectral overlap increases FRET efficiency decreases. In addition as it is shown in Figure 11 there is no FRET beyond 10 Å as it is stated before.

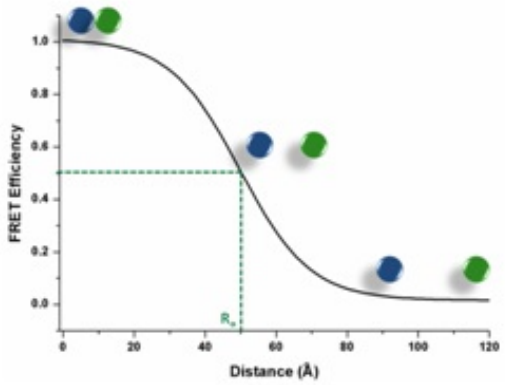

Figure 11. Distance dependence of FRET efficiency

There are two main patways to determine the efficiency of FRET; the first one of them is the steady state approach and the second one of them is time-resolved approach. [32] Steady state approach is used to follow the decrease in the donor unit's quantum yield. The only problem here is the re-absorption of the emitted light by the same molecule which is also called as inner filter effect. This problem is overcome by the utilization of very dilute solutions. [33,34]

Efficiency of FRET with steady state is given below;

$$\mathbf{E = 1 - (\Phi_{DA} / \Phi_D)}$$

where Φ_{DA} represents the quantum yield of donor in the presence of acceptor and Φ_D represents the quantum yield of donor in the absence of acceptor. There is also another formula, that is related to the increase of acceptor unit's fluorescence, to calculate FRET efficiency;

$$\mathbf{E = A_A (\lambda_D) / A_D (\lambda_D) * [I_{AD}(\lambda_A^{em}) / I_A(\lambda_A^{em}) - 1]}$$

where A_A is the absorbance of acceptor and A_D is the absorbance of donor at a wavelength at which the absorbance of donor is maximum, integrated area of the acceptor is denoted as I_{AD} and I_{AD} in the presence and absence of donor at λ_A^{em}, respectively.

FRET efficiency calculation is much more accurate with the second pathway; time resolved approach that uses time-resolved emissions of acceptor and donor as its name implies. FRET efficiency can be calculated by using the formula below [32];

$$\mathbf{E = \tau_D * k_{FRET} / (1 + \tau_D * k_{FRET})}$$

$$\mathbf{k_{FRET} = 1/\tau_{DA} - 1/\tau_D}$$

where τ_{DA} and τ_D represents lifetime of the excited state of donor in the presence and absence of acceptor, respectively.

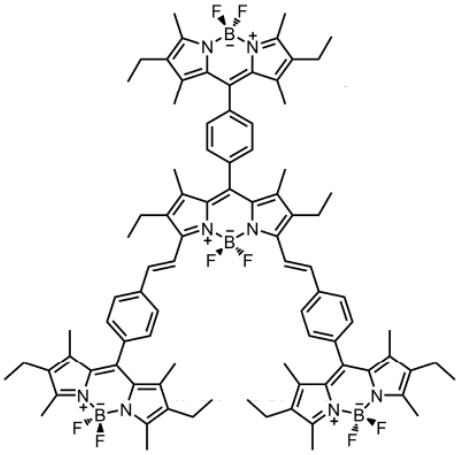

Figure 12. An example of FRET system (Copyright ©, 2009, Elsevier. Reprinted with permission from Ref. 35)

An example of FRET system can be seen in Figure 12. The emission of the core Bodipy increases as the number of terminal Bodipy donors are increased. [35]

2.2 Molecular Logic Gates

Human life is extended and reached to a more comfortable condition in novadays. The improvement of computers and digital devices has a great impression on this

development of life conditions. Their function and contribution in sharing information, saving and generating data and communication between people all around the world can be shown as the base of the civilization. Contemporary technology is proceeded enough to use electronic signal as a carrier for these kind of information sharing, storing and communication by means of miniaturization. Information is encoded as a series that is composed of a combination of zeros and ones which represent low and high voltage, respectively, in this kind of digital systems. [36,37]

The fundamental building blocks of silicon circuitry depends on the logic gates which are a kind of electronic devices and carry out Boolean functions. [38] There should be one or more logical inputs for a logical operation and for the creation of an output. There are 16 different types of Boolean logic operations. [39] Here, the most commonly used logic operations are; AND, OR, NOR, XOR, NAND, XNOR, INH and NINH. The interconnection of AND, OR, XOR and INH which are the basic logic operations results in the others; NOR, NAND, XNOR and NINH operations.

Table 1 displays the truth tables for all these commonly used logic gate operations. If and only if the both inputs are 1 then the output is 1 which indicates a state above a specified threshold, otherwise the output is 0 which indicates a state below a specified threshold in any combination of inputs in an AND gate. In an OR gate, it is enough for a one input to be 1 for the output to be 1. The output will be 0 only when the two inputs are 0. In an XOR gate, when the both inputs are at the same logic state the output becomes 0, if the inputs have different state from each other the output is 1. For an INH gate, one of the input determines whether the output is 1 or 0. It is seen that the outputs of NAND, NOR, XNOR and NINH are the reverse of AND, OR, XOR and INH gates, respectively.

There are also more complex logic gate systems that are composed of the integration of Boolean logic operations. Some of them are half adder, half substractor, full adder, full substractor, multiplexer and demultiplexer. [40]

Inp1	Inp2	Outp	Outp	Outp	Outp	Outp	Outp	Outp	Outp
A	B	OR	AND	XOR	INH	NOR	NAND	XNOR	NINH
0	0	0	0	0	0	1	1	1	1
1	0	1	0	1	0	0	1	0	1
0	1	1	0	1	1	0	1	0	0
1	1	1	1	0	0	0	0	1	1

Table 1. Truth tables for the commonly used logic operators that have 2 inputs

Transistors are the main components of the logic gates in computers which makes them to be used as electronic switches. When the current is turned on in the transistor, it is symbolized as 1, when it is turned off it is symbolized as 0. [41] With the emergency of silicon based transistors there occurred a chance to combine the transistors in a small chip which makes it possible to profit from space, energy, cost and performance. [42]

Molecular logic devices are the extended version of the macroscopic logic devices. Molecules can be synthesized and designed in such a way that they can be capable of performing some special functions. There is a need for energy and signal to operate and communicate with the operator. [43] The energy here can be light such as luminescence, electrical energy or chemical energy and electronic and/or nuclear rearrangements are used to operate. [43] The prominent study in molecular logic gates was proposed by de Silva in 1993 which then gained a great importance in the area of molecular mimicry. [1] There should be an ion responsive molecule to carry out a logical operation due to a given input in molecular logic gates. The output of the molecular logic system is followed by a signal which might be fluorescent or an other optical signal. Fluorocesce phenomenon is opted in general because of its advantages on selectivity and sensitivity. With help of chemical stimuli fluorescence switches between “on” and “off” states. It is obvious that these kind of molecular logic gates are design to work with on/off switching systems such as photoinduced electron transfer, internal charge transfer and energy transfer.

After the first application of logic gates into the molecular world a variety of different molecular logic gates are upgraded. [44] Figure 13 represents the receptor molecule that is designed and synthesized by de Silva et al. in 1993, which acts as a logic gate having two inputs. [1] It is proposed to be an AND gate in which H^+ and Na^+ are represented as inputs and the molecule of interest binds selectively to that ions. Binding to the both ions selectively results in an increase in the intensity of fluorescence, in all other ways intensity of fluorescence will be lower.

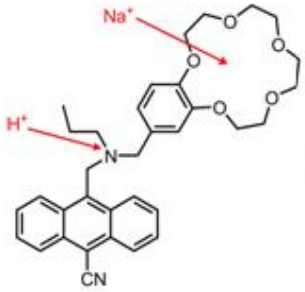

In1 (Na^+)	In2 (H^+)	Output (F. Intensity)	Q. Yield	F. Enhancement
0	0	0	0.011	1.0
1	0	0	0.020	1.8
0	1	0	0.013	1.2
1	1	1	0.068	6.2

Figure 13. Two-input molecular logic gate by de Silva et. al. (1993) (Copyright ©, 2014, Elsevier. Reprinted with permission from Ref. 1)

2.2.1 A Higher Function Molecular Logic Gate - Molecular Demultiplexer

Although for the basic logic operations fundamental logic gates are satisfactory, there is a need for more complex logic systems for performing higher level functions. By connecting the simple logic gates to each other in a compatible manner generation of complex logic systems is carried out. The important thing here is that, the output of the one logic gate should be used as the input of the other logic gate. However, because the molecular logic gates use different types of signals such as electrical, chemical and optical, this input-output homogeneity is not the actual fact for the molecular logic gates. Although it seems hard to integrate simple gates to each other scientists found out an easier way; designing such a molecule that minimizes the problem of physical integration of simple logic gates, by this way mimicking higher functions logic gates with molecules has found a place in literature. [45] A demultiplexer (DEMUX) is such a logic gate that takes one input and selects between different outputs. There is an address input that effect the selection of output process. Nowadays, scientists have developed chemical systems that are

capable of operating as DEMUX by combining organic molecules, lasers and nanocrystalline semiconductures. [46] There is an example below that works as a 1:2 DEMUX;

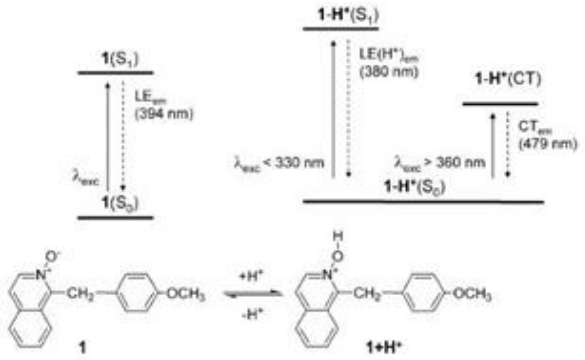

H+ (In)	λexc (c)	Em at 380 nm (Out1)	Em at 479 nm (Out2)
0	λexc<330 nm (c=0)	0	0
1	λexc<330 nm (c=0)	1	0
0	λexc≥360 nm (c=1)	0	0
1	λexc≥360 nm (c=1)	0	1

Figure 14. Chemical structure and proton equilibrium of a 1-2 Molecular Demultiplexer and its truth table [47] (Copyright ©, 2008, Elsevier. Reprinted with permission from Ref. 47)

There are two basic parts of the molecule which are activated photochemically and linked by a methylene bridge. Here, the output-1 or output-2 are photonically addressed by the proton,which is the input, due to the control input, c. [47]

2.3 Photodynamic Therapy

Photodynamic therapy is a new clinically used method that is found about a century ago for the treatment of certain diseases such as melanoma, cardiovascular diseases, pancreas cancer, lung cancer, and many other malignant diseases. [48] It is asserted as an alternative curing method to the chemotherapy and radiotherapy by being less harmless then these. A light sensitive drug or a photosensitizer (PS) is taken orally and after 1 to 3 days of administration it is exposed to a certain wavelength of light which then generates toxic singlet oxygen. [48] Hence, the main components of PDT are light, photosensitizer and singlet oxygen. Using visible/near infrared light makes PDT less harmless than radiotherapy in which the light with high energy is used. A photosensitizer is an organic molecule which is a fundamental element of PDT. It is important because it is responsible for the generation of singlet oxygen from the molecular oxygen. The highly reactive singlet oxygen damages the diseased cell

which is exposed to the light. To summarize, it can be said that by activating the PS by photons with appropriate energy results in the formation of singlet oxygen from the molecular oxygen. The place of the PS determines where the cellular attack of singlet oxygen will occur, it can damage lipids, DNA or proteins oxidatively. [49] the cellular response is given as apoptosis or necrosis and the vascular supply is broken down so hypoxia or activation of immune system takes place. [50,51] In PDT, either a laser source of light emitting diodes (LEDs) that are red or near infrared are used as a light sources because these red or near IR light penetrates to the tissues better. [52]

2.3.1 A Brief History of Photodynamic Therapy

The story of PDT began with the observation of some chemicals caused cell death in the presence of certain intense light about a century ago. Oscar Raab, a pharmacology student, observed that a certain bacteria was dead due to the toxic affect of acridine red molecule when it was subjected to the light. [53] He found out that a flurorophore was needed for the corresponding light induced toxicity. After the first emergency of PDT, eosin dye was used as the first PS for the medical treatment of skin cancer by Tappeiner and Jesionek. [54] Year 1979 has a great importance for the development and understanding of PDT. It is the year that the mechanism of oxygen dependent toxicity of photoactive molecules was found due to monitoring the generation of singlet oxygen by electron spin resonance technique. [55] Meyer-Betz, a scientist, made the first trial of human PDT on himself and suffered from an extensive phototoxic reactions and felt extreme pain. [56] The clinical application of PDT was performed by Dougherty et al. in 1978. [57] After that, the first PS approved by FDA was photofrin. The commercialization of photofrin was completed in Canada for the treatment of bladder cancer ,n 1993. By being the most used PDT drug, it has been approved in USA for oesophagel cancer, in Netherlands and France for lung cancer, in Japan for gastric cancer and in Germany for early stage lung cancer. . Following this, a lot of PS were approved by FDA and this leaded to a great success in the treatment of diseases by PDT.

2.3.2 Mechanism of Photodynamic Action

The most important step of the photodynamic action is the generation of singlet oxygen which occurs due to the photoactivation of the fluorophore. The Jablonski diagram below that demonstrates the steps of singlet oxygen generation is given in Figure 15.

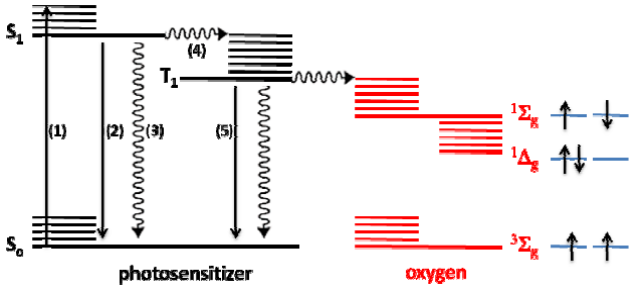

Figure 15. Jablonski Diagram PDT Action

The first step in the generation of $^1O_2$ is the excitation of the fluorophore to its singlet excited state with a photon that is in appropriate energy level. After the relaxation to the vibrational ground state there are two possible ways of relaxation to the ground state besides radiationless relaxation (step 3); one of them is the fluorescence (step 2) in which the electron falls back to its electronic ground state, the other one is the intersystem crossing to triplet state. (step 4). If there are heavy atoms attached to the interested molecule that can favor the intersystem crossing pathway generation of singlet oxygen takes place due to the energy transfer from triplet excited state to ground state, else it prefers phosphorescence (step 5). [58] Photodynamic therapy depends on the formation of reactive singlet oxygen species and its oxidative damage to the diseased cell. It is known that life time of the singlet oxygen is very short (about 0.6 µs) and the diffusion distance is about 0.1µm so it is accepted as the cellular damage begins around the photosensitizer. [59] Therefore, the localization of the PS is important for the PDT in terms of targeting the cell that is in interest.

2.3.3 Biochemistry Beyond the Photodynamic Action

There are two different mechanisms for the cell death in PDT. In the first one, unstable radicals are formed due to the reaction between excited PS and a substrate,

which is called as a biomolecule. These radicals are used to generate singlet oxygen. In the second one, there is an energy transfer from excited PS to oxygen that leads to the formation of singlet oxygen. It is accepted that both of the mechanisms occurs concurrently. [50] The newly generated singlet oxygen ($^1O_2$) reacts with biomolecules such as membrane lipids whose structure and integrity are changed due to the formation of radicals and other destructive chemicals that lead to an increase in the oxidative stress in cell. [60] Hydroxyl radicals generated by reactions of $^1O_2$ attack to the deoxyribose sugar and bases of DNA and this mutation causes an immediate cell death. [61]

Cell death in PDT can take place in two different morphological ways; apoptosis and necrosis. [62] Apoptosis is known as the programmed cell death. Apoptosis causes some characteristic morphological changes in the cell, such as; DNA fragmentation, blebbing, cell shrinkage and chromatin condensation. Caspases, as known as proteolytic enzymes exist in all cells as inactive precursors or procaspases and activated by other caspases cleavage process and produces a proteolytic caspase cascade, intercede apoptosis by cleaving specific proteins in cytoplasm and nucleus. [63] It is activated with an apoptotic signal which is triggered by radiation, an increase in intracellular calcium concentration, viral infection and lack of nutrition. With the initiation of the activation intracellular adaptor molecules begin to aggregate and activate procaspases, and the cell death exist. Necrosis is the second way of cell death by PDT. Unlike apoptosis, it is known as being traumatic and unnatural cell death. It can be fatal to the organism. Cell membrane integrity is lost and products of cell death are set free in the cell membrane, in necrosis. Both apoptosis and necrosis can be observed as outcome of the PDT.

2.3.4 Properties of Photosensitizers

There are some special requirements for the photosensitizer which is sent to the cell before the light is applied for being an efficient agent. For the PDT takes place, there should be a generation of singlet oxygen which requires appropriate physical and chemical properties in a specific molecule. The transition from triplet ground state of molecular oxygen to singlet oxygen excited state is spin forbidden. Its probability is increased with the spin-orbit (SO) coupling which provides a singlet character to the

triplet state by mixing the spin angular momentum and the orbital angular momentum.

$$\mathbf{Hso=[(e^2Z^4)/(2a_0m^2c^2n^3)]LS}$$

SO-Hamiltonian formula is given[64] above shows that SO-Hamiltonian term is proportional to the fourth power of atomic number , Z, where e is charge of electron, a_0 is Bohr's radius, m is the mass of electron, c is the speed of light, n is the principle quantum number, L is the angular momentum and S is the spin operator. It is clear that heavy atom attachment to the molecule of interest increases the spin-orbit coupling and so the spin forbidden transition from singlet to triplet state. Heavy atom effect on efficacy of the photosensitizer was verified on BODIPY dyes with bromine attachment by O'Shea *et al.* [65] Therefore, photosensitizers with heavy atoms have a better singlet oxygen generation capability.

In addition, because of the reactive singlet oxygen generated during the PDT action most of the photosensitizers are degraded which is called photobleaching. Hence, photosensitizer should be designed as a photostable molecule for the sake of PDT.

The depth of the penetration of light to the tissue is another important issue. It is known that penetration of light is decreased substantially beyond 1150 nm because of the absorbance of water. Visible light is absorbed by flavins, collogens, melanin and hemoglobins. Near UV region is absorbed by some aromatic amino acids such as phenylalanine, tyrosine and tryptophan. When all these conditions are considered it gives out that maximum penetration of light is obtained in the range of 620-850 nm which is called therapeutic window. To produce reactive singlet oxygen the chosen or designed photosensitizer should absorb light in this region sufficiently. [66]

Besides the properties mentioned above a photosensitizer should meet the other requirements for biological application such as it should be biocompatible, effervescent and should have dark toxicity which means it is inactive until the light is exposured.

CHAPTER 3

3 PEGylated Calix[4]arene as a Carrier for a Bodipy-based Photosensitizer

This work is partially described in the following publication
Yusuf Çakmak, Tuğrul Nalbantoğlu, Tuğçe Durgut, Engin U. Akkaya
Tet. Lett., **2014**, Vol. 55, pp. 538-540

3.1 Introduction

Photodynamic therapy (PDT) is accepted as an alternative method to the other traditional therapeutic methods that includes chemotherapy, radiation therapy and surgery because of being less invasive than them.[50] PDT is a selective method by performing the cytotoxic action only in the presence of light, sensitizer and dissolved oxygen. Its selectivity depends on the capability of controlling the region of irradiation.

There is a great interest in generating and controlling the photodynamic action of late years. In addition, there is an increase in the introduction of novel chromophore families such as Bodipy dyes as potential photosensitizers. [67] Bodipy dyes are seen as one of the most promising and efficient photosensitizers although they were ascribed to be chemically and photochemically stable hence unavailable to form triplet state and so the interaction with ambient oxygen is reduced which is necessary for PDT at first. However, with incorporation of heavy atoms such as iodine or with the increase in degeneracy of the excited state frontier orbitals an efficient photosensitizer can be obtained from a Bodipy dye. [68]

The wavelength of irradiation is the other important point that should be considered. The dyes with weak absorptions in the red end of the visible spectrum where the mammalian tissues are most transparent are preferred in the PDT studies. Studies on obtaining dyes that have absorptions in the red and near IR region of the spectrum are acceptable in this point of view. Porphyrin family is an example to these kinds of dyes. [69] Bodipys give a chance to tune their absorption bands in a wide range. For

example, by substituting one or two styryl groups to a Bodipy dye its absoption peak can be moved between 500 nm and 850 nm. [70] With the consideration of this practical property of the Bodipy dye we come up with a new type of scaffold carrying this dye and also enabling it to absorb near IR light.

Furthermore, calix[4]arene which has a hydrophobic core and special geometry is a very useful molecule for organic chemists. Up to this point in time there are only a few examples that incorporate Bodipy dyes and calix[4]arenes. Akkaya et al. have synthesized a bodipy around a monoformylated tetrahydroxycalix[4]arene for pH sensing with the help of the working principle of photoinduced electron transfer (PeT).[71] In this design, the bodipy is synthesized around the formyl unit which ensures obtaining the bodipy unit attached to the calix[4]arene unit. It is notable that π conjugation is faded due to the orthogonalty of the phenyl of calix[4]arene and the bodipy. By this way absorption spectrum of the bodipy does not change. In our design, we improved the aforementioned system in terms of absorbance, application, route of synthesis and the number of bodipy units attached to the calix[4]arene backbone.

3.2 Design and Synthesis

Incorporation of maximum number of bodipy molecules to the calix[4]arene scaffold is the main principal of our design. Our aim was putting forward a new type of molecule that would function effectively in other potential applications. The number of bodipy unit is important for the enhancement of the phototoxic effect. Therefore, our design of PS (Fig. 16), there are two bodipy chromophores that are attached to the calix[4]arene core.

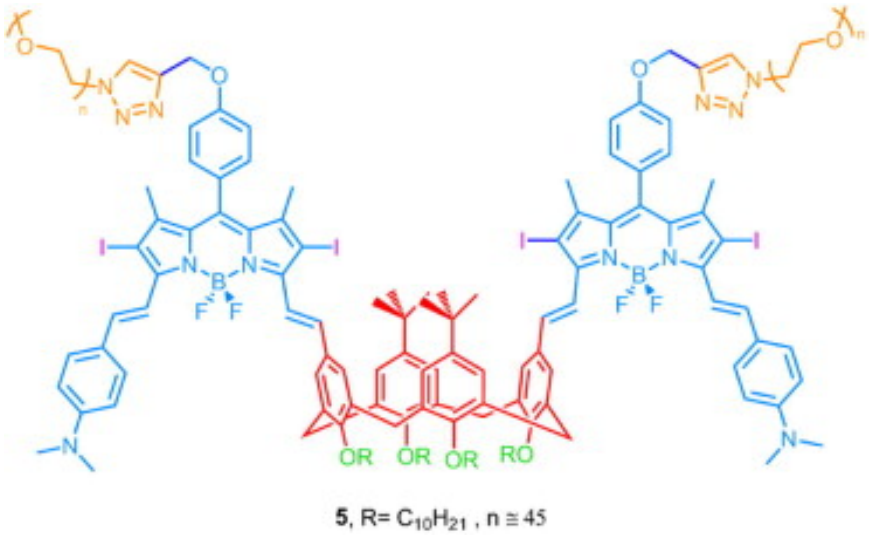

Figure 16. Design of the final molecule[72] (Copyright ©, 2014, Elsevier. Reprinted with permission from Ref. 72)

The absorption wavelength of the PS is the second important parameter of a good PS as it is mentioned before. Therefore, we thought that there should be a π-bond character in the bond between the bodipy units and calix[4]arene for the extension of π-conjugation of the bodipy units which causes a red shift in the absorbance of wavelength. This type of organization of the molecule is the first example that includes both bodipy and any kind of calixarene. The third design parameter is increasing the molecule's solubility in organic solvents, and therefore four decyl groups attached to the lower rim of the calix[4]arene. This attachment makes one side of the molecule hydrophobic and so it is possible to go inside the cell via diffusion by interacting with the hydrophobic moieties around the cell. As a fourth property, this molecule has two poly(ethyleneglycol) polymers attached to the bodipy which makes the molecule water soluble, in other words these two moieties act as complementary for the molecule to gain amphiphilic character. Fifth, 4-Dimethylaminobenzaldeyde units are attached to the bodipy to increase the π-conjugation more and to guarantee the maximum absorbance wavelength at around 700 nm. Finally, our design includes iodine atoms on the bodipy core. By this way, rate of intersystem crossing for the production of singlet oxygen increases which is necessary for the PDT.

The synthesis of the final compound was completed in eleven steps at all which is shown in Figures 17-19.

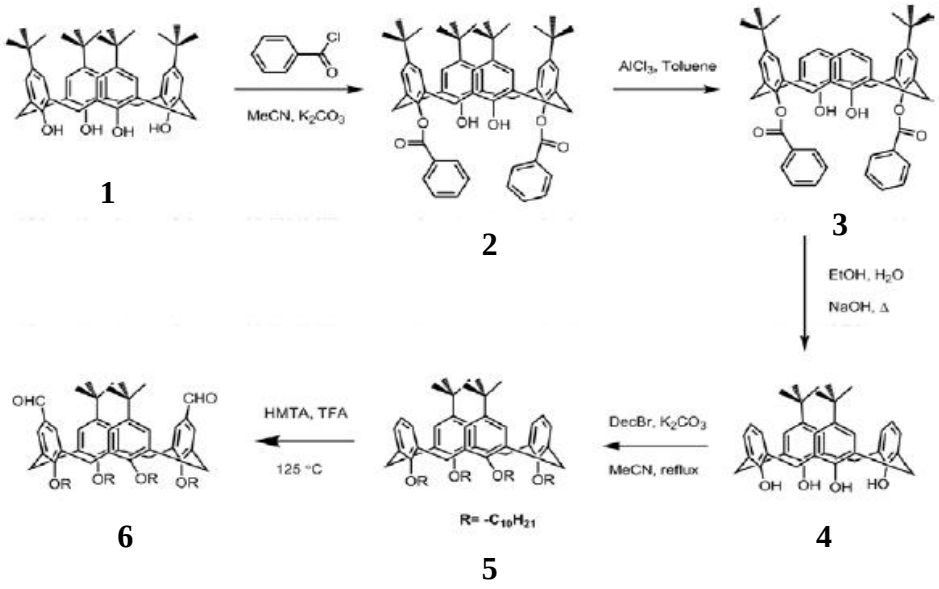

Figure 17. Synthesis of calix[4]arene derivative

Compound **6** was synthesized in five steps to be ready for the reaction with bodipy derivative. First of all, for the de-*tert*-butylation step, **1** and benzoyl chloride reaction was performed to get the compound **2** as the protected group. Two of the four tert-butyl groups were de-*tert*-butylated in step 2 by using $AlCl_3$ and toluene to yield compound **3**. For the removal of the protecting groups hydrolysis reaction was performed with NaOH and EtOH. Compound **5** was yielded by the alkylation reaction of compound **4** with 1-bromodecane. Compound **5** was diformylated at elevated temperature with hexamethylenetetramine and TFA to get compound **6.**

Synthesis of diiodinated bodipy derivative was performed in three steps which are shown in Figure 18.

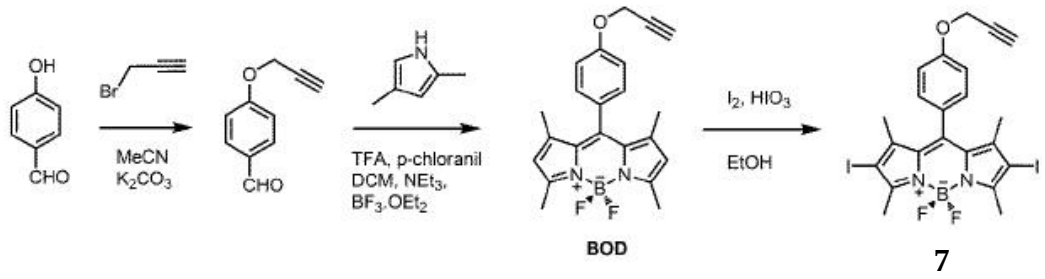

Figure 18. Synthesis of diiodinated bodipy derivative

First step is the reaction of the propargyl bromide and 4-hydroxybenzaldehyde. Product of this reaction was reacted with 2,4-dimethylpyrrole with an ordinary bodipy synthesis procedure and yielded alkynyl bodipy derivative, which was then diiodinated with iodine and iodic acid to yield compound **7**.

Compound **8** was obtained due to the Knoevenagel reaction of compound **6** and compound **7**. (Fig. 19). Another typical Knoevenagel reaction on compound **8** with 4-(Dimethylamino)benzaldehyde yielded in compound **9**, which then forms compound **10** due to a click reaction with pre-prepared PEG-N_3.

^{1}H NMR, ^{13}C NMR and ESI or MALDI mass spectroscopy were used for the characterization of the compounds. Because of the large molecular weights of the compound **9** and compound **10** characterization of them was hard. However, by comparing their ^{1}H NMR data analysis, the structure of the photosensitizer, compound **10** was verified. (Fig. 20)

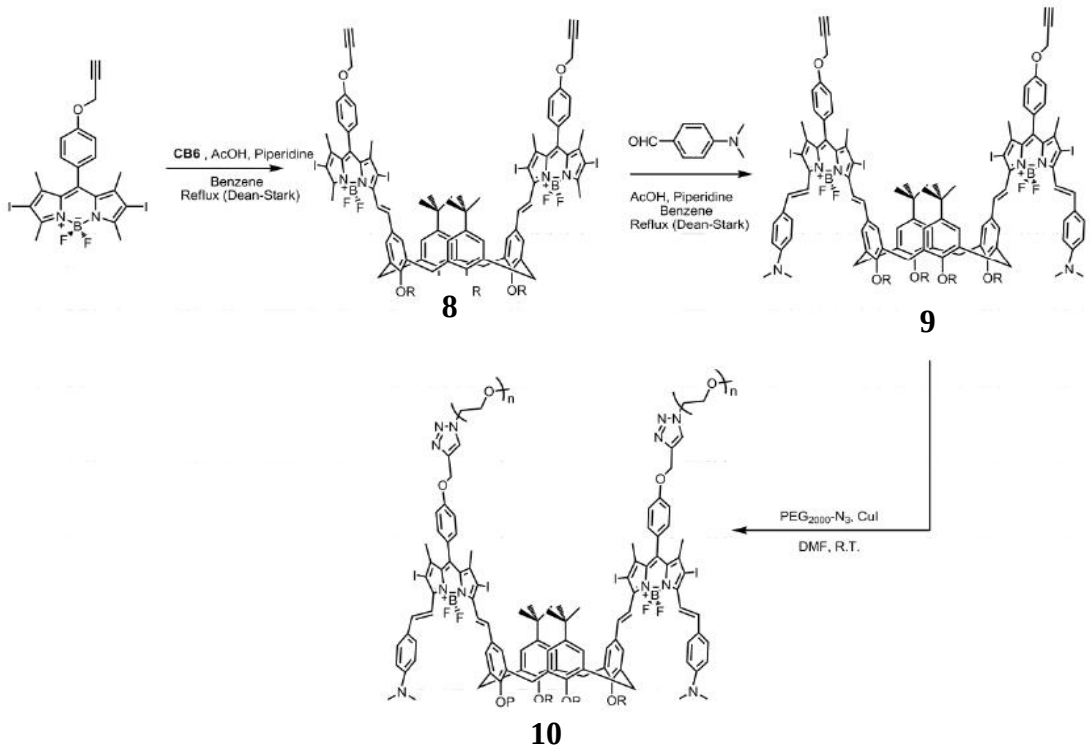

Figure 19. Schematic synthesis of the photosensitizer, compound 10

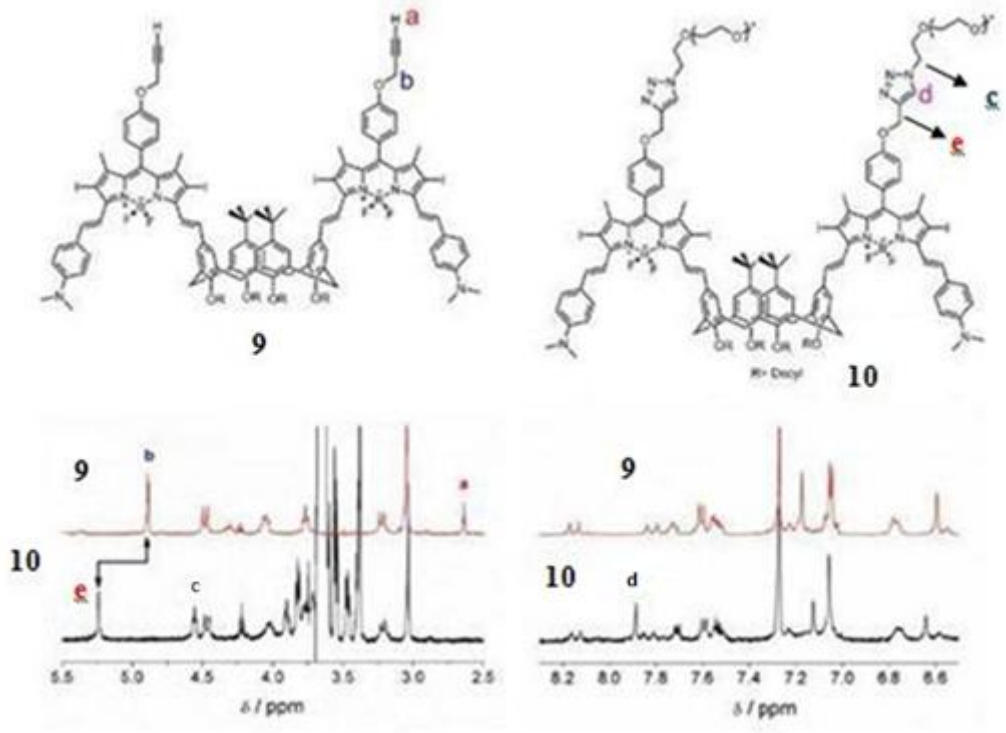

Figure 20. Comparative ^{1}H NMR data analysis of compound 9 and compound 10

A comparative ^{1}H NMR spectra of compound **9** and compound **10** are given in Figure 20. There are three differences in aliphatic regions of the ^{1}H NMR spectra of these two compounds due to the successful final click reaction. First of all, disappearance of the acetylenic proton at 2.61 ppm (proton a, in Fig. 20) is a proof of the accomplishment of the click reaction. The second difference is that, a methylene proton that belongs to the PEG group linked directly to the triazole is appeared at 4.58 ppm (proton d, in Fig.20). And lastly, there is a shift of methylene bridge protons which connects the triazole unit to the phenoxy unit of the Bodipy from 4.89 ppm to 5.25 ppm is observed (proton shifting from b to e, in Fig. 20). This kind of a peak shift is also observed in a similar compound that is synthesized by Erbas *et al*.[73] In the aromatic region of the spectra, there exists a triazole proton at 7.90 ppm. (proton e, in Fig. 20). Because the electronic structure and the geometric shape of the molecule do not change too much, there are no such important changes in the aromatic region of the ^{1}H NMR spectra.

3.3 Results and Discussion

After synthesizing the photosensitizer, compound 10, we focused on the PDT experiments. For this aim, we planned two experiments; one of them is in organic medium and the other one is in the aqueous medium because our final compound is amphiphilic. We used 1,3-diphenylisobenzofuran (DPBF) which is known as a universal oxygen scavenger compound for the experiments took place in the organic medium. Maximum absorbance of DPBF in a broad range of organic solvent types is about at 410 nm and intensity of the absorbance peak at 410 nm is decreased due to the reaction with oxygen that is generated by the PS in action. Therefore, we focused on the decrease in the intensity of the peak at 410 nm.

First of all, we performed control experiments without PS, compound **10**. We used only DPBF (10μM), light and bubbled air (5 min.) in isopropanol. We started the photodynamic experiments in dark by withdrawing light and recording the absorbance spectra for 15 minutes. After that, irradiation with LED light array of 725 nm was applied with 5 min time intervals for 60 min. The normalized absorbance graph (Black dotted line in Fig. 21, below) shows that the absorbance of trap

molecule does not change with time, by proving that there is no cytotoxic $^1O_2$ formation.

Secondly, we included compound **10** (46 nM) to the control experiments in isopropanol. For this case, again 15 min. dark toxicity experiment was applied and it was observed that the absorbance did not change with time and there was no cytotoxic $^1O_2$ formation. (Red dotted line in Fig. 21) Then, it was irradiated by 725 nm light for 60 min. with 5 min time intervals again for the photodynamic activity. There was a successful decrease in the absorbance of scavenger with time which was a proof of $^1O_2$ formation.

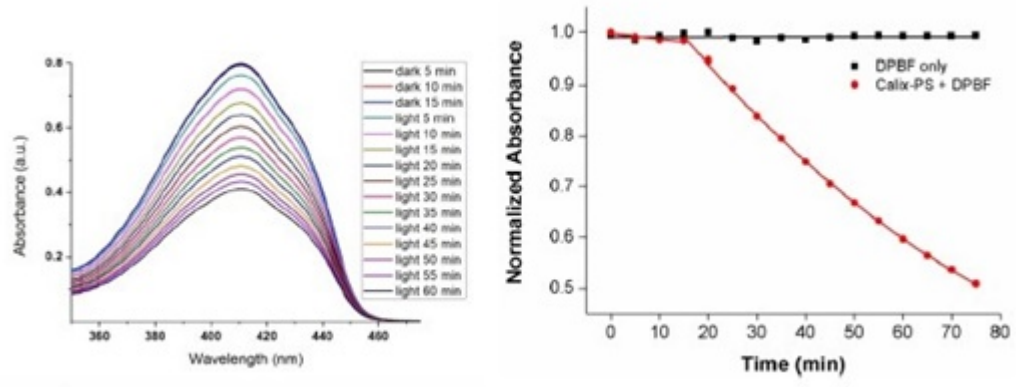

Figure 21 Change in absorbance spectrum of DPBF in the absence of compound 10 and in the presence of compound 10 in IPA; first 15 min dark and then 60 min irradiation with 725 nm LED array (above). Normalized absorbance vs. time graph of DPBF; control experiment without (black dotted line) and with (red dotted line) compound 10 (below). (Copyright ©, 2014, Elsevier. Reprinted with permission from Ref. 72)

Afterward, we performed singlet oxygen experiments in aqueous medium. Because DPBF is not soluble in such polar solvents we needed a water soluble trap molecule. For this reason we synthesized an anthracene derivative substituted with malonic acid groups (2,2'-(anthracene-9,10-diylbis(methylene))dimalonic acid, ADMDA). Figure 22 shows the schematic synthesis of ADMDA that tracks $^1O_2$ formation. Dioxygen bridges are formed as a result of the reaction with $^1O_2$ and there is a decrease in the absorbance signal around 380 nm of the original compound.

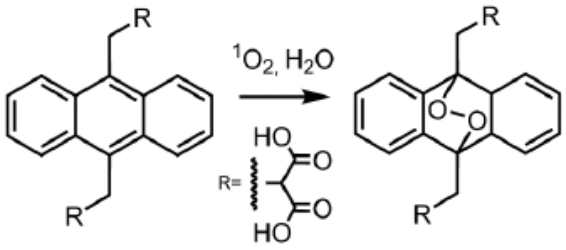

Figure 22. Structure of 2,2'-(anthracene-9,10-diylbis(methylene))dimalonic acid that is used to track $^1O_2$ production in aqueous media. (Copyright ©, 2014, Elsevier. Reprinted with permission from Ref. 72)

The absorbance of the trap molecule (1 µM) first in dark and then 60 min irradiation was recorded in PBS at pH 7.4 as a control experiment. It is seen that there is a minimum decrease in absorbance in Fig. 23 (Black dotted line, below).

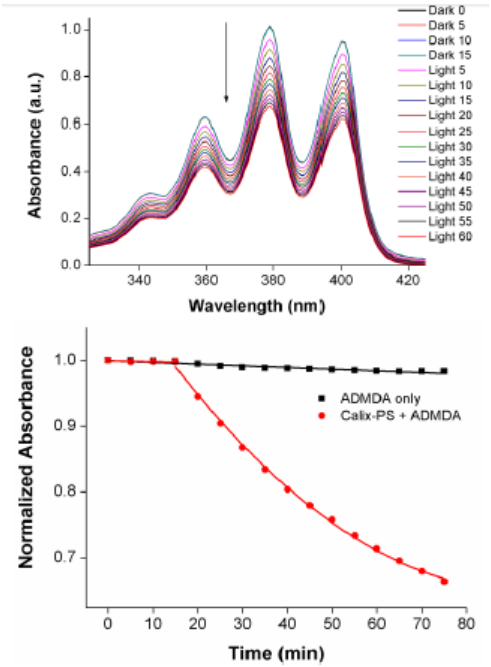

Figure 23. Change in absorbance spectrum of ADMDA in the absence of compound 10 and in the presence of 2.3 µM of compound 10 in PBS at pH 7.4; first 15 min dark and then 60 min irradiation with 725 nm LED array (above). Normalized absorbance vs. time graph of ADMDA; control experiment without (black dotted line) and with (red dotted line) compound 10 (below). (Copyright ©, 2014, Elsevier. Reprinted with permission from Ref. 72)

After the control experiments a PBS solution at pH 7.4 was prepared. Because the compound **10** did not dissolved in PBS well because of the polar ethylene glycol units we first dissolved in tiny amount of ethanol and then studied with PBS. There was no precipitation and it worked well. We used 2.3 µM of compound **10** for the photodynamic activity experiment in PBS. It was mandatory to use 50 folds of compound **10** due to the short lifetime of the $^1O_2$ (2 µs) in aqua. The same procedure with organic media was applied to the this experiment; there was no change in absorbance in the first 15 min dark experiment, and a sharp decrease in the absorbance with 60 min irradiation with 725 nm LED array (Figure 23).

Eventually, we observed the singlet oxygen formation and photodynamic activity in both organic (IPA) and aqueous (10% EtOH in PBS) media due to amphiphilic structure of the calix-bodipy photosensitizer.

3.4 Conclusion

Initially, we came up with an idea such that getting a carrier molecule having four bodipy units. In addition, we were planning to link this carrier molecule to an antibody of a cancer tissue to recognize it and act as a targeting group. Because characterization of the structure of antibody, reacting it with our previously designed photosensitizer and functionalizing the calix[4]arene to react with bodipy would be difficult we redesigned it with decyl groups in the end.

The selectivity of the designed photosensitizer that have decyl groups is very low in biological media. However, it is well known that hydrophobicity ensures the interaction between the molecule and the cell membrane and also facilitates diffusing into cells. It is an advantage because nuclei are responsible for the cell destruction which is a strong effect of the photodynamic action. Moreover, amphiphilic character of the photosensitizer mimics biological molecules, so a molecule that reflects the truth of life was synthesized.

The other problem was that low yields of the reaction steps made it difficult to study our PS *in vitro* and *in vivo* cytotoxic experiments. Especially, the yield of the two Knoevenagel condensation reactions were very low (10-20%) and restricted our

studies. The long reaction steps that reached to eleven steps limited the final amount of the aforementioned molecule as well.

In conclusion, although we faced such problems through the project we finally succeeded in synthesizing the amphiphilic photosensitizer that is photoactive in both organic and aqueous media. This π-conjugated bodipy calix[4]arene scaffold may be used in future works for another applications.

3.5 Experimental Details

3.5.1 Methods and Materials

Chemicals for the experiments were purchased from Merck and Sigma-Aldrich and used without further purification. Reactions were monitored by thin layer chromatography using Merck TLC Silica gel 60 $F_{254.}$ Merck Silica Gel 60 (particle size: 0.040-0.063 mm, 230-400 mesh ASTM) was used for the column chromatography. ^{1}H NMR and ^{13}C NMR spectra were recorded on Bruker DPX-400 in $CDCl_3$ where the internal standard is tetramethylsilane. Chemical shifts were given in parts per million and the coupling constants (*J*) were in Hz. Mass spectra were performed on Agilent Technologies 6224 TOF LC/MS and Accurate Mass Q-TOF LC/MS. MALDI spectra were recorded in Izmir Institute of Technology, Chemistry Department by Bruker MALDI-TOF-TOF. Varian Cary-100 spectrophotometer and Varian Cary 5000 UV-VIS-NIR absorption spectrophotometer were used for the absorption spectra. Varian Eclipse Spectrofluometer was used for the fluorescence measurements. 1,3-Diphenylisobenzofuran was used as a singlet oxygen trap in organic medium singlet oxygen measurement and purchased from supplier. For aqueous medium singlet oxygen measurement 2,2'-(Anthracene-9,10-diylbis(methylene))dimalonicacid was synthesized via literature procedure. [74] Compound 4[75] and Compound 7[73] were synthesized according to literature.

3.5.2 Synthesis of Compounds

Compound 5

NaH (60% dispersion in oil – 2.23 g, 55.7 mmol) was washed with hexane and filtrate was added to the dry DMF (40 mL) with care. Then Calix[4]arene-OH (1.79 g, 3.34 mmol) and 1-Bromodecane (7.38 mL, 33.4 mmol) were added to the solution. The reaction mixture was heated at 60^0 C for 12 hours. After reaction it was allowed to cool down. Ice/water was added (100 mL) and the mixture was extracted with dichloromethane (3×50 mL). Organic layer was washed with water (3×50 mL), aqueous ammonium chloride solution (2×50 mL) and brine (50 mL) and dried with K2CO3. Then organic layer was evaporated in low pressure and yellow solution was obtained. Upon waiting overnight the compound precipitatedin MeOH. The compound was filtrated and washed with MeOH to get the pure product as a white solid (2.4 g, 60%). ^{1}H NMR : 7.09 (s, 4H; ArH), 6.21 (t, 2H, *J* = 7.5 Hz; ArH), 6.09 (d, 4H,*J* = 7.5 Hz; ArH), 4.45 (d, 4H, *J* = 13.2 Hz; CH_2), 4.05 (t, 4H, *J*=8.3; OCH_2), 3.72 (t, 4H, *J*=6.5; OCH_2), 3.11 (d, 4H; *J*=13.3), 1.95-2.01 (m, 4H; CH_2), 1.81- 1.95 (m, 4H; CH_2), 1.51-1.65 (m, 4H; CH_2), 1.15-1.50 (m, 70H; CH_2, CH_3), 1.00-0.85 (m, 12H; CH_2, CH_3). ^{13}C NMR : 155.5, 155.3, 144.2, 135.9, 133.6, 127.2, 125.6, 122.0, 75.1, 75.0, 34.1, 32.0, 31.8, 31.3, 30.6, 30.4, 30.2, 29.9, 29.8, 29.5, 26,7, 26.1, 22.8, 14.1. HRMS (TOF-ESI): m/z calcd for $C_{76}H_{120}O_4Na$: 1119.9084 [M+Na]+; found: 1119.9138 [M+Na]+, Δ = 4.82 ppm.

Compound 6

A mixture of Compound **5** (1 g, 0.91 mmol), Hexamethylenetetraamine(4.52 g, 27.34 mmol) and Trifluoroacetic acid (20 mL) was stirred at 125^0 C for 4 h in a screw-capped vial, then the reaction mixture was cooled to room temperature. Diluted with aqueous 1 M HCl (150 mL) and CH_2Cl_2 (50 mL) and it was stirred for 3 h vigorously. The organic layer was taken and extracted with dichloromethane (50 mL). Then dried with K_2CO_3 and evaporated in vacuo. The compound was obtained pure after column chromatography with chloroform (1.044 g, 99%). ^{1}H NMR: 9.15 (s, 1H; CHO), 7.11 (s, 4H; ArH), 6.59 (s, 4H; ArH), 4.49 (d, 4H,*J*=13.4; CH_2), 4.10 (t, 4H, *J*=8.3; OCH_2), 3.75 (t, 4H, *J*=6.5; OCH_2), 3.18 (d, 4H, *J*=13.6, CH_2), 1.80-2.00 (m, 8H; CH_2), 1.50-1.62 (m, 4H; CH_2), 1.41 (s, 18H; CH_3), 1.18-1.41 (m, 52H; CH_2), 0.88-0.98 (m, 12H; CH_3). ^{13}C NMR : 191.5, 160.7, 155.0, 145.3, 135.4, 134.9, 131.1, 129.1, 126.1, 75.3, 75.0, 34.2, 32.0, 31.7, 31.2, 30.4, 30.2, 30.1, 29.8, 29.7,

29.5, 29.4, 26.6, 26.0, 22.7, 14.1. HRMS (TOF-ESI): m/z calcd for C78H121O6: 1153.9163 [M+H]+; found: 1153.9107 [M+H]+, Δ = 4.85 ppm.

Compound 8

Compound **6** (100 mg, 86×10-3) and Diiodobodipy (Compound **7**) (173×10-3) were dissolved in benzene (50 mL). Piperidine (0.3 mL) and then acetic acid (0.3 mL) was added to the solution. The reaction mixture was heated to reflux in Dean-Stark apparatus. When most of the solvent has been evaporated the compound was started to compose and the product was tracked by TLC with $CHCl_3$ as an eluent. After product formed in majority EtOAc (20 mL) was added and extracted with H_2O (3×30 mL). Organic layer was dried with Na_2SO_4, and evaporated in vacuo. In order to eliminate polar impurities evaporated mixture a short column chromatography done by using chloroform as an eluent. The product then recrystallized with $CHCl_3$ and Hexanes. The product precipitates in hexane which was filtrated to yield the pure product as blue solid (22 mg, 11 %). ^{1}H NMR: 7.80 (d, 2H, *J*=16.0; CH), 7.11-7.21 (m, 6H; CH and ArH), 6.98-7.10 (m, 8H; ArH); 6.51 (s, 4H; ArH), 4.85 (s, 4H; OCH_2), 4.48 (d, 4H, *J*=12.9 Hz; CH_2), 4.05 (t, 4H, *J*=7.9 Hz; OCH_2), 3.73 (t, 4H, *J*=6.0 Hz; OCH_2), 3.20 (d, 4H, *J*=12.9 Hz; CH_2), 2.60-2.68 (m, 8H, $ArCH_3$ and CH), 2.00-2.10 (m, 4H, CH_2), 1.82-1.95 (m, 4H, CH_2), 1.50-1.61 (m, 4H, CH_2), 1.41 (s, 6H, $ArCH_3$), 1.35 (s, 18H, CH_3), 1.10 (s, 6H, $ArCH_3$), 0.80-1.00 (m, 12H, CH_3). ^{13}C NMR : 158.2, 157.1, 155.1, 145.8, 145.2, 140.7, 135.4, 134.0, 132.4, 131.4, 130.5, 129.5, 128.4, 127.3, 126.0, 116.3, 115.7, 78.0, 76.2, 75.5, 75.2, 56.2, 34.2, 32.0, 31.7, 31.0, 30.5, 30.3, 30.2, 29.9, 29.8, 29.5, 29.4, 26.6, 26.2, 22.7, 17.7, 16.9, 14.1.
MALDI 2483.722 measured as 2483.558.

Compound 9

Compound **8** (50 mg, 0.021 mmol) and N,N-Dimethylaminobenzaldehyde (7.46 mg, 0.05 mmol) were dissolved in Benzene (50 mL).Piperidine (0.3 mL) and then acetic acid (0.3 mL) was added to the solution. Then the reaction mixture was heated to reflux in Dean-Stark apparatus. When most of the solvent has been evaporated the compound was started to form and tracked by TLC and $CHCl_3$ used as an eluent.

After product formed in majority EtOAc (20 mL) was added and extracted with H_2O (3×30 mL). Organic layer was dried with Na_2SO_4, and evaporated in vacuo. The mixture was obtained as a pure product after column chromatography with $CHCl_3$: Hexane (3:1) as a green solid(17 mg, 31%). ^{1}H NMR: 8.15 (d, 2H, *J*=16.7 Hz; CH), 7.81 (d, 2H, *J*=16.6 Hz; CH), 7.59 (d, 4H, *J*=8.8 Hz; ArH), 7.53 (d, 2H, *J*=16.8 Hz ; CH), 7.15-7.24 (m, 6H; ArH and CH), 7.00-7.09 (m, 8H; ArH), 6.77 (d, 4H, *J*=8.1 Hz; ArH), 6.53-6.62 (m, 4H; ArH), 4.89 (d, 4H, *J*=2.4 Hz; CH_2), 4.48 (d, 4H, *J*=12.8 Hz; CH_2), 4.05 (t, 4H, *J*=8.1 Hz; CH_2), 3.75 (t, 4H, *J*=6.6 Hz; CH_2), 3.21 (d, 4H, *J*=12.9 Hz; CH_2), 3.01 (s, 12H; $N(CH_3)_2$), 2.61 (t, 2H, *J*=2.4 Hz; CH), 2.00-2.10 (m, 4H; CH_2), 1.82-1.95 (m, 4H; CH_2), 1.51-1.65 (m, 4H; CH_2), 1.48 (s, 6H; $ArCH_3$), 1.20-1.42 (m, 70H; CH_3 and CH_2), 1.18 (s, 6H; $ArCH_3$), 0.80-0.97 (m, 12H, CH_3). ^{13}C NMR :158.1, 156.9, 154.9, 145.4, 135.3, 133.9, 130.9, 129.8, 129.3, 128.8, 127.4, 125.9, 115.7, 112.2, 78.1, 76.0, 75.5, 75.2, 68.2, 56.2, 40.4, 38.8, 37.1, 34.1, 32.0, 31.9, 31.8, 31.7, 31.0, 30.5, 30.4, 30.2, 30.1, 30.0, 29.9, 29.8, 29.7, 29.5, 29.4, 26.6, 26.2, 23.8, 22.7, 17.7, 17.6, 14.1. MALDI 2639.972 measured as 2639.604.

Compound 10

Compound **9** (17 mg, 6.44×10-3mmol) and PEG_{2000}-N_3 (25.76 mg, 0.0129 mmol) were dissolved in dry DMF (5 mL). Argon was bubbled through the solution for 10 minutes and CuI (2.94 mg, 15.4×10-3 mmol) was added to the deaerated solution. The reaction mixture was stirred at 60^0 C overnight. Then 5 mL of $CHCl_3$ was added and CuI was filtrated. Then solution was evaporated and compound was separated through column chromatography in MeOH: $CHCl_3$ (7:93) as green solid (10 mg , 24%) ^{1}H NMR: 8.15 (d, 2H, *J*=16.2 Hz; CH), 7.90 (s, 2H; CH), 7.85 (d, 2H, *J*=16.6 Hz; CH), 7.61 (d, 4H, *J*=8.1 Hz; ArH), 7.53 (d, 2H, *J*= 15.6 Hz;CH), 7.21 (d, 2H, *J*=17.1 Hz, CH), 7.11-7.17 (m, 4H, ArH), 6.72-6.81 (m, 4H, ArH), 6.58-6.70 (m, 4H, ArH), 5.22-5.28 (m, 4H; OCH_2), 4.58 (t, 4H, *J*=3.8 Hz; NCH_2), 4.48 (d, 4H, *J*=12.0 Hz; CH_2), 4.03 (t, 4H, *J*=7.9 Hz; OCH_2), 3.91 (t, 4H, *J*= 4.9 Hz; OCH_2), 3.35-3.88 (m, 364 H, OCH_2), 3.23 (d, 4H, *J*=11.0 Hz; CH_2), 3.05 (s, 12H; $N(CH_3)_2$), 1.83-2.11 (m, 8H; CH_2), 1.51-1.63 (m, 4H; CH_2), 1.47 (s, 6H; $ArCH_3$), 1.23-1.43 (m, 70 H; CH_2), 0.87-0.95 (m, 12H, CH_3). MALDI calculated as 6736.998, found 6728.428.

CHAPTER 4

4 SYNTHESIS OF MODULES FOR A MOLECULAR DEMULTIPLEXER

4.1 Introduction

The potential application of linking molecular logic gates for diagnosis and therapeutic purposes is very exciting. As it is reported in de Silva article[1] molecules that can perform like logic gates are seen as prerequisites for the molecular information processing. Although they have some limitations according to their inspired precedents, Boolean logic, one of these limitations "input-output heterogeneity" can create a positive situation that one can design a single molecule that may perform two different logic gate operations. [76] Demultiplexer is a kind of logic gate operation that uses this advantage. It is a combinational device that takes one input and selects between multiple outputs depending upon the control groups.

It is discussed previously that molecular logic operations are now seen as the backbone of photodynamic therapy where the selectivity is seen as the supreme key of the theranostics. It is known that a simple logic gate operation, an AND gate, can enhance the selectivity and brings advantages for the diagnosis. [77] Demultiplexer, can be very effective in this from this point of view by being a dual selective in outputs such as light and cytotoxic singlet oxygen. In this thesis we designed the modules of such molecular demultiplexer that can be used for further researches in theranostics.

4.2 Design and Synthesis

Design of a molecular logic gate with a proper application is quite hard. It is known that a demultiplexer can switch between the two outputs with one input and a control group. In this project we aimed to synthesize the modules of such a molecular demultiplexer that can diagnose the carcinogenic cells and can apply therapy by killing the cancer cells via generation of singlet oxygen with the help of emission property. Our modules are composed of three different parts; first one is the

photosensitizer, the second one is the fluorophore and the last one is the linker that links the PS and FL.

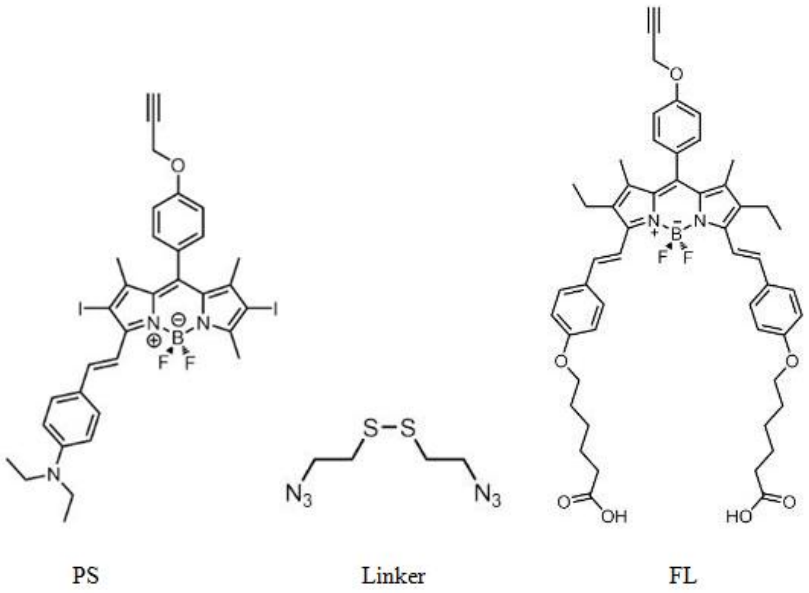

Figure 24. Molecular structures of PS, Linker and FL

In this design, we figured out the synthesis of modules of molecular demultiplexer. We design them to act as a molecular demultiplexer when we combine FL and PS with the linker by click reaction. We expect the energy of FL to be less than the energy of PS according to the literature examples. The PS is similar to the molecule in Figure 71[78], so we expect its maximum absorbance at about 700 nm. The FL is similar to the molecule in Figure 72[79] and we expect its maximum absorbance at around 650 nm so their spectra might intersect. so we expect an energy transfer from PS to FL when the PS is excited. In addition, there should be an acidic medium for the excitation step and so the protonation of the PS. We know that the carcinogenic cells are acidic. [80] To sum up, we can say that PS can produce singlet oxygen in the acidic medium but it prefers energy transfer. However, when there is Glutathione in that acidic medium, because it is also known that glutathione uptake is increased in carcinogenic cells[81], the S-S bond of the linker is broken and singlet oxygen production is set free due to the long distance between the FL and the PS.

Here, the PS module has heavy atom groups which includes iodine to increase rate of singlet oxygen production by making the intersystem crossing process easier.

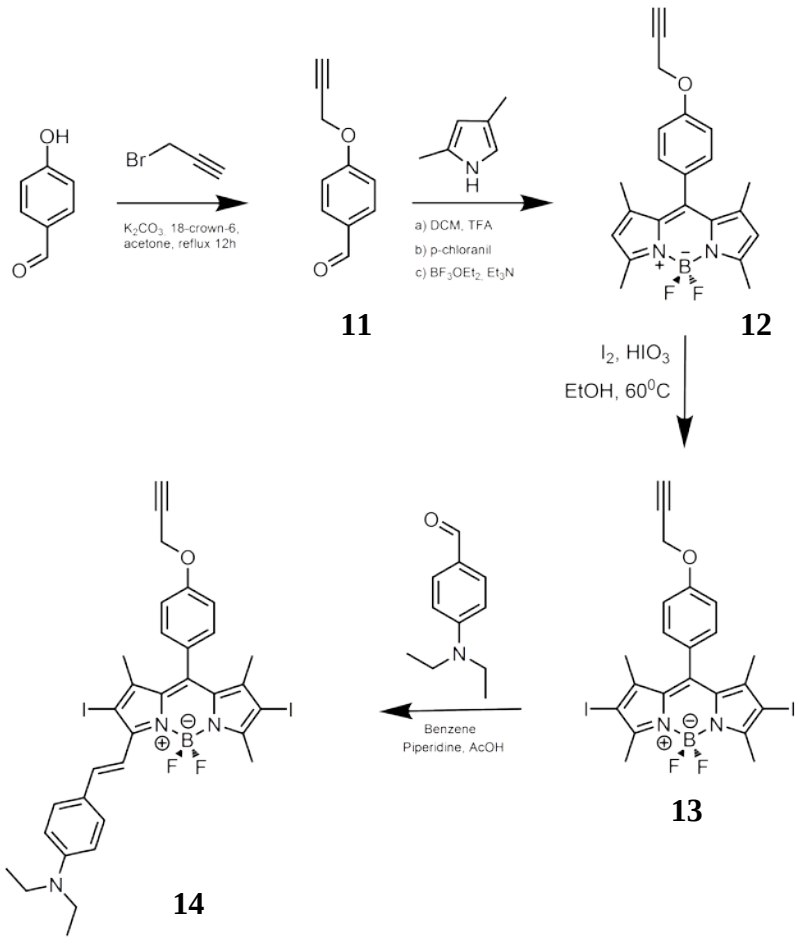

Figure 25. Schematic synthesis of PS

We first synthesized the propargyl aldehyde (compound **11**) from 4-Hydroxybenzaldehyde and propargyl bromide, and then used it for the simple BODIPY reaction (compound **12**) with 2,4-Dimethylpyrrole. After iodination reaction of the BODIPY (compound **13**), Knoevenagel condensation reaction was used with 4-Diethylaminobenzaldehyde and the targeted PS (compound **14**) was obtained as it is seen in Figure 25.

The FL module is designed to be fluorescent. We used pre-synthesized propargyl aldehyde and 2,4-dimethyl-3-ethyl pyrrole to synthesize the BODIPY (compound **15**). Then we synthesized the compound **16** by using 4-hydroxybenzaldeyde and 6-bromohexanoic acid. After that we used these two compounds to synthesize the FL module (compound **17**) by Knoevenagel condensation reaction as it seen in Figure 26.

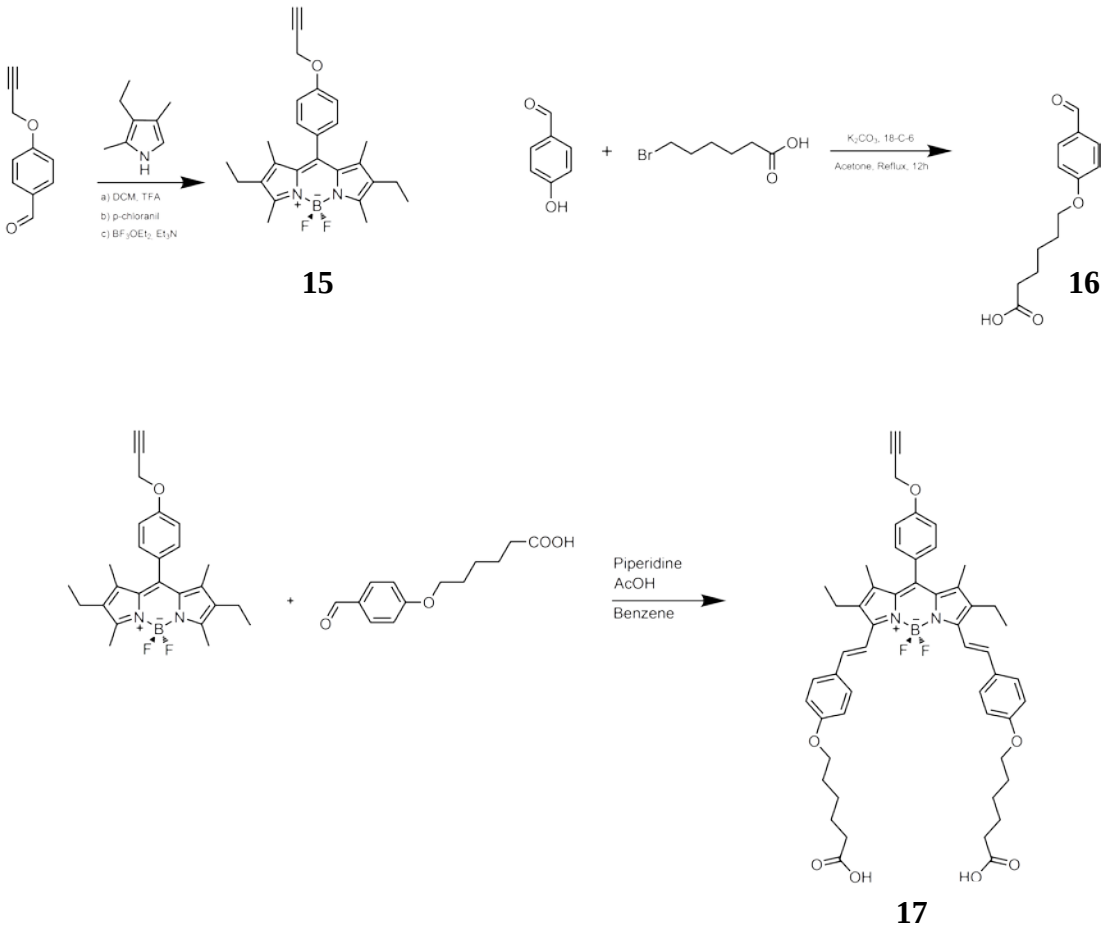

Figure 26. Schematic synthesis of FL

The synthesis of the linker is important because we need S-S bond, for the design of the molecular DEMUX.

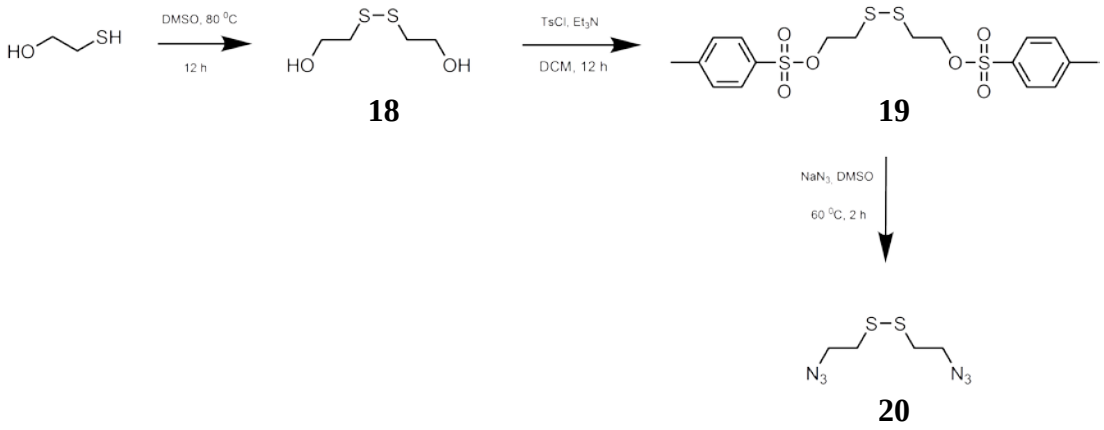

Figure 27. Schematic synthesis of the linker

We began with the disulfide synthesis by using 2-mercaptoethanol, as it is seen in Figure 27. Then we used the product, 2-hydroxyethyldisulfide (compound **18**), in tosylation reaction with 4-Toluenesulfonyl chloride for the synthesis of compound

19. And finally, we made an azide synthesis (compound **20**) from this compound by using sodium azide.

4.3 Results and Discussion

In this project we designed and synthesized the necessary modules for the concept of molecular demultiplexer. As it is mentioned before, molecular logic gates have opened a new door to the exciting research areas. In addition when they are integrated with the life necessity such as diagnosis and therapy of some cancer types imputed as undeterred diseases it becomes an attractive field to discover. Photodynamic therapy is such a sort of therapy that can easily be combined with logic gate approach. However, it is a serious application for diseased people so it might be controlled in a detailed way. Molecular demultiplexer is one of the unique molecular logic gate. It is unique because it has an ability to select between the two different outputs when it receives an input. It should define the diseased region of the tissue and then select the right patway of the outputs to operate.

Photodynamic therapy based on the excitation of the specialized photosensitizer that is in the tumor tissue and then generation of the singlet oxygen to destroy aforementioned tissue. It can be seen that molecular DEMUX can be a very effective way in the photodynamic therapy context. It can be designed to select between the two outputs such as energy transfer or the generation of singlet oxygen.

In this project, we expect the energy of the FL be less than the energy of the PS. In a molecular DEMUX, one can combine FL and PS with a linker such that we synthesized here. If one excites the molecule in a normal tissue, there will be no change in the molecule. If one excites the PS in an acidic medium at a certain wavelenght, energy transfer is expected from PS to FL and there is no harm for the tissue. If there is GSH in that acidic medium than the molecule prefers to generate singlet oxygen because the breakage of the S-S bond causes FL and PS to be seperated and energy transfer becomes impossible because of the distance between them. It can be seen clearly in Figure 28.

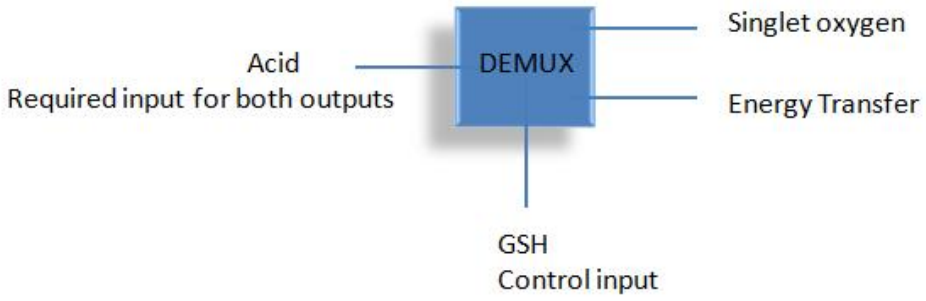

acid	GSH	Singlet oxygen	ET
0	0	0	0
1	0	0	1
0	1	0	0
1	1	1	0

Figure 28 Logic gate function of the DEMUX

Synthesis of these compounds are important for the application of logic gates in real life. As it is mentioned before our design composed of three important modules; PS, linker and FL. In the synthesis of PS, it is important that it has heavy atoms like iodine because it is known that Bodipys become more efficient photosensitizers with the incorporation of heavy atoms. As it is implied heavy atom substituted Bodipys have intersystem crossing step faster which then causes generation of singlet oxygen. In addition one can adjust the absorption band of a Bodipy. Tunable absorption band is an important phenomenon for a PDT agent. Absorption peak of the module can be tuned in between 550-800 nm wavelenght with the substitution of styryl groups to the Bodipy core because the ligth that can be used for PDT should be in this range. The NMR spectra show that the compound was synthesized successfully.

Our second target compound was the linker. As it is mentioned before the S-S bond system was designed according to the gluthathione's structure. A simple azide synthesis procedure was applied to get the compound. Mass data and NMR spectra indicate that the synthesis of the linker was accomplished.

The synthesis of FL was the most arduous part of the project. Because there are two carboxylic acid groups on the molecule, applying column chromatography was difficult. However, the synthesis was completed assuring the target compound was

yielded. NMR spectrum and mass spectrum verify the final compound was the target compound.

4.4 Conclusion

In this Project we made progress with the idea that includes design and synthesis of a possible molecular logic gate; DEMUX as a theranostic device. Our design is composed of a three different modules; a photosensitizer that is able to generate singlet oxygen upon excitation with the help of the heavy atom substitution, a fluorophore that is fluorescent especially upon protonation and linker that is able to link these two modules to each other and is able to break up in the presence of GSH.

In conclusion we can say that although we faced a lot of difficulties in the purification steps of the modules we are able synthesize these three PDT modules in a successful manner. Our mass spectra and NMR spectra support the synthesis is successful. We expect our modules to be used can be used as we envisoned in the synthesis of a functional threnostic device based on a molcular demultiplexer. This in turn will be a radical departure from the current approaches for obtaining theranostic agents, with hopefully much better results.

4.5 Experimental Details

4.5.1 Methods and Materials

Chemicals for the all experiments were purchased from Merck and Sigma-Aldrich and used without further purification. ^{1}H NMR and ^{13}C NMR spectra were recorded on Bruker DPX-400 in $CDCl_3$ where the internal standard is tetramethylsilane. s (singlet), d (doublet), t (triplet), q (quartet), dd (doublet of doublet) and m (multiplet) are used for the indication of splitting pattern. Reactions are monitored by thin layer chromatography using Merck TLC Silica gel 60 $F_{254.}$ Merck Silica Gel 60 (particle size: 0.040-0.063 mm, 230-400 mesh ASTM) was used for the column chromatography. Mass spectroscopy was performed on Agilent Technologies 6530 Accurate-Mass Q-TOF LC/MS.

4.5.2 Synthesis of Compounds

Compound 11

After solving 2.45 g (20 mmol) of 4-hydroxybenzaldehyde in 100 ml acetone, 2.5 g (30 mmol) of propargyl bromide was added to the solution. 5.5 g (39.8 mmol) of K_2CO_3 and a small crystal of 18-crown-6 were added. The reaction mixture was refluxed until 4-hydroxybenzaldehyde was consumed. Acetone was evaporated and the product was extracted with CH_2Cl_2 and dried over anhydrous Na_2SO_4. Organic phase was evaporated in vacuo and the product was purified via silica gel column chromatography using CH_3Cl/Hexane (50/50; v/v) as eluent. Compound 11 was obtained after the solvent was removed. (2.72 g, 16.98 mmol, 85%) ^{1}H NMR ($CDCl_3$, 400 MHz, δ ppm) 2.59 (q, *J*=1.00 1H), 4.75 (q, *J*=1.00 2H), 7.12 (t, *J*=1.00 2H), 7.88 (q, *J*=1.00 2H), 9.92 (s, 1H), ^{13}C NMR ($CDCl_3$, 400 MHz, δ ppm) 190.75, 162.38, 131.89, 115.19, 77.34, 77.02, 76.70, 76.35, 55.95. HRMS-ESI: calculated for M+Na 183.0422, found 183.0422, Δ= 0 ppm.

Compund 12

300 ml of CH_2Cl_2 was purged for 30 minutes with argon. 1.00 g (6.24 mmol) of Compund **11** and 1.31 g (13,7 mmol) of 2,4-dimethyl pyrrole were dissolved in it. a few drops of trifluoroacetic acid was added to the solution and the mixture was stirred for 12 h at room temperature. 1.52 g (6.24 mmol) of p-chloranil was added to the mixture and it was stirred for 45 minutes at room temperature. Triethylamine (5 ml) and boron trifluoride diethyl etherate (5 ml) were added, respectively. The product was extracter with diethylether after 30 minutes stirring. Organic phase was dried with Na_2SO_4 and evaporated under vacuum. Purification of the product was performed with silica gel column chromatography by using Hexane/Ethyl Acetate (8/1; v/v) as mobile phase. Fraction containing compound 1**2** was collected and the solvent was evaporated. (256 mg, 0.68 mmol, 11%) ^{1}H NMR ($CDCl_3$, 400 MHz, 1.43 (s, 6H), 2.56-2.58 (m, 6H+1H), 4.77 (d, *J*=2.4 Hz, 2H), 5.99 (s, 2H), 7.10 (d, *J*=8.7 Hz), 7.21 (d, *J*=8.7 Hz, 2H). ^{13}C NMR ($CDCl_3$, 100 MHz, d ppm) 14.5, 14.6, 56.0, 75.9, 78.0, 115.6, 121.2, 128.0, 129.2, 131.8, 141.5, 143.1, 155.4, 158.1. HRMS-ESI: calculated for M+Na 401.1617, found 401.1644, D= 6.7 ppm.

Compund 13

0.256 g (0.677 mmol) of compound 1**2** was dissolved in 100 ml ethanol. 0.429 g (1.692 mmol) of I_2 was added to the solution. 0.238 g (1.354 mmol) of HIO_3 was dissolved in a few drops of water and added to the previous mixture. The reaction mixture was stirred at 60 ^{0}C and monitored with TLC. When all BODIPY was consumed 50 ml of saturated solution of sodiumthiosulfate was added and stirred for an extra 30 minutes. Extraction was performed with DCM. The purification of the product was done with column chromatography by using Hexane/DCM (50/50 ;v/v) as eluent. The product was obtained through the evaporation of the organic solvent. (0.382 g, 0.607 mmol, 90%) ^{1}H NMR ($CDCl_3$, 400 MHz, δ ppm) 1.36 (s, 6H), 2.49 (s, 1H), 2.56 (s, 6H), 4.70 (s, 2H), 7.04 (d, *J*=8.8 Hz, 2H), 7.09 (d, *J*=8.8 Hz, 2H). ^{13}C NMR ($CDCl_3$, 400 MHz, δ ppm) 16.0, 17.1, 56.1, 76.1, 85.8, 100.1, 116.0, 127.8, 129.1, 131.6, 141.4, 146.0, 156.7, 158.6. HRMS-ESI: calculated for M+Na 652.9550, found 652.9515, Δ= 5.4 ppm.

Compound 14

0.200 g (0.317 mmol) of compound **13** and 0.050 g (0.285 mmol) of 4-diethylaminobenzaldehyde were dissolved in 30 ml benzene. 0.45 ml of piperidine and 0.45 ml of acetic acid were added. The reaction mixture was refluxed by using Dean-Stark. Extraction was done with DCM and water. The organic layer was dried with sodium sulfate and its solvent was evaporated under vacuum. The product was purified by column chromatography where the mobile phase was DCM/Hexane (2/1; v/v). Fraction containing compound **14** was collected and the solvent was evaporated. (0.045 g, 57 μmol, 18%) ^{1}H NMR ($CDCl_3$, 400 MHz, δ ppm) 1.24 (m, Hz, 6H), 1.51 (s, 3H), 2.60 (t, *J*=10.8, 3H), 3.44 (m, 4H), 4.79 (d, *J*=2.4, 2H), 6.69 (d, *J*=8.9, 2H), 7.15 (m, 2H), 7.48 (s, 2H), 7.54 (t, *J*=8.8, 3H), 8.22 (d, *J*=16.5, 1H) ^{13}C NMR ($CDCl_3$, 400 MHz, δ ppm) 158.83, 140.84, 129.81, 129.54, 115.90, 113.36, 111.60, 76.00, 56.21, 44.56, 29.74, 17.88, 16.96, 16.25, 12.77 HRMS (TOF-ESI): m/z calcd for $C_{33}H_{32}BF_2I_2N_3O^-$ 787.0666 $[M-H]^-$, found: 787.06594 [M-H], Δ = -0.84 ppm.

Compound 15

1.5 g (9.36 mmol) of compound **11** was dissolved in 300 ml DCM to which Argon was purged for 30 min. 2.78 ml (2.54 g, 20.60 mmol) of 2,4-dimethyl-3-ethyl pyrrole was added to the solution. 3 drops of trifluoroacetic acid was added dropwise. The reaction mixture was stirred for 12 h at room temperature. Then 2.31 g (9.36 mmol) of p-chloranil was added and the mixture was stirred for 45 min. After that 8 ml of triethyl amine and 8 ml of boron trifluoride diethyl etherate were added, in sequence. The reaction mixture was stirred for an extra 30 min. Then it was extracted with water. The organic phase was dried over Na_2SO_4 and evaporated. Silica gel column chromatography was applied to the product by using Hexane/EtOAc solvent system (8/1; v/v). The fraction that contains compound 15 was collected and its solvent was evaporated under vacuum. (0.6 g, 1.38 mmol, 15%) ^{1}H NMR ($CDCl_3$, 400 MHz, δ ppm) 7.22 (m, 2H), 7.10 (t, J = 0.02 Hz, 2H), 4.78 (d, J = 2.40 Hz, 2H), 2.55 (m, 5H), 2.32 (t, J=7.49, 5H), 1.60 (s, 5H), 1.28 (s, 3H) 1.00 (t, J= 0.01, 3H). ^{13}C NMR ($CDCl_3$, 400 MHz, δ ppm) 158.0, 153.6, 140.0, 138.4, 132.8, 131.1, 129.8, 128.9, 115.6, 78.1, 75.8, 56.0, 17.1, 14.6, 12.5, 11.8.

Compound 16

1 g (8.19 mmol) of 4-Hydroxybenzaldehyde and 1.36 g (6.96 mmol) of 6-Bromohexanoic acid were dissolved in 150 ml acetone. A few crystals of 18-Crown-6 was added to the mixture. Then 3.40 g (24.57 mmol) of K_2CO_3 was added. The reaction mixture was refluxed for 12 h and then filtered. The filtrate was dissolved in water and then neutralized with 4 M HCl. White precipitate was filtered and dried. ^{1}H NMR (400 MHz, DMSO) 1.56 (q, *J*=2.00 2H), 1.75 (q, *J*=2.00, 2H), 2.24 (t, *J*=2.00, 2H), 2.50 (m, 2H), 4.08 (t, *J*=2.00, 2H), 7.12 (t, *J*=1.00, 2H), 7.86 (q, *J*=1.00, 2H), 9.86 (s, 1H), 11.92 (s, 1H), ^{13}C NMR ($CDCl_3$, 400 MHz, δ ppm) 191.75, 174.89, 164.14, 132.28, 115.37, 68.40, 40.59, 40.39, 40.18, 39.97, 39.76, 39.56, 39.34, 34.06, 28.69, 25.51, 24.68 HRMS (TOF-ESI): m/z calcd for $C_{13}H_{16}O_4^-$ 235.0961 $[M-H]^-$, found: 235.09758 $[M-H]^-$, Δ = 6.26 ppm.

Compound 17

0.10 g (0.24 mmol) of compound 15 was dissolved in 30 ml of benzene. 0.13 g (0.60 mmol) of compound **16** was added to the solution. Then 0.3 ml of acetic acid and 0.3

ml of piperidine were added. The reaction mixture was refluxed for 2 h with Dean-Stark apparatus. It was extracted with DCM and water. After the solvent of organic phase was removed silica gel column chromatography was applied for purification with Methanol/EtOAc (1/9; v/v). The fraction containing the product was evaporated under vacuum. (0.027 g, 0.032 mmol, 13%). ^{1}H NMR (400 MHz, DMSO) 1.10 (q, *J*=8.44, 4H), 1.34 (d, *J*=7.02, 4H), 1.45 (d, *J*=7.48, 6H), 1.56 (s, 4H), 1.72 (s, 6H), 2.25 (s, 4H), 4.02 (s, 4H), 4.39 (t, *J*=6.08, 4H), 4.46 (s, 1H), 4.89 (d, *J*=2.47, 2H), 7.01 (t, *J*=8.91, 4H), 7.07 (d, *J*=8.60, 2H), 7.17 (d, *J*=8.88, 2H), 7.31 (d, *J*=8.89, 2H), 7.53 (d, *J*=8.82, 2H), 7.68 (s, 2H), 7.89 (d, *J*=11.02, 2H), 12.06 (s, 2H), HRMS (TOF-ESI): m/z calcd for $C_{52}H_{57}BF_2N_2O_7^-$ 868.4191 $[M-H]^-$, found: 868.41904 $[M-H]^-$, Δ = -0.11 ppm.

Compound 18

2 g (25.6 mmol) of mercapto ethanol was dissolved in 10 ml DMSO. The mixture was stirred at 80 ^{0}C for 12 hours. After cooling the mixture to room temperature extraction was performed with brine and ethyl acetate. Organic layer was dried with sodium sulfate and after evaporation silica gel column chromatography was applied with Hexane/Ethyl Acetate (3/1; v/v) as eluent. Solvent of the fraction that contain compound **5** was removed and product was obtained. (1.79 g, 11.6 mmol, 45%) ^{1}H NMR ($CDCl_3$, 400 MHz, δ ppm) 3.90 (t, 4H, J = 5.84 Hz; OCH_2), 7.30 (t, 4H, J = 5.88 Hz; SCH_2). ^{13}C NMR ($CDCl_3$, 400 MHz, δ ppm) 60.4, 41.3.

Compound 19

1 g (6.48 mmol) of compound **18** was dissolved in DCM/Et_3N solvent system (10/1; v/v). As the solution was being cooled with ice bath 1.22 g (12,96 mmol) of p-toluene sulfonyl chloride was dissolved in 10 ml DCM and added dropwise to the solution. The mixture was stirred for 12 h. Extraction was done with DCM and water. Organic phase was dried with sodium sulphate and evaporated. Silica gel column chromatography was applied with $CHCl_3$ as eluent. Fraction that contained product was evaporated and a white solid was obtained. (2.82 g, 6.1 mmol, 94%) ^{1}H NMR ($CDCl_3$, 400 MHz, δ ppm) 7.83 (d, 4H, J = 8.04 Hz; ArH), 7.38 (d, 4H, J = 7.93 Hz; ArH), 4.21 (t, 4H, J = 6.61 Hz; OCH_2), 2.85 (t, 4H, J = 6.53 Hz; SCH_2),

2.48 (s, 6H, $ArCH_3$). ^{13}C NMR ($CDCl_3$, 400 MHz, δ ppm) 145.2, 130.0, 128.0, 67.5, 36.9, 21.7. HRMS (TOF-ESI): m/z calcd for $C_{18}H_{22}NaO_6S_4^+$ 485.0191 $[M+Na]^+$, found: 485.0104 $[M+Na]^+$, Δ = 17.94 ppm.

Compound 20

1 g (2.16 mmol) of compound **19** was dissolved in 10 ml DMSO. Then 0.648 g of (9.98 mmol) sodium azide was added to the solution. The reaction mixture was stirred at 60 ^0C for 2 hours. Extraction was done with ethyl acetate and water after cooling the reaction mixture to room temperature. Organic layer was dried with Na_2SO_4 and evaporated under vacuum. The yellow oily product was obtained. (0.42 g, 2.05 mmol, 95%) ^1H NMR ($CDCl_3$, 400 MHz, δ ppm) 3.63 (t, 4H, J = 6.76 Hz; NCH_2), 2.89 (t, 4H, J = 6.76 Hz; SCH_2). ^{13}C NMR ($CDCl_3$, 400 MHz, δ ppm) 49.9, 37.6.

CHAPTER 5

5 CONCLUSION

In this thesis we focused on the two different projects. The first project was the design and synthesis of a PEGylated Calix[4]arene as a carrier for a Bodipy that is substituted by heavy atoms and has complementary water soluble units. It is obvious that calix[4]arene molecule can be functionalized with two Bodipy units having a high tendency to intersystem crossing property due to heavy iodine atoms. Some hydrophobic character was gained due the long alkyl chains on the lower rim of the calixarene. There are two PEG groups that adds hydrophilic character which then make the compound amphiphilic. The styryl group make long wavelength absorption ensured.. In the second project, we designed and synthesized the modules of molecular logic gate, DEMUX. There are three main compounds for this kind of molecular logic gates geared for theranostic potential, these are, photosensitizer, fluorophore and a analyte responsive linker between them. The synthesis part was completed successfully. It will be a significant progress for future work.

To conclude, we can say that PDT is a promising area for scientists and when it is coupled with logic gate concepts, the potetial for information processing therapeutic agents is enormous.

BIBLIOGRAPHY

[1] A. P. De Silva, N. H. Q. Gunaratte and C. P. McCoy, “A molecular photoionic AND gate based on fluorescent signalling” Nature, vol. 364, pp. 42-44, 1993.

[2] A. Urruticoechea, R. Alemani, J. Balart, A. Villanueva, F. Vinals, and G. Capella, PubMed, vol. 16, no. 1, pp. 3-10, 2010.

[3] A. Gorman, J. Killoran, C. O’Shea, T. Kenna, W. M. Gallagher and D. F. O’Shea, “In Vitro Demonstration of the Heavy-Atom Effect for Photodynamic Therapy” J.Am. Chem. Soc., vol. 126, pp. 10619–10631, 2004.

[4] I. Roy, T. Y. Ohulchanskyy, H. E. Pudavar, E. J. Bergey, A. R. Oseroff, J. Morgan T. J. Dougherty and P. N. Prasad, “Ceramic-based nanoparticles entrapping water-insoluble photosensitizing anticancer drugs: a novel drug-carrier system for photodynamic therapy,” J. Am. Chem. Soc., vol. 125, pp. 7860- 7865, 2003.

[5] B. Wardle, “Principles and Applications of Photochemistry,” Wiley, pp. 33, 2009.

[6] B. R. Henry, W. Siebrand, “Spin–Orbit Coupling in Aromatic Hydrocarbons. Analysis of Nonradiative Transitions between Singlet and Triplet States in Benzene and Naphthalene”, J. Chem. Phys. vol. 54, No. 3, pp. 1072-1085, 1971.

[7] K. Szacilowski, W. Macyk, A. Drzewiecka Matuszek, M. Brindell, G. Stochel, “Bioinorganic photochemistry: frontiers and mechanisms” Chem. Rev. vol. 105, no. 6, pp. 2647-2694, 2005.

[8] J. C. Cosiar, D. O. Cowan, “Photochemical Heavy-Atom Effects”, Acc. Chem. Res. vol. 11, no. 9, pp. 334-341, 1978.

[9] M. Colombo, M. W. George, J. N. Moore, D. I. Pattison, R. N. Perutz, I. G. Virrels, T. Q. Ye, “Ultrafast reductive elimination of hydrogen from a metal carbonyl dihydride complex; a study by time-resolved IR and visible spectroscopy” Dalton Trans., pp.2857-2859, 1997.

[10] M. Kasha, “Discussions of the Faraday Society”, The Faraday Society, vol. 9, pp. 14-19, 1950.

[11] J. R. Lalowicz, “Principles of Fluorescence Spectroscopy” 3rd Edition, Springer, pp. 6, 2006.

[12] M. R. Wasielewski, “Photoinduced Electron Transfer in Supramolecular Systems for Artificial Photosynthesis”, Chem. Rev., vol. 92, pp. 435-461, 1992.

[13] A. P. de Silva, H. Q. Gunaratne, T. Gunnlaugsson, A. .J. Huxley, C. P. McCoy, J. T. Rademacher, T. E. Rice, “Signaling Recognition Events with Fluorescent Sensors and Switches”, Chem. Rev., vol.97, no.5, pp. 1515-1566, 1997.

[14] V. Balzani, A. Credi, M. Venturi, “Molecular Devices and Machines”, Nanotoday, vol. 2, no. 2, 2007.

[15] A. P. De Silva, B. McCauhan, B. O. F. McKinney and M. Querol, “Newer optical-based molecular devices from older coordination chemistry”, Dalton Trans., pp. 1902-1913, 2003.

[16] A. P. de Silva, S. A. de Silva, “Fluorescent signalling crown ethers; ‘switching on’ of fluorescence by alkali metal ion recognition and binding *in situ*”, J. Chem. Soc., Chem. Commun., pp.1709-1710, 1986.

[17] A. P. de Silva, R. A. D. D. Rupasinghe, “A new class of fluorescent pH indicators based on photo-induced electron transfer” J. Chem. Soc., Chem. Commun., Issue. 23, pp. 1649-1740, 1985.

[18] B. Valeur, F. Badaoui, E. Bardez, J. Bourson, P. Boutin, A. Chatelain, I. Devol, B. Larrey, J. P. Lefe`vre, A. Soulet, Eds. J. P. Desvergne, A. W. Czarnik, “Chemosensors of Ion and Molecule Recognition”, NATO ASI Series, Vol. 492, pp. 195-196, 1997.

[19] B. Valeur, I. Leray, “Design principles of fluorescent molecular sensors for cation recognition” Coord. Chem. Rev., Issue. 1, vol. 205, pp.3-40, 2000.

[20] R. E. Gawley, H. Mao, M. M. Haque, J. B. Thorne, J. S. Pharr, “Visible fluorescence chemosensor for saxitoxin” J. Org. Chem. vol. 72, no. 6, pp.2187-2191, 2007.

[21] E. Deniz, G. C. Isbasar, O. A. Bozdemir, L. T. Yildirim, A. Siemiarczuk, E. U. Akkaya, “Bidirectional switching of near IR emitting boradiazaindacene fluorophores” Org. Lett., vol. 10, Issue. 16, pp. 3401-3403, 2008.

[22] V. Balzani, A. Credi, M. Venturi, “Molecular Devices and Machines – A Journey into the Nano World”, Wiley-VCH, 2002.

[23] N. J. Turro, “Modern Molecular Photochemistry”, University Science Books, Sausalito, 1991.

[24] M. D. Yilmaz, O. A. Bozdemir, E. U. Akkaya, “Light harvesting and efficient energy transfer in a boron-dipyrrin (BODIPY) functionalized perylenediimide derivative”Org. Lett., vol. 8, Issue. 13, pp.2871-2873, 2006.

[25] D. L. Dexter, “A Theory of Sensitized Luminescence in Solids” J. Chem. Phys., vol. 21, Issue. 5, pp. 836-850, 1953.

[26] S. Prathapan, T. E. Johnson, J. S. Lindsey, “Building-Block Synthesis of Porphyrin Light-Harvesting Arrays” J. Am. Chem. Soc., vol. 115, pp.7519-7520, 1993.

[27] A. Loudet, K. Burgess, “BODIPY dyes and their derivatives: syntheses and spectroscopic properties” Chem. Rev. Vol. 107, Issue. 11, pp. 4891-4932, 2007.

[28] T.G. Kim, J.C. Castro, A. Loudet, J.G.S. Jiao, M.R. Topp, R.M. Hochstrasser, K. Burgess, M.R. Topp, “Correlations of structure and rates of energy transfer for through-bond energy-transfer cassettes” J. Phys. Chem. A., vol. 110, pp. 20-27, 2006.

[29] T. Förster, “Zwischenmolekulare Energiewanderung und Fluoreszenz” Annalen der Physik, vol. 437, Issue. 1-2, pp. 55-75, 1948.

[30] T. Förster, “Experimentelle und theoretische Untersuchung des zwischenmolecularen Uebergangs von Electronenanregungsenergie” Z. Naturforsch, vol. 4, pp.321-327, 1949.

[31] T. Förster, “Transfer Mechanisms of Electronic Excitation”, Discussions Faraday Soc., vol. 27, Issue. 7, 1959.

[32] B. Valeur, “Molecular Fluorescence: Principles and Applications”, Wiley-WC, 2002.

[33] J. R. Lakowicz, Principles of Fluorescence Spectroscopy, Kluwer Acadamic, Plenum Publishers, 1999.

[34] A. Sharma, S. G. Schulman, Introduction to Fluorescence Spectroscopy, Wiley Science, 1999.

[35] G. Barin, M. D. Yilmaz, E. U. Akkaya, “Boradiazaindacene (Bodipy)-based building blocks for the construction of energy transfer cassettes” Tet. Lett., vol. 50, pp. 1738-1740, 2009.

[36] T. L. Floyd, Digital Fundamentals, Prentice-Hall International Inc., Upper Saddle River, NJ, 1997.

[37] A. Saba, N. Manna, Digital Principles & Logic Design, Infinity Science Press, London, 2007.

[38] S. Gibilisco, The Illustrated Dictionary of Electronics, McGraw-Hill, New York, 2001.

[39] J. Millman, A. Grabel, Microelectronics, McGraw-Hill, London, 1988.

[40] Szacilowski, “Digital information processing in molecular systems” Chem. Rev., vol. 108, pp. 3481-3548, 2008.

[41] N. Hush, “Molecular electronics: Cool computing” Nature Materials, vol.2, pp. 134-135, 2003.

[42] P. Siffert, E. Krimmel, Silicon: Evolution and Future of a Technology, Springer, Berlin, 2004.

[43] V. Bojinov, N. Georgiov, Molecular Asensors and Molecular Logic Gates (Review), Journal of the University Chemical Technology and Metallurgy, vol. 46, no. 1, pp.3-26, 2011.

[44] J.F. Callan, A.P. de Silva and N.D. McClenaghan, "Switching between Molecular Switch Types by Module Rearrangement: Ca^{2+}-enabled, H^{+}-driven 'Off-On-Off', H^{+}-driven YES and PASS 0 as well as H^{+}, Ca^{2+}-driven AND Logic Operations", Chem. Commun., vol. 18, pp. 2048-2049, 2004.

[45] K. Szacilowski, "Digital Information Processing in Molecular Systems" Chem. Rew., vol. 108, pp. 3481-3548, 2008.

[46] K. Szacilowski, W. Macyk, "Working prototype of an optoelectronic XOR/OR/YES reconfigurable logic device based on nanocrystalline semiconductors

" Solid-State Electron, Vol. 50, Issues 9-10, pp.1649-1655, 2006.

[47] E. Perez-Inestrota, J-M. Montenegro, D. Collado, R. Suau, "A Molecular 1:2 Demultiplexer", Chem. Commun., pp. 1085-1087, 2008.

[48] M. Triesscheijn, P. Baas, J. H. M. Schellens, F. A. Stewart, "Photodynamic Therapy in Oncology" The Oncologist, vol. 11, pp. 1034- 1044, 2006.

[49] S. Miyamoto, G. E. Ronsein, F. M. Prado, M. Uemi, T. C. Correa, I. N. Toma, A. Bertolucci, M. C. B. Oliveira, F. D. Motta, M. H. G. Medeiros, "Biological hydroperoxides and singlet molecular oxygen generation" IUBMB Life, vol. 59, pp. 322-331, 2007.

[50] D. E. Dolmans, D. Fukumura, R. K. Jain, "Photodynamic Therapy for Cancer", Nat. Rev. Cancer, vol. 3, pp.380-387, 2003.

[51] A. P. Castano, P. Mroz, M. R. Hamblin, "Photodynamic therapy and anti-tumour immunity" Nat. Rev. Cancer, vol. 6, pp. 535-545, 2006.

[52] K. Szaciowski, W. Macyk, A. Drzewiecka-Matuszek, M. Brindell, G. Stochel, “Bioinorganic photochemistry: frontiers and mechanisms”, Chem. Rev. Vol. 105, pp. 2647-2694, 2005.

[53] O. Z. Raab, “Ueber die wirking fluoreszierender stoffe auf infusorien” Zeitschrift fuer Biologie, vol. 39, pp.524-526, 1900.

[54] H. von Trappeiner, A. Jesionek, “Therapeutische Versuche mit fluoreszierenden Stoffen” Med Worchenschr, vol. 47 pp. 2042-2044, 1903.

[55] J. Moan, E. Wold, “Detection of singlet oxygen production by ESR” Nature, vol. 279, pp. 450-451, 1979.

[56] R. Ritz, “Visualization and Photodynamic Therapy in Malignant Glioma - An Overview and Perspectives, Advances in the Biology, Imaging and Therapies for Glioblastoma, Prof. Clark Chen (Ed.), pp. 183, 2011.

[57] T. J. Dougherty, J. E. Kaufman, A. Goldfarb, K. R. Weishaupt, D. Boyle, A. Mittleman, “Photoradiation therapy for the treatment of malignant tumors” Cancer Res., vol. 38, pp. 2628-2635, 1978.

[58] J. R. Lacowicz, “Principles of Fluorescence Spectroscopy”, Springer, 2nd Ed. Kluwer/Plenum, New York, 1999.

[59] B. W. Henderson, T. J. Dougherty, “How does photodynamic therapy work?” Photochem. Photobiol., vol. 55, pp. 145-157, 1992.

[60] A. Wright, C. Hawkins, M. Davies, “Photo-oxidation of cells generates long-lived intracellular protein peroxides” Free radical biology & medicine. Vol. 34 pp. 637-647, 2003.

[61] J. Cadet, P. Di Mascio, “Peroxides in Biological Systems” John Wiley and Sons Ltd, Chichester., pp. 915-999, 2006.

[62] N. L. Oleinick, R. L. Morris, I. Belichenko, “The role of apoptosis in response to photodynamic therapy: what, where, why, and how. “ Photochem. Photobiol. Sci., vol. 1, pp. 1-21, 2002.

[63] B. Alberts, A. Johnson, J. Lewis et al. “Molecular Biology of the Cell”, 4th edition, New York: Garland Science; 2002.

[64] N. J. Turro, “In Modern Molecular Photochemistry; University Science Books” Sausalito, CA, pp. 191-195, 1991.

[65] A. Gorman, J. Killoran, C. O’Shea, T. Kenna, W. M. Gallagher, D. F. O’Shea, “In vitro demonstration of the heavy-atom effect for photodynamic therapy.”J. Am. Chem. Soc., pp. 10619–10631, vol. 126, 2004.

[66] A. Graczykowa “Photodynamic method of diagnosis and therapy of tumors (in Polish); Dom Wydawniczy Bellona” Warszawa, 1999.

[67] L. Huang, X. R. Yu, W. H. Wu, J. Z. Zhao, “Styryl Bodipy-C_{60} Dyads as Efficient Heavy-Atom-Free Organic Triplet Photosensitizers” Org. Lett., vol. 14, pp. 2594-2597, 2012.

[68] Y. Cakmak, S.Kolemen, S. Duman, Y. Dede, Y. Dolen, B. Kilic, Z. K ostereli, L. T. Yildirim, A. L. Dogan, D. Guc, E. U. Akkaya, “Designing Excited States: Theory Guided Access to Efficient Photosensitizers for Photodynamic Action” Angew. Chem. Int. Edit. Vol. 50, pp. 11937-11941, 2011.

[69] M. Ethijaran, Y. H. Chen, P. Joshi, R. K. Pandey, “The Role of the Porphyrin Chemistry in Tumor Imaging and Photodynamic Therapy” Chem. Soc. Rev. Vol. 40, pp. 340-362, 2011.

[70] Z. Kostereli, T. Ozdemir, O. Buyukcakir, E. U. Akkaya, “Tetrastyryl-BODIPY Based Dendritic Light Harvester and Estimation of Energy Transfer Efficiency” Org. Lett. Vol. 14, pp. 3636-3639, 2012.

[71] C. N. Baki, E. U. Akkaya, “Boradiazaindacene-appended calix[4]arene: Fluorescence sensingof pH near neutrality” J. Org. Chem., vol.66, pp.1512-1513, 2001.

[72] Y. Cakmak, T. Nalbantoglu, T. Durgut, E. U. Akkaya, “PEGylated calix[4]arene as a carrier for a Bodipy-based photosensitizer”, Tetrahedron Letters, Vol. 55, Issue. 2, pp. 538-540, 2014.

[73] S. Erbas, A. Gorgulu, M. Kocakusakogullari, E. U. Akkaya, Noncovalent Functionalized SWNTs as Delivery Agents for Novel Bodipy Based Potential PDT Sensitizers”, Chem. Commun., Vol. 33, pp. 4956-4958, 2009.

[74] G. R. Martinez, F. Garcia, L. H. Catalani, J. Cadet, M. C. B. Oliveira, G. E. Ronsein, S. Miyarnoto, M. H. G. Medeiros, P. di Mascio, “Synthesis of a Hydrophilic and non-ionic Anthracene Derivative, the N,N’-di-(2,3-dihydroxypropyl)-9,10-anthracenedipropanamide As a Chemical Trap for Singlet Molecular Oxygen Detection in Biological Systems” Tetrahedron, Vol. 62, pp. 10762-10770, 2006.

[75] O. J. Dalbavie, J. B. Regnouf-De-Vains, R. Lamartine, S. Lecocq, M. Perrin, “Complexation of Cobalt(II) At The Upper Rim of Two New calix[4]arene/bipyridine-based Podands” Eur. J. Inorg. Chem., Vol. 4, pp. 683-691, 2000.

[76] O. A. Bozdemir, R. Guliyev, O. Buyukcakir, S. Selcuk, S. Kolemen, G. Gulseren, T. Nalbantoglu, H. Boyaci, E. U. Akkaya, “Selective Manipulation of ICT and PET Processes in Styryl-Bodipy Derivatives: Applications in Molecular Logic and Fluorescence Sensing of Metal Ions” J. Am. Chem. Soc., Vol. 132, p.p. 8029-8036, 2010.

[77] S. Ozlem, E. U. Akkaya, “Thinking Outside the Silicon Box: Molecular AND Logic As an Additional Layer of Selectivity in Singlet Oxygen Generation for Photodynamic Therapy” J. Am. Chem. Soc., Vol. 131, p.p. 48-49, 2009.

[78] A. Kamkaew, S. H. Lim, H. B. Lee, L. V. Kiew, L. Y. Chunq, K. Burgess, “BODIPY Dyes in photodyamic therapy”Chem. Soc. Rew. Vol. 42, pp.78-78, 2013.

[79] Z. Kostereli, T. Ozdemir, O. Buyukcakir, E. U. Akkaya, “Tetrastyryl-BODIPY-Based Dendritic Light Harverster and Estimation of Energy Transfer Efficiency” Org. Lett. Vol. 14, pp.3636-3639, 2012.

[80] A. Thiry, J.-M. Dogne, B. Maereel, C. T. Supuran, “Targeting tumor-associated carbonic anhydrase IX in cancer therapy” Trends Pharmacol. Vol.11, pp.566-573, 2006.

[81] L. Chaiswing, T. D. Oberley, “Extracellular/Microenvironmental Redox State” Antioxid. Redox Sign. Vol. 13, pp. 449-465, 2010.

APPENDIX

A.1 PEGylated Calix[4]arene as a Carrier for a Bodipy-based Photosensitizer

A.1.1 ^{1}H NMR and ^{13}C NMR Spectra

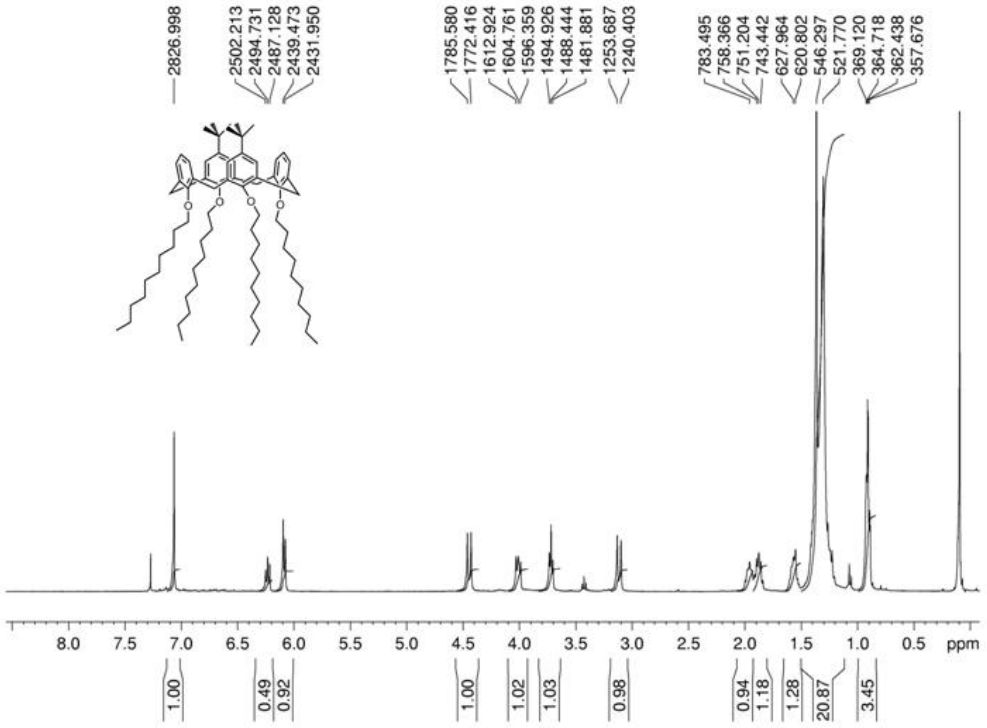

Figure 29. ^{1}H NMR of Compound 5 (Copyright ©, 2014, Elsevier. Reprinted with permission from Ref. 72)

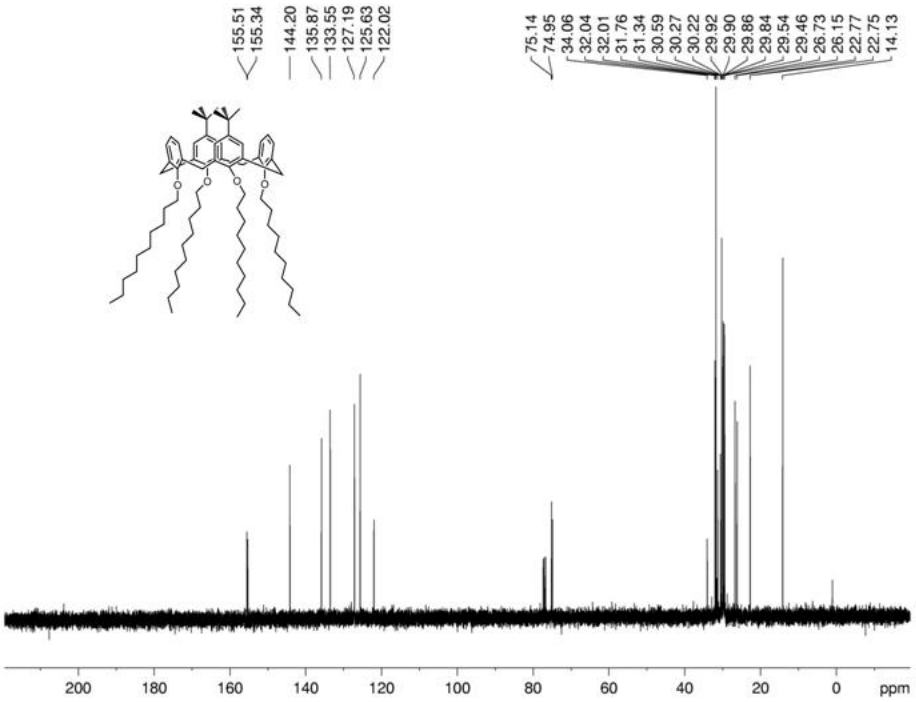

Figure 30. ^{13}C NMR of Compound 5 (Copyright ©, 2014, Elsevier. Reprinted with permission from Ref. 72)

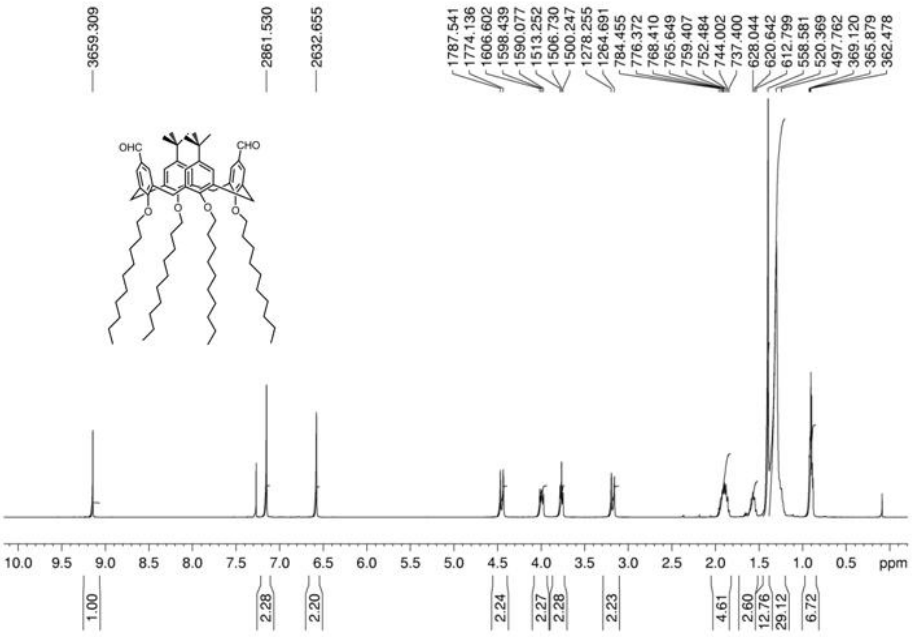

Figure 31. ^{1}H NMR of Compound 6 (Copyright ©, 2014, Elsevier. Reprinted with permission from Ref. 72)

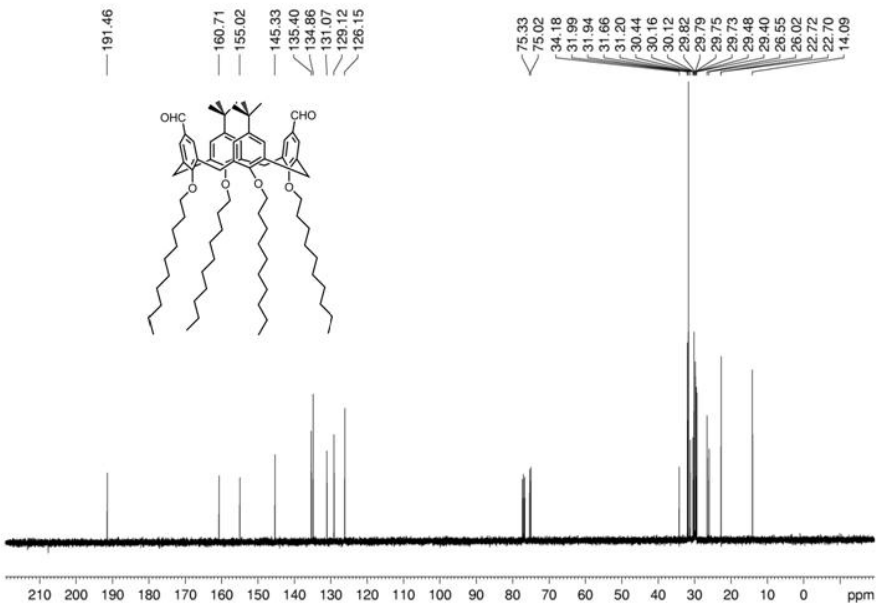

Figure 32. ^{13}C NMR of Compound 6 (Copyright ©, 2014, Elsevier. Reprinted with permission from Ref. 72)

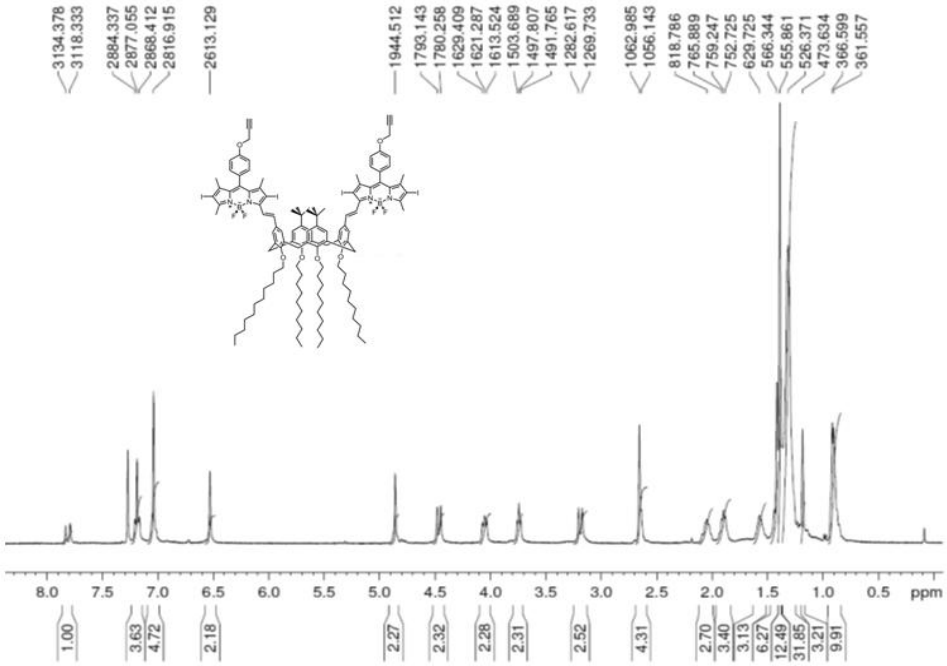

Figure 33. ^{1}H NMR of Compound 8 (Copyright ©, 2014, Elsevier. Reprinted with permission from Ref. 72)

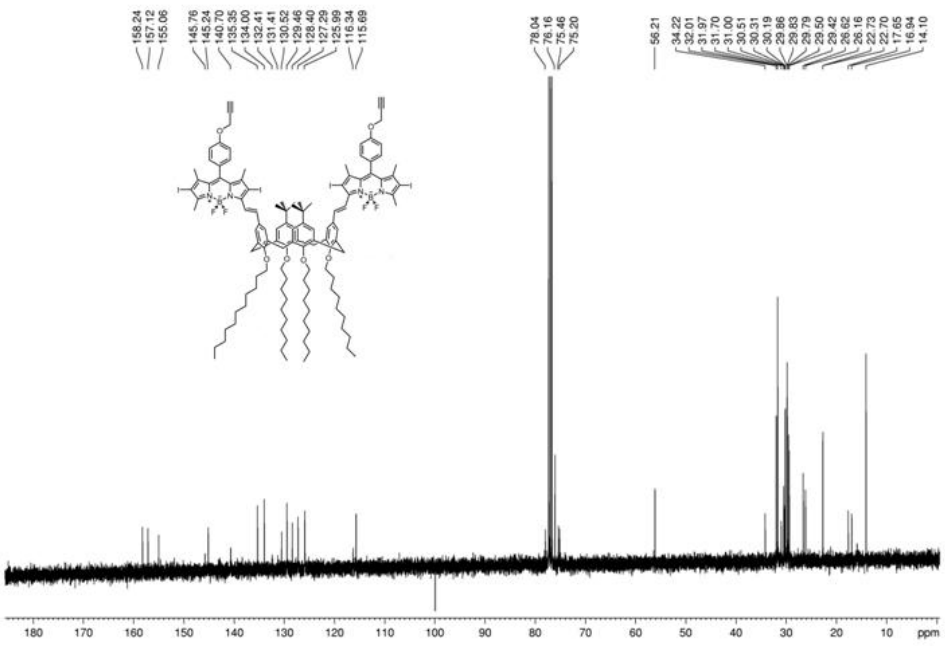

Figure 34. ^{13}C NMR of Compound 8 (Copyright ©, 2014, Elsevier. Reprinted with permission from Ref. 72)

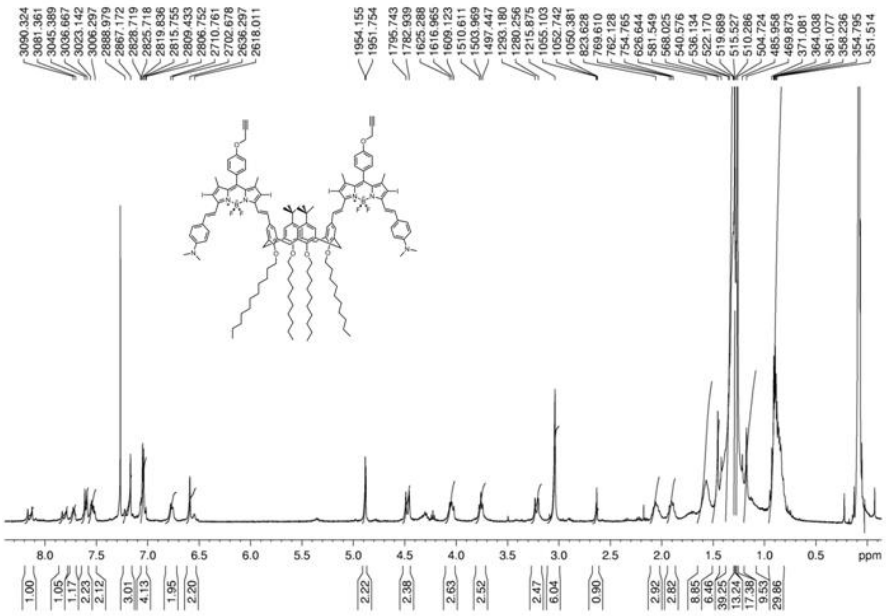

Figure 35. ^{1}H NMR of Compound 9 (Copyright ©, 2014, Elsevier. Reprinted with permission from Ref. 72)

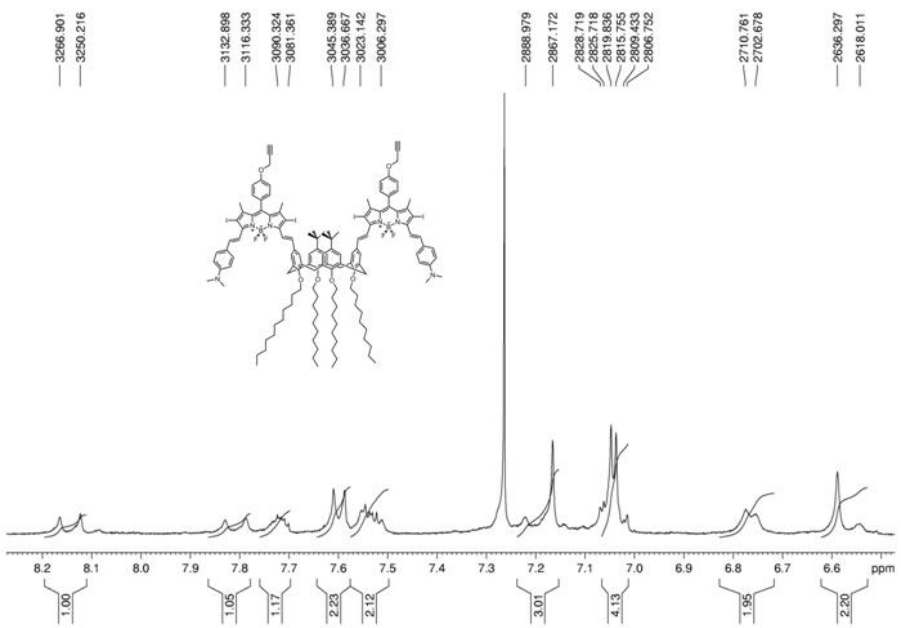

Figure 36. Aromatic part of the ^{1}H NMR of Compound 9 (Copyright ©, 2014, Elsevier. Reprinted with permission from Ref. 72)

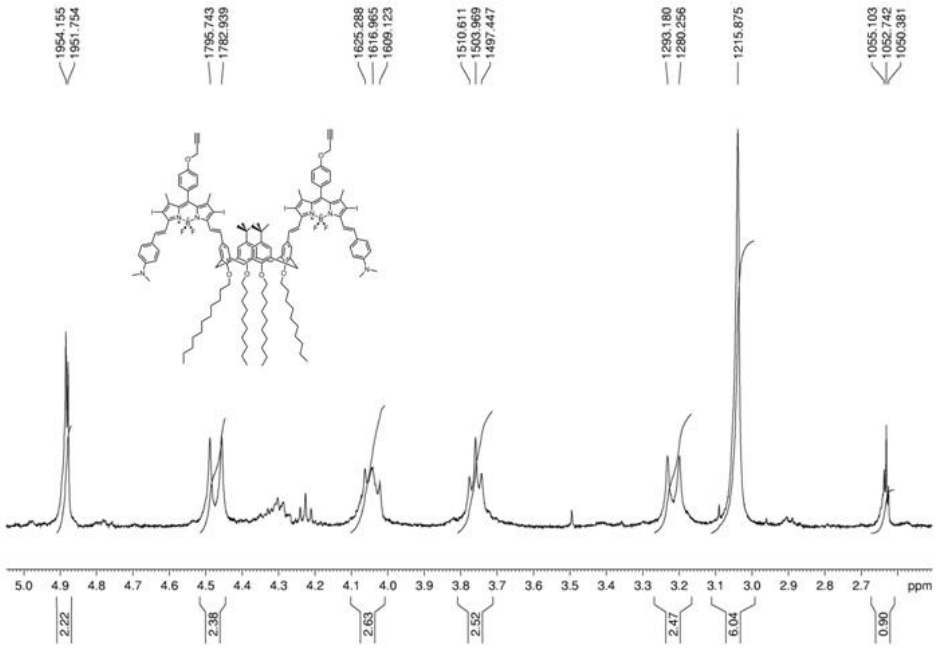

Figure 37. Aliphatic part of the ^{1}H NMR of Compound 9 (Copyright ©, 2014, Elsevier. Reprinted with permission from Ref. 72)

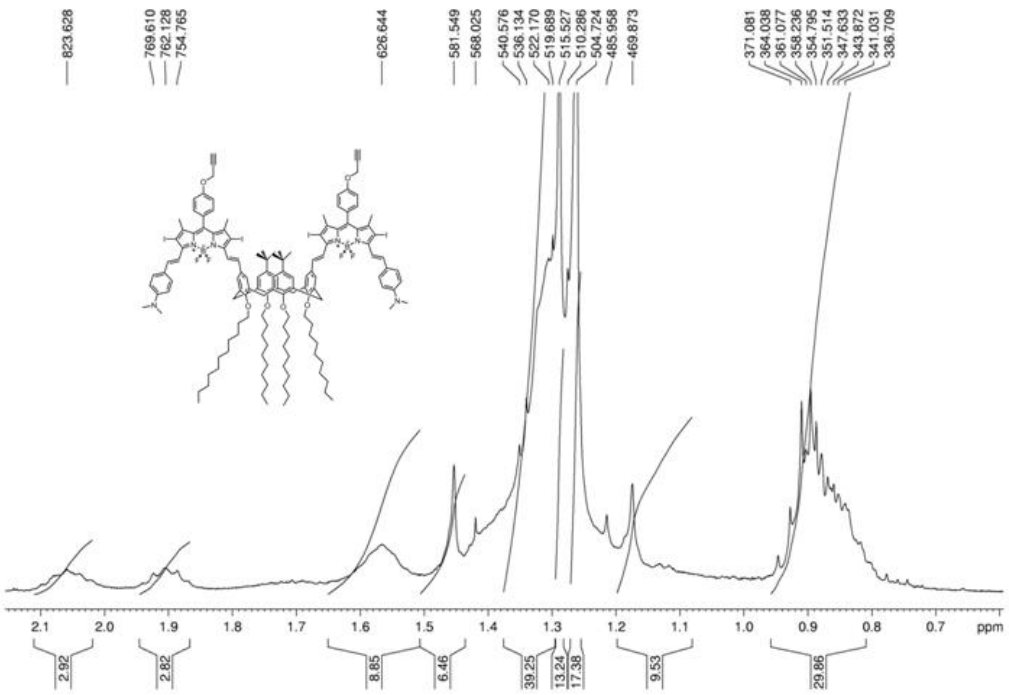

Figure 38. Detailed aliphatic part of the ^{1}H NMR of Compound 9 (Copyright ©, 2014, Elsevier. Reprinted with permission from Ref. 72)

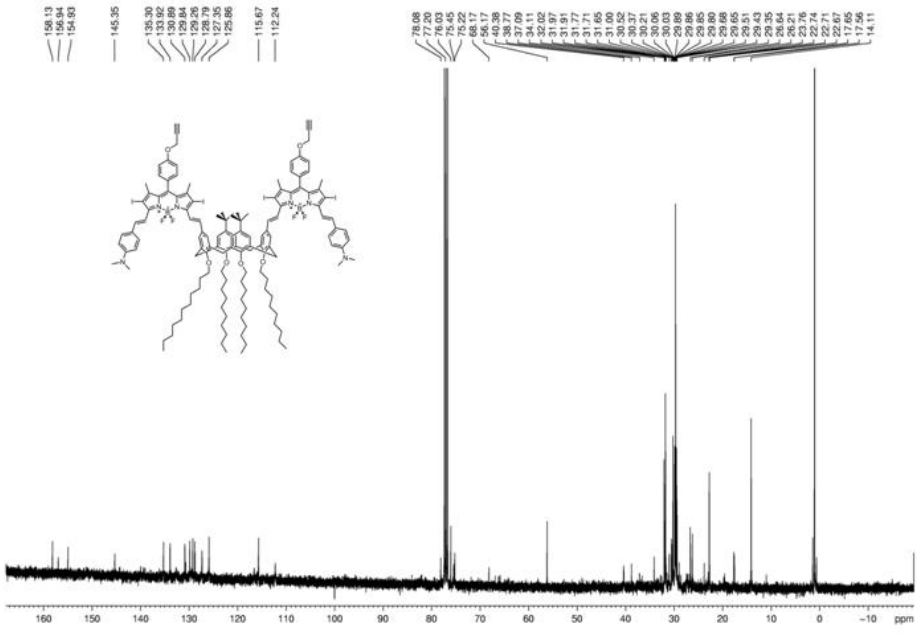

Figure 39. ^{13}C NMR of Compound 9 (Copyright ©, 2014, Elsevier. Reprinted with permission from Ref. 72)

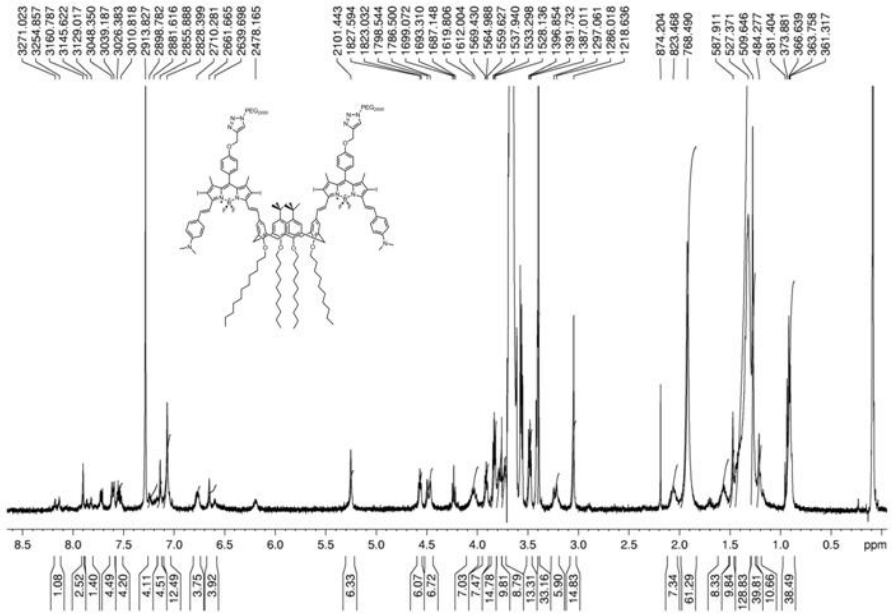

Figure 40. ^{1}H NMR of Compound 10 (Copyright ©, 2014, Elsevier. Reprinted with permission from Ref. 72)

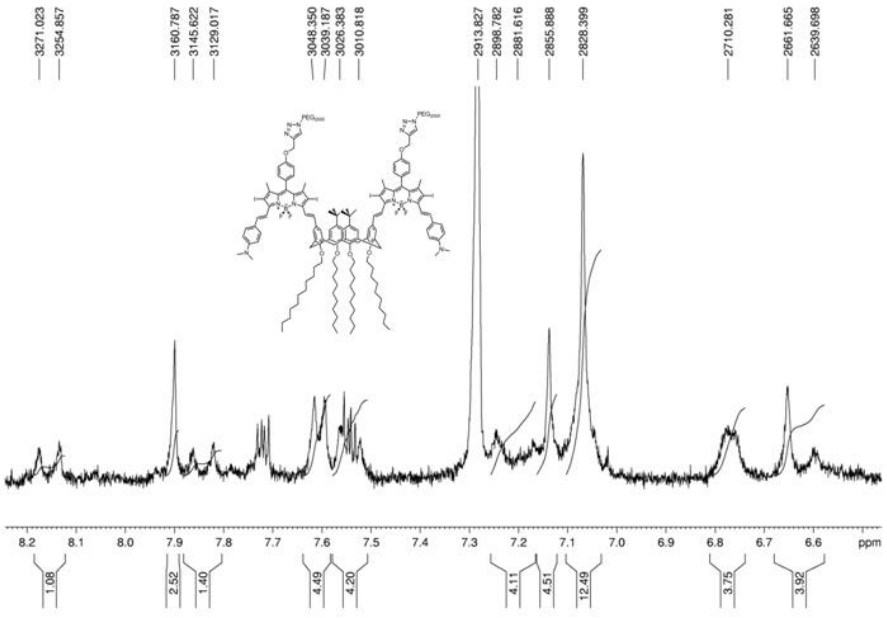

Figure 41. Aromatic part of the ^{1}H NMR of Compound 10 (Copyright ©, 2014, Elsevier. Reprinted with permission from Ref. 72)

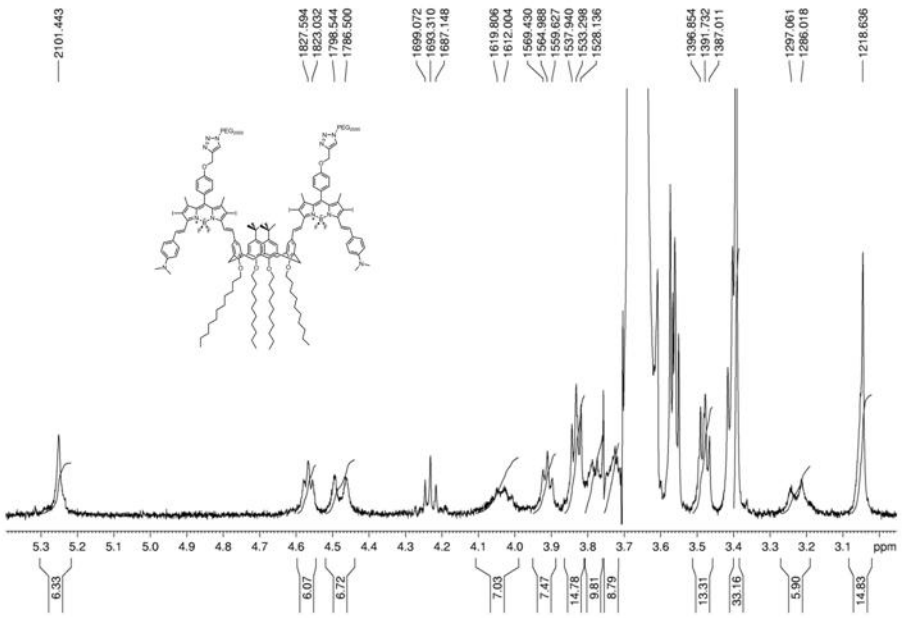

Figure 42. Aliphatic part of the ^{1}H NMR of Compound 10 (Copyright ©, 2014, Elsevier. Reprinted with permission from Ref. 72)

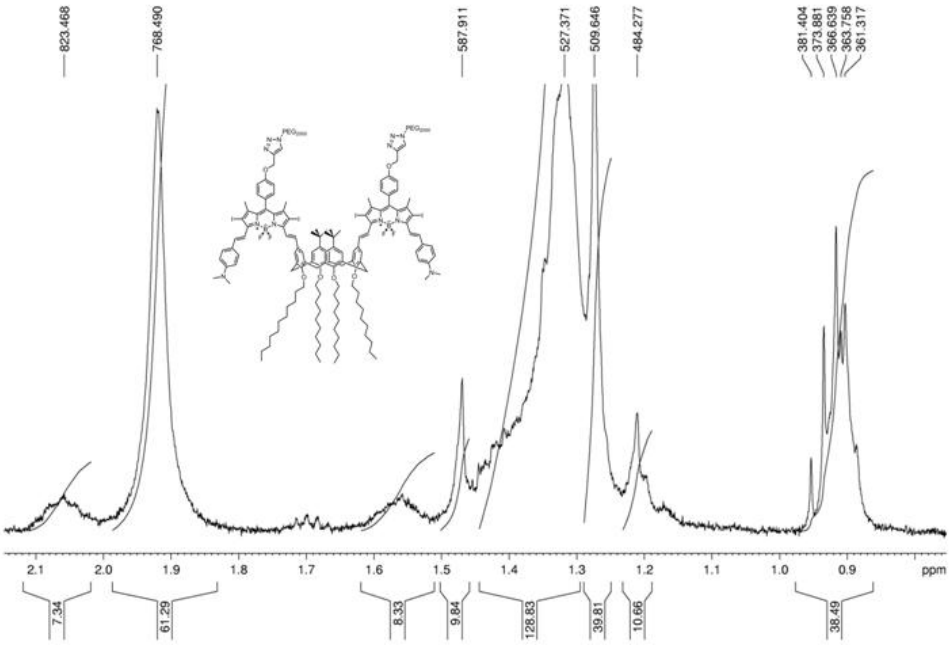

Figure 43. Detailed aliphatic part of the ^{1}H NMR of Compound 10 (Copyright ©, 2014, Elsevier. Reprinted with permission from Ref. 72)

A.1.2 MASS Spectra

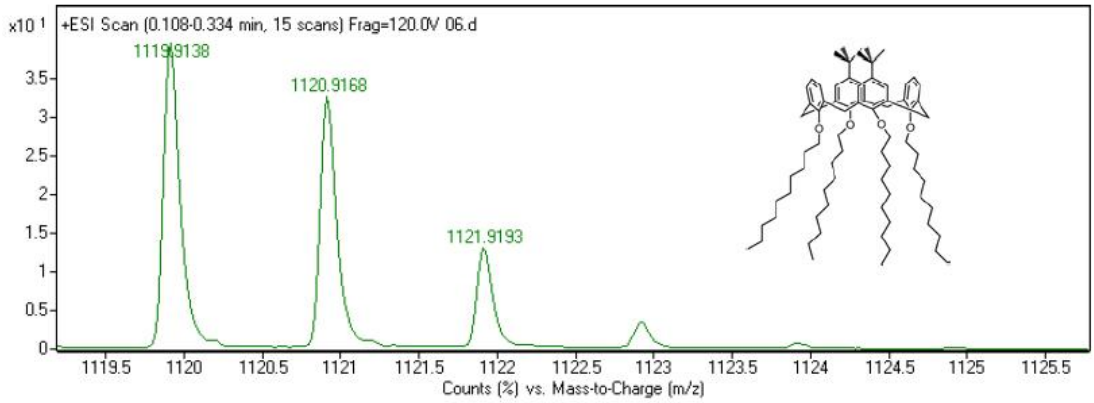

Figure 44. MALDI Spectrum of compound 5 (Copyright ©, 2014, Elsevier. Reprinted with permission from Ref. 72)

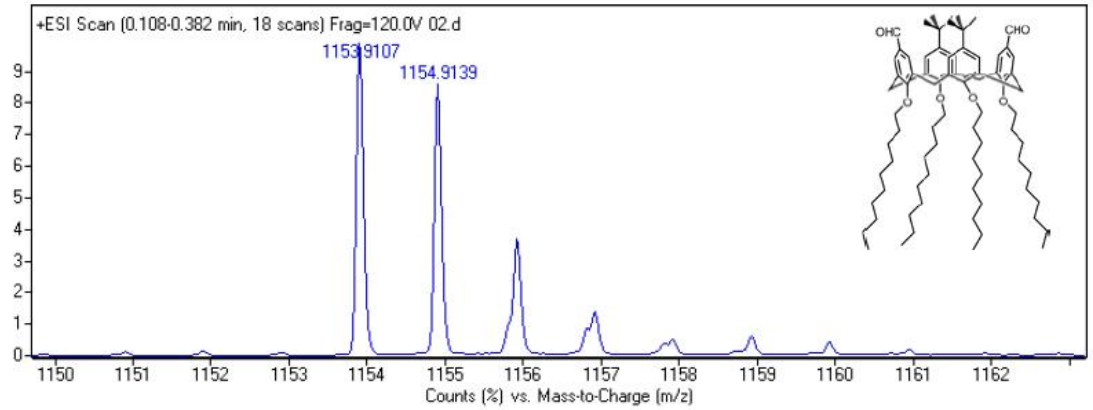

Figure 45. MALDI Spectrum of compound 6 (Copyright ©, 2014, Elsevier. Reprinted with permission from Ref. 72)

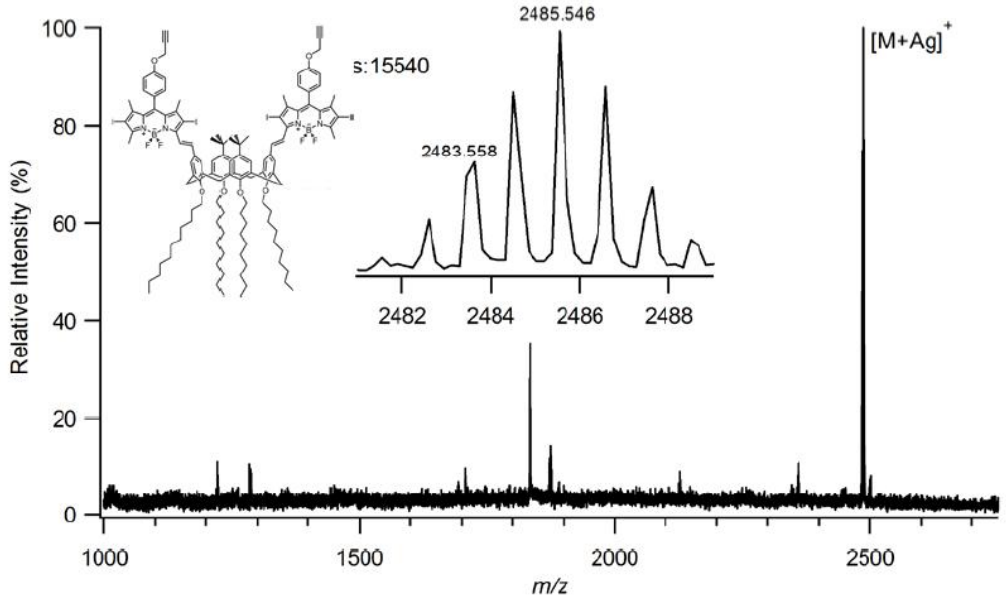

Figure 46. MALDI Spectrum of compound 8 (Copyright ©, 2014, Elsevier. Reprinted with permission from Ref. 72)

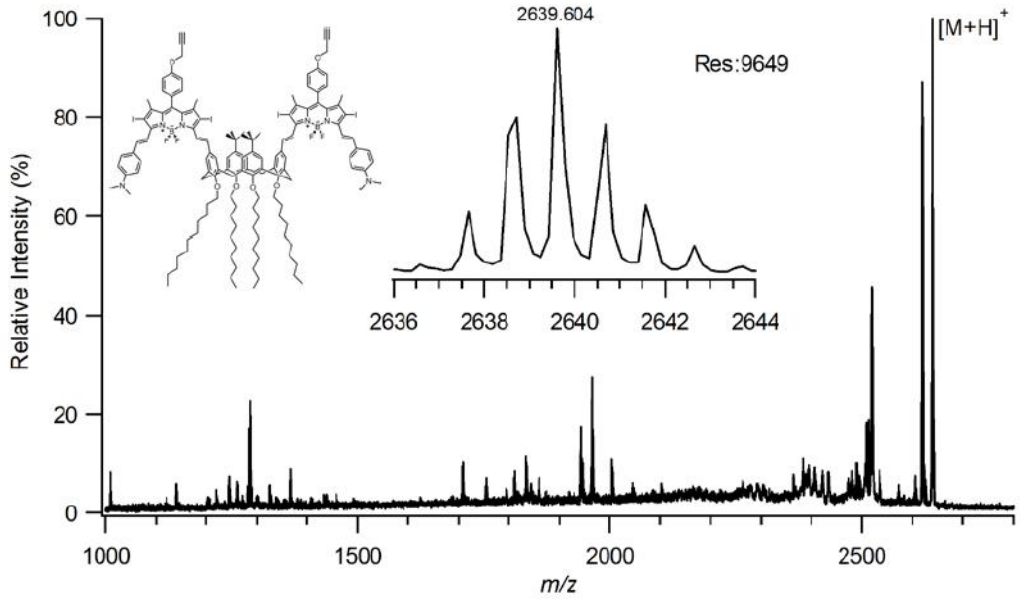

Figure 47. MALDI Spectrum of compound 9 (Copyright ©, 2014, Elsevier. Reprinted with permission from Ref. 72)

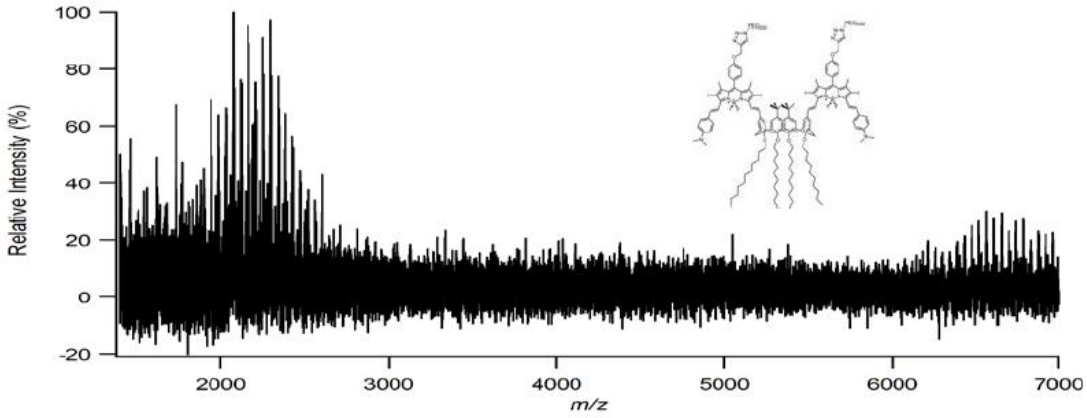

Figure 48. MALDI Spectrum of compound 10 (Copyright ©, 2014, Elsevier. Reprinted with permission from Ref. 72)

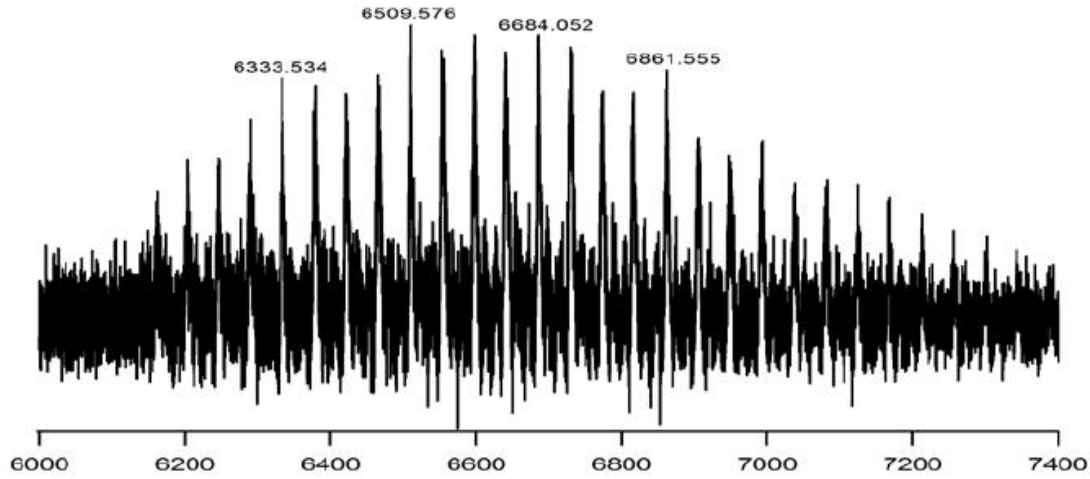

Figure 49. Detailed MALDI Spectrum of compound 10 (Copyright ©, 2014, Elsevier. Reprinted with permission from Ref. 72)

A.2 Synthesis of Molecular Demultiplexer Modules

A.2.1 ^{1}H NMR and ^{13}C NMR Spectra

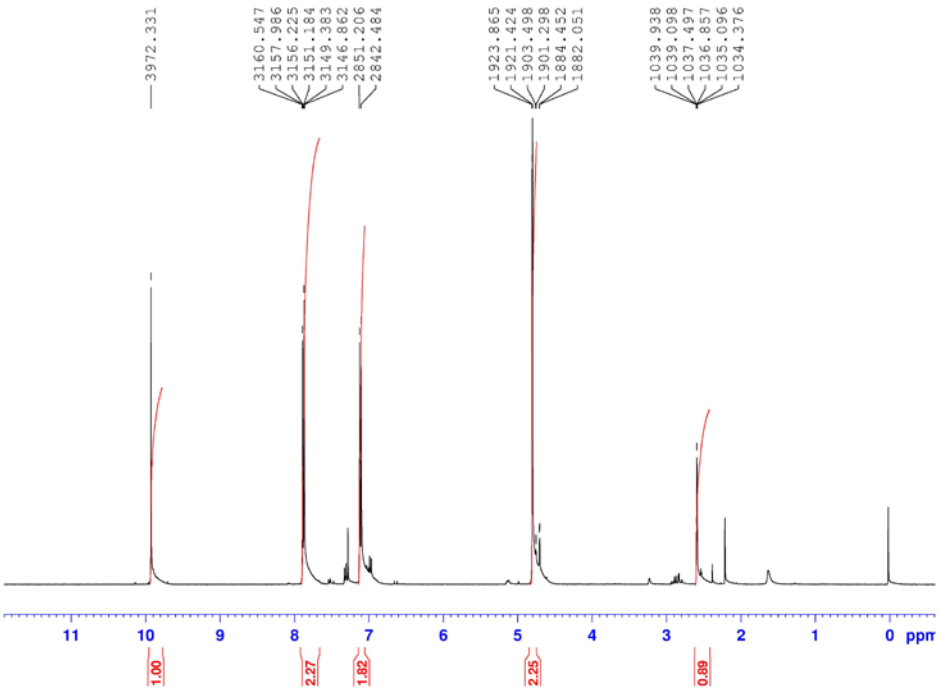

Figure 50. ^{1}H NMR of Compound 11

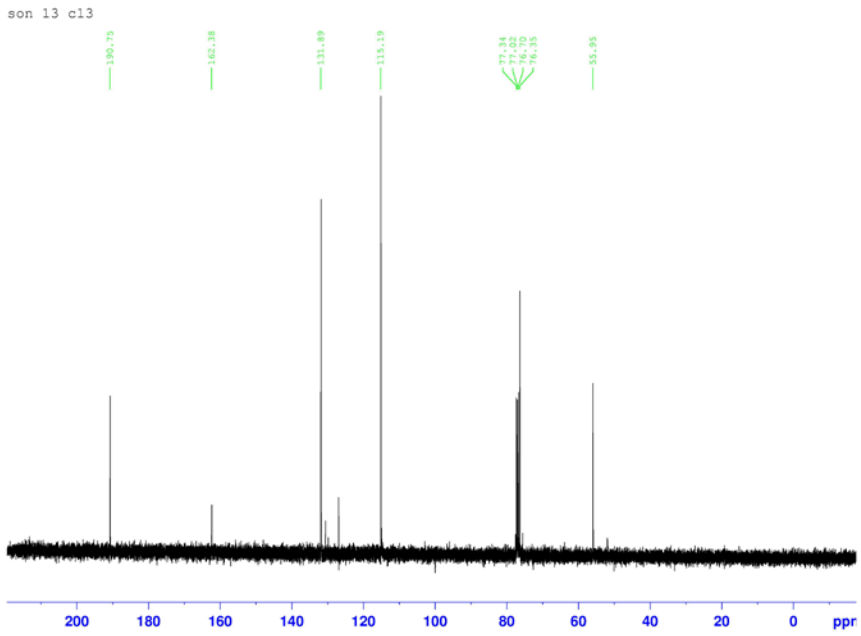

Figure 51. ^{13}C NMR of Compound 11

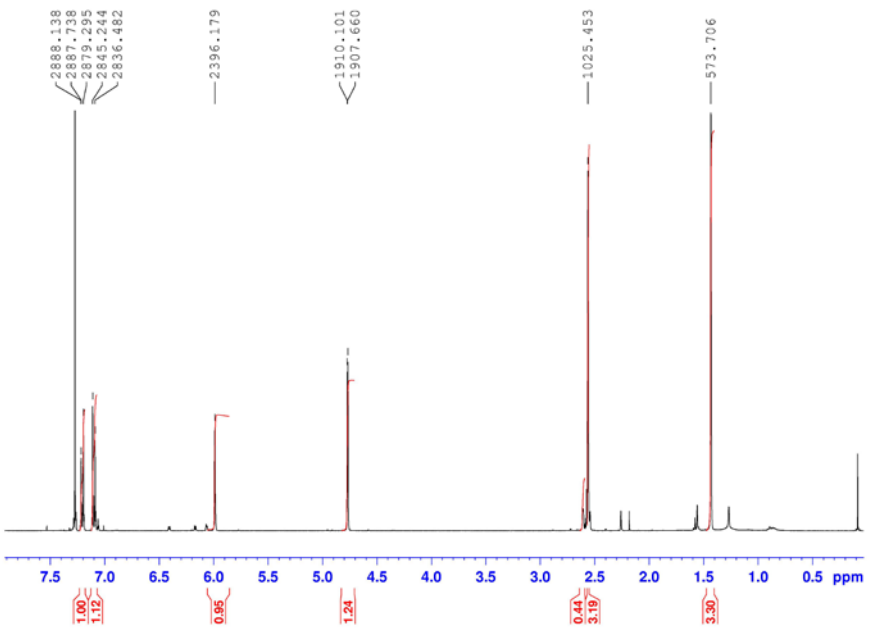

Figure 52. ^{1}H NMR of Compound 12

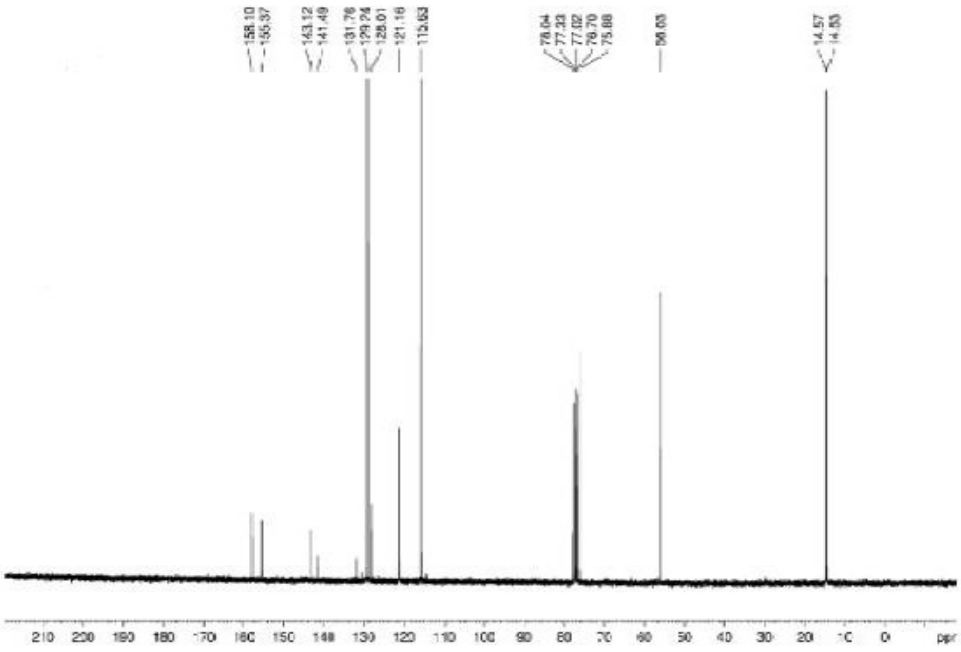

Figure 53. ^{13}C NMR of Compound 12

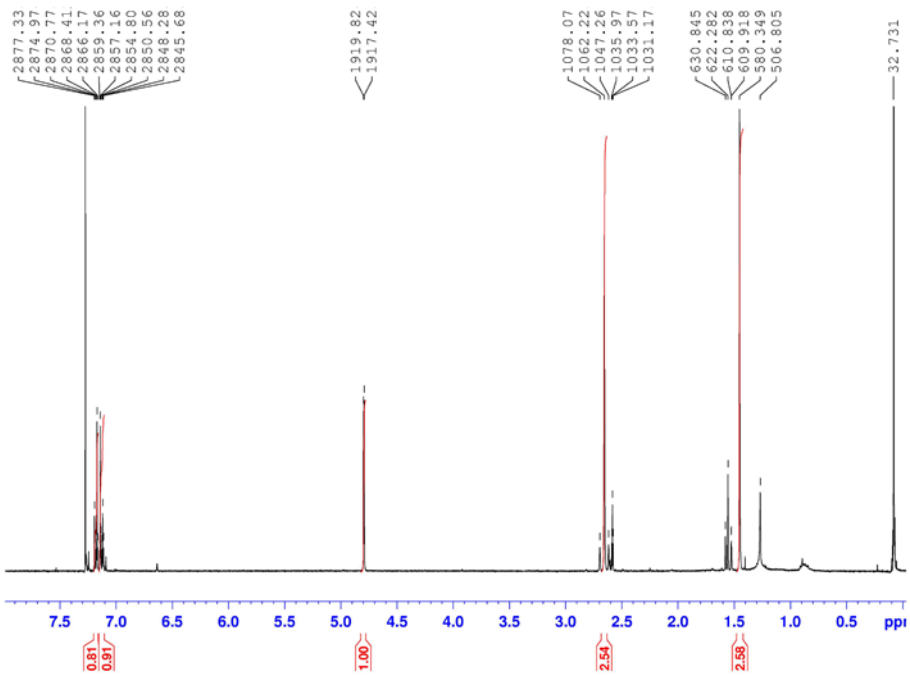

Figure 54. ^{1}H NMR of Compound 13

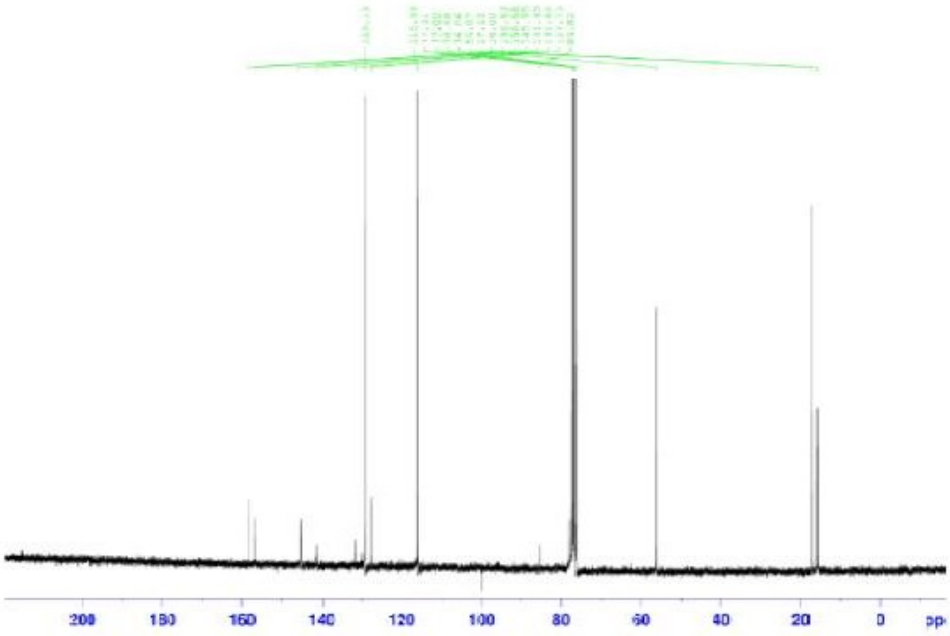

Figure 55. ^{13}C NMR of Compound 13

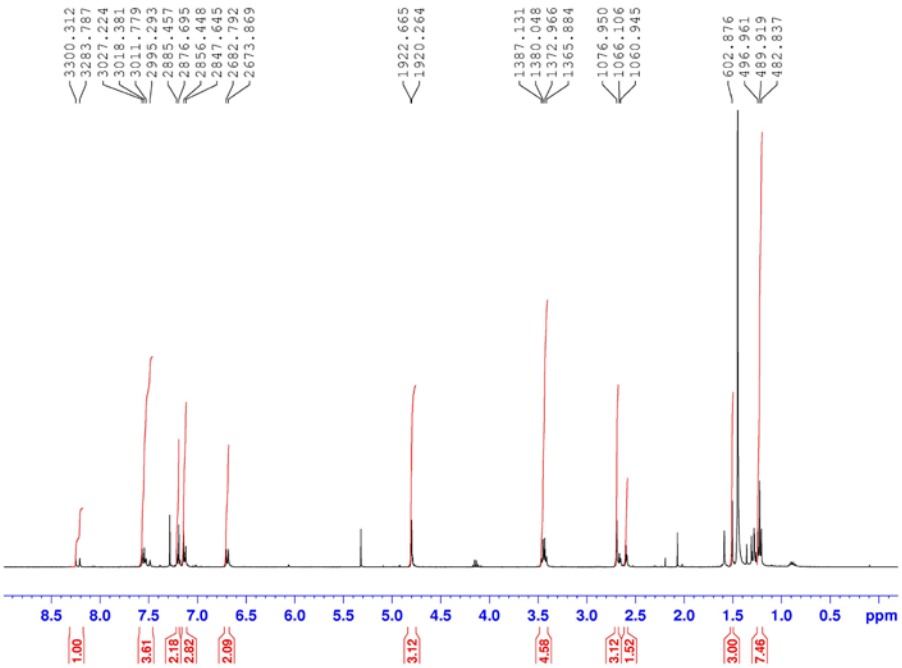

Figure 56.^{1}H NMR of Compound 14

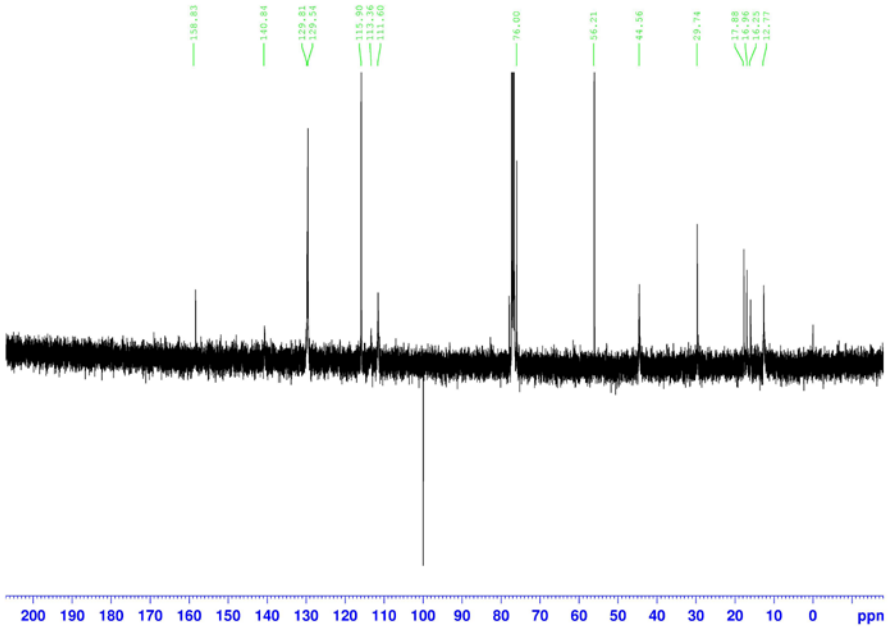

Figure 57. ^{13}C NMR of Compound 14

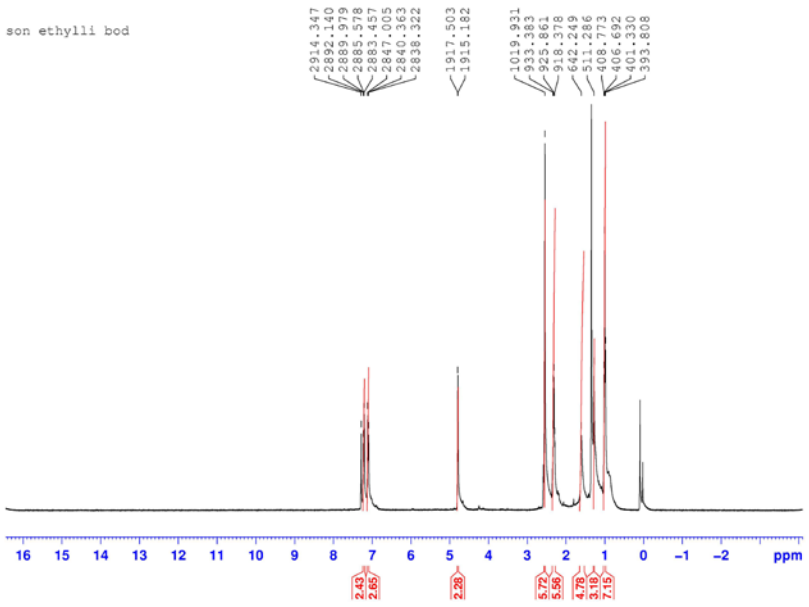

Figure 58. ^{1}H NMR of Compound 15

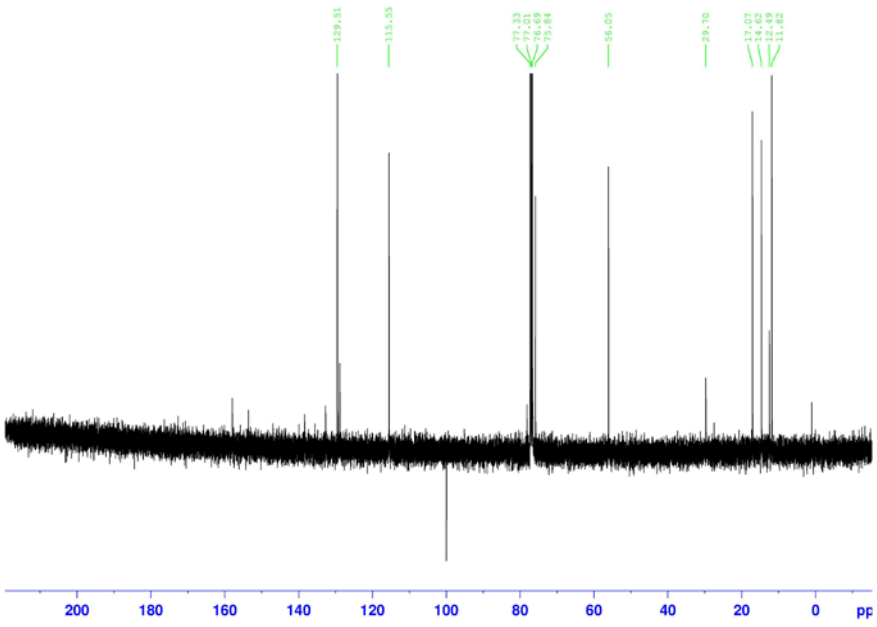

Figure 59. ^{13}C NMR of Compound 15

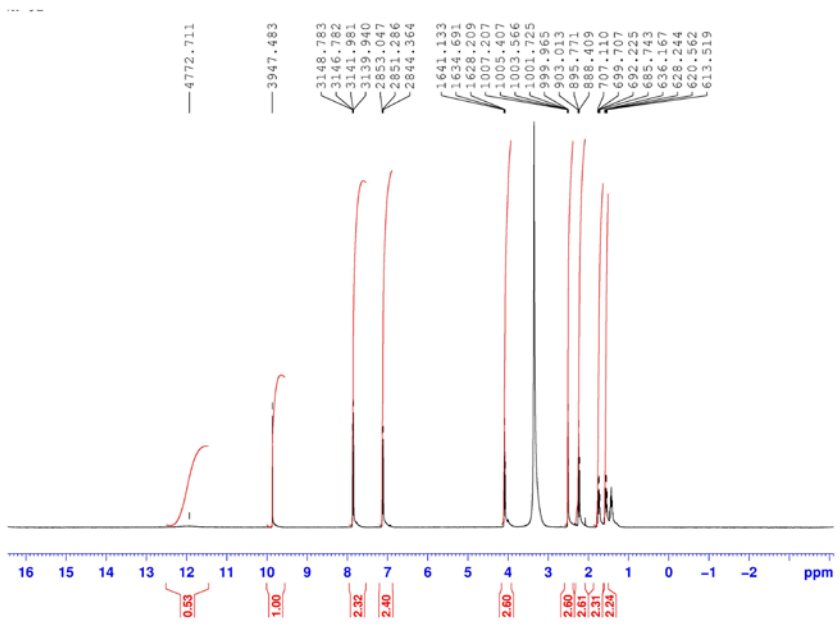

Figure 60. ^{1}H NMR of Compound 16

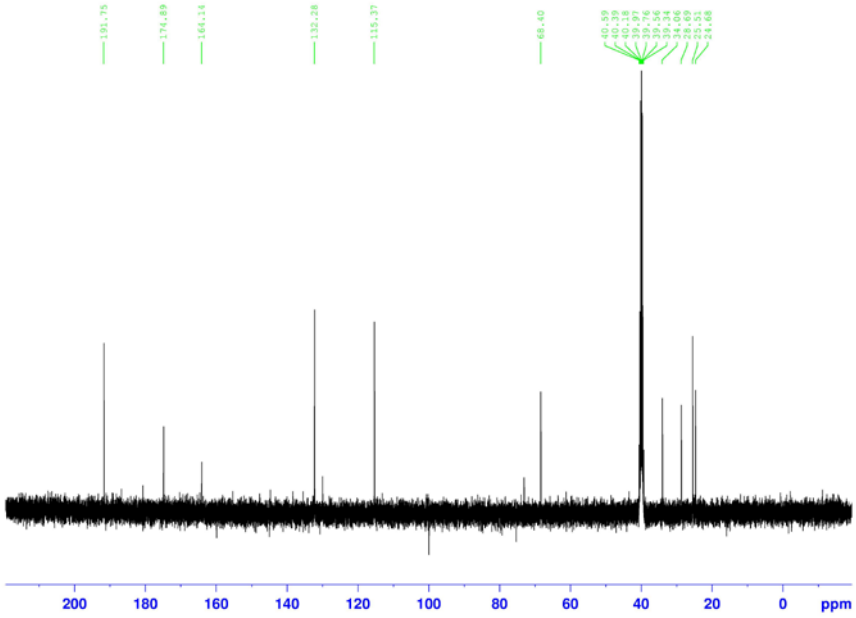

Figure 61.[13]C NMR of Compound 16

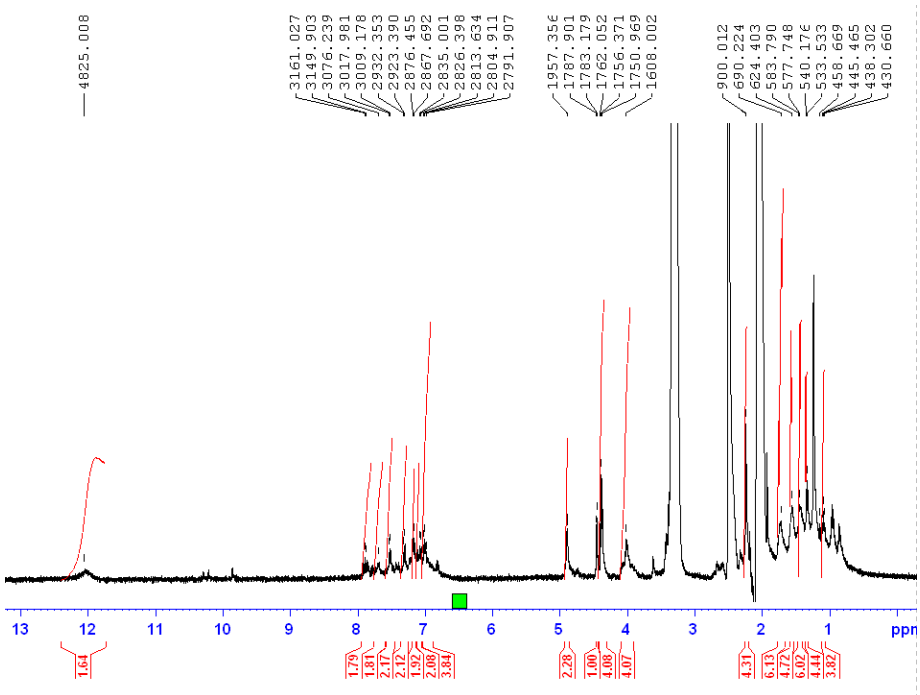

Figure 62. [1]H NMR of Compound 17

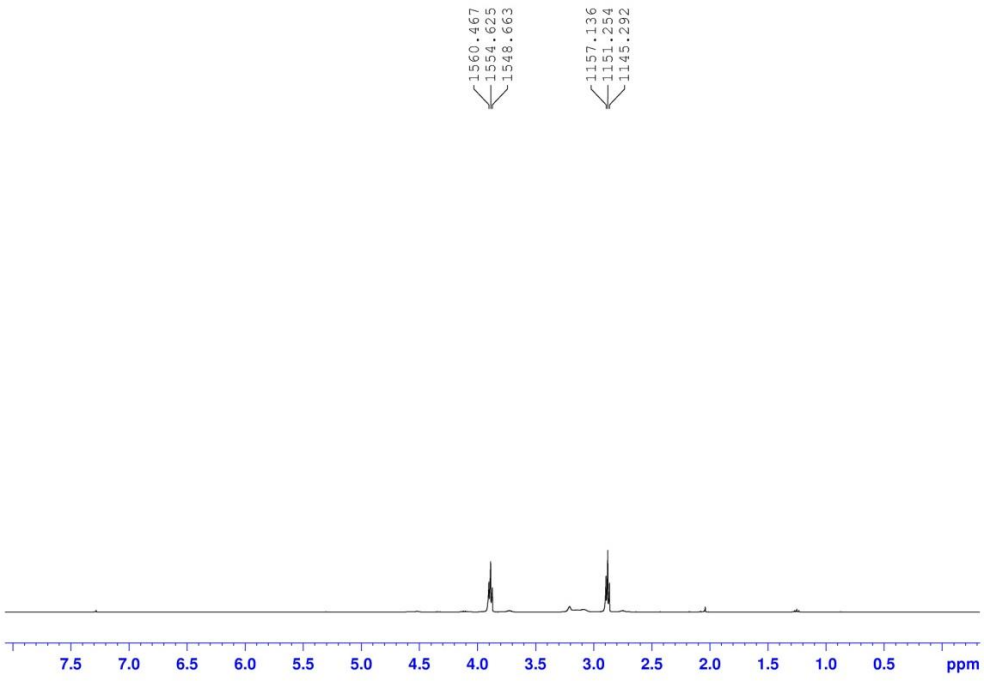

Figure 63. ^{1}H NMR of Compound 18

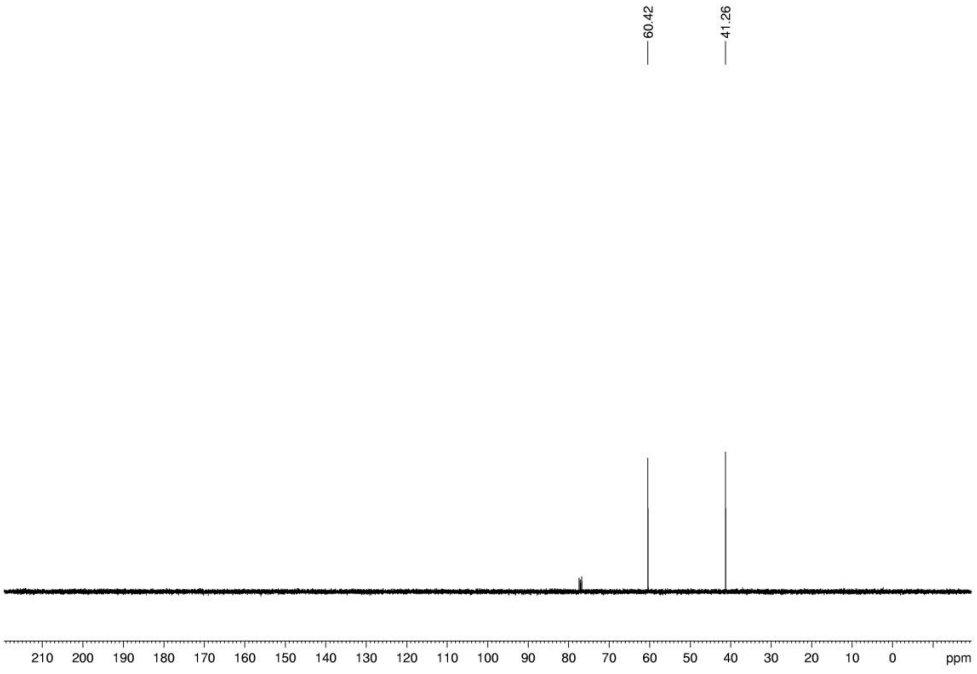

Figure 64. ^{13}C NMR of Compound 18

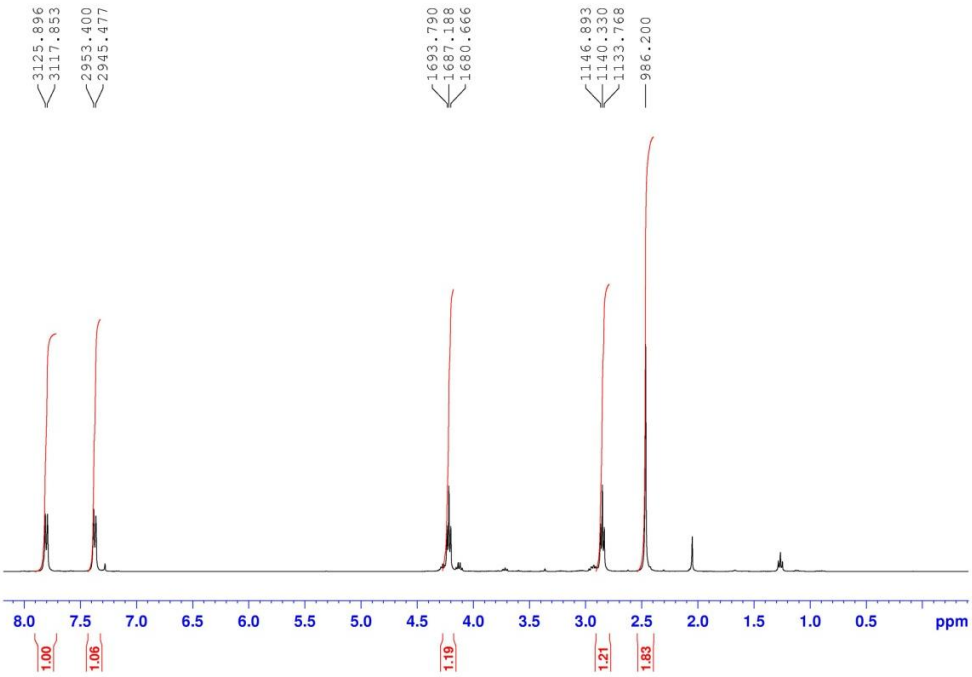

Figure 65. ^{1}H NMR of Compound 19

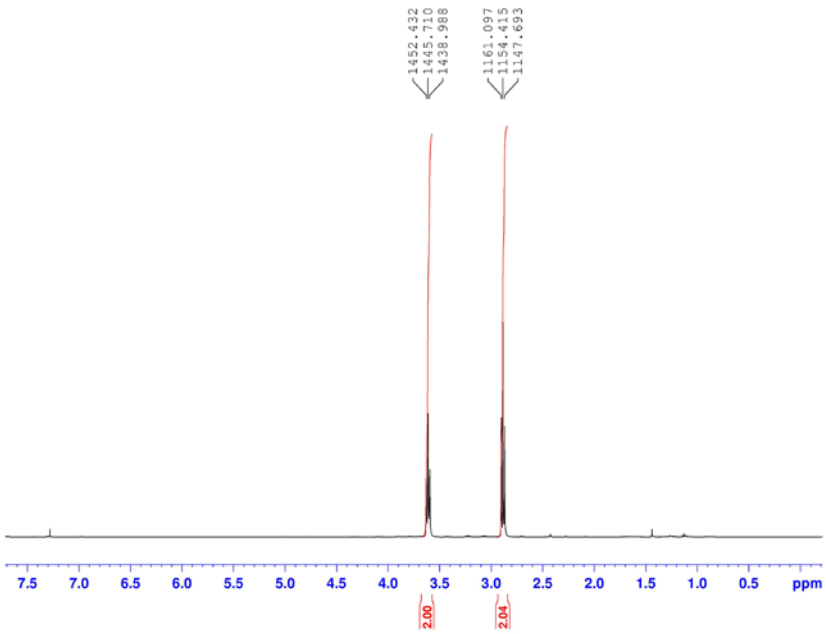

Figure 66. ^{1}H NMR of Compound 20

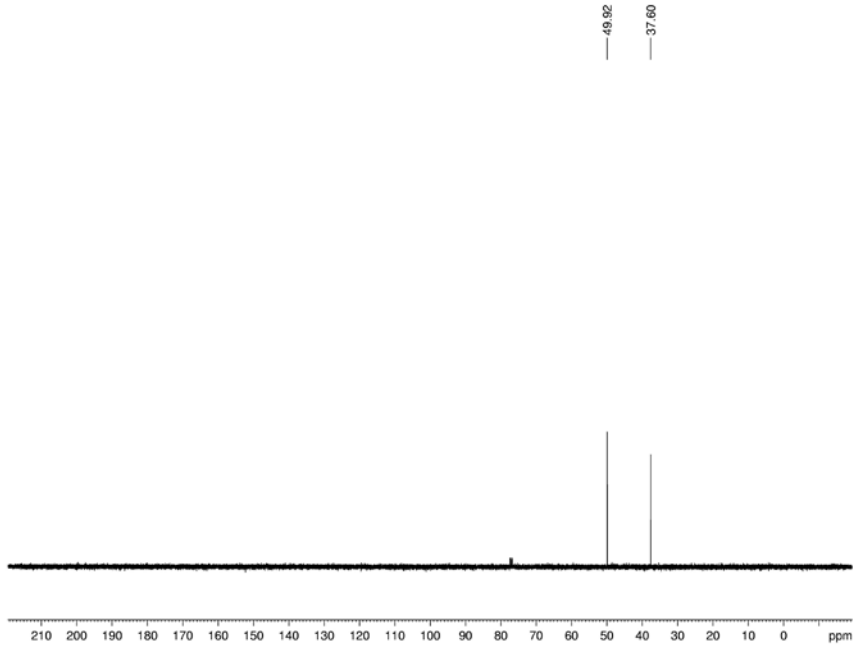

Figure 67. ^{13}C NMR of Compound 20

A.2.2 Mass Spectra

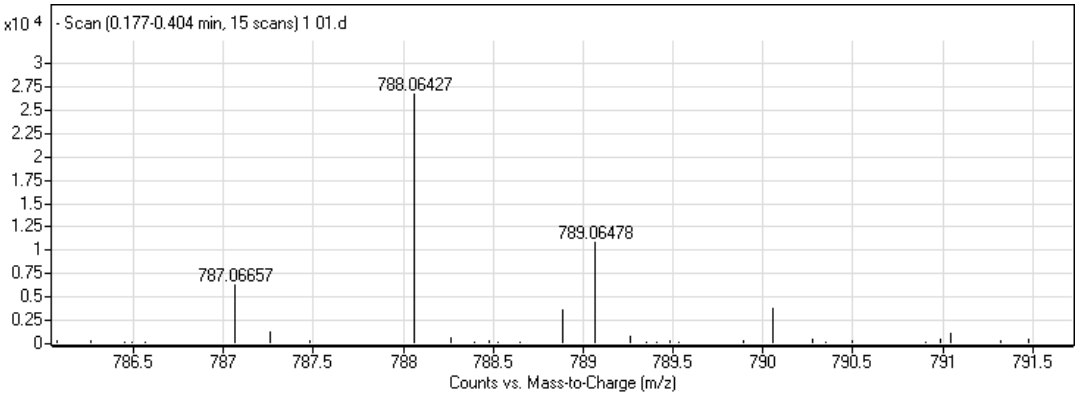

Figure 68. Mass Spectrum of Photosensitizer (Compound 14)

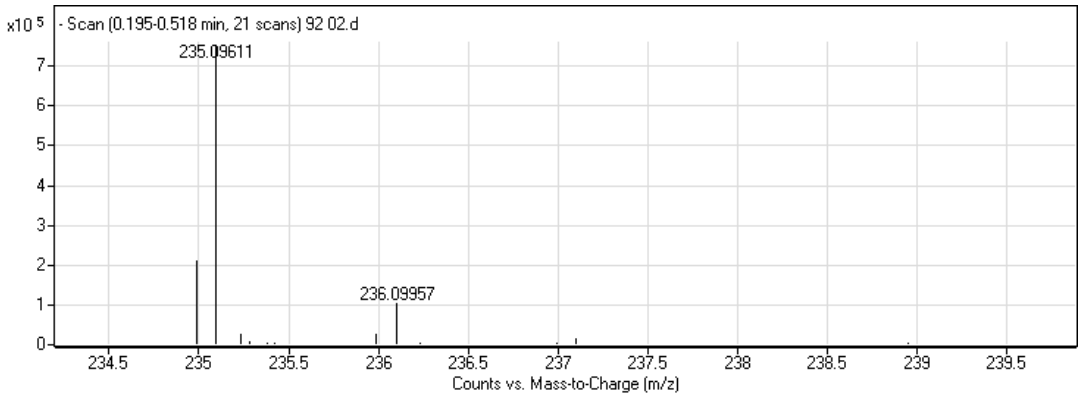

Figure 69. Mass Spectrum of Compound 16

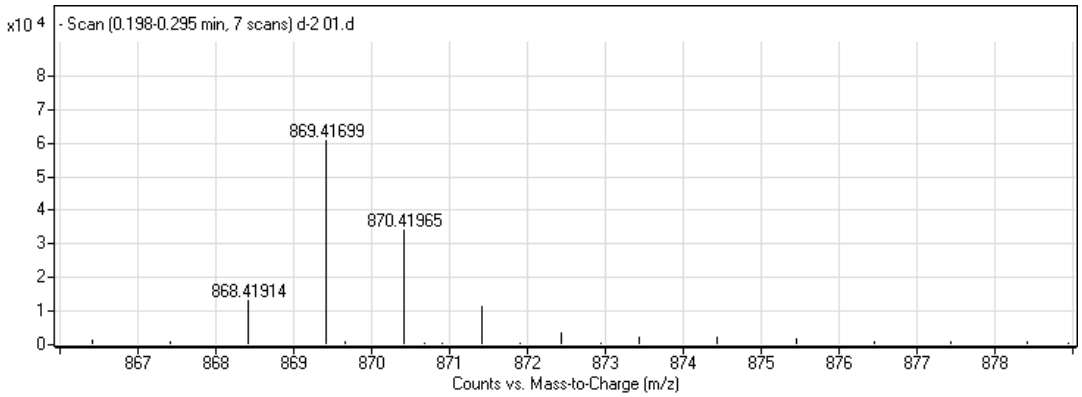

Figure 70. Mass Spectrum of Fluorophore (Compound 17)

A.2.3 Literature Examples

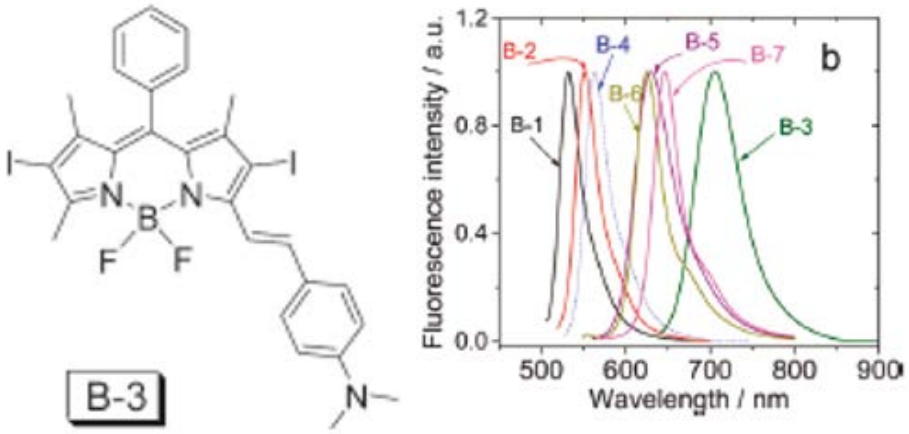

Figure 71. Literature example for PS (Copyright ©, 2012, Elsevier. Reprinted with permission from Ref. 78)

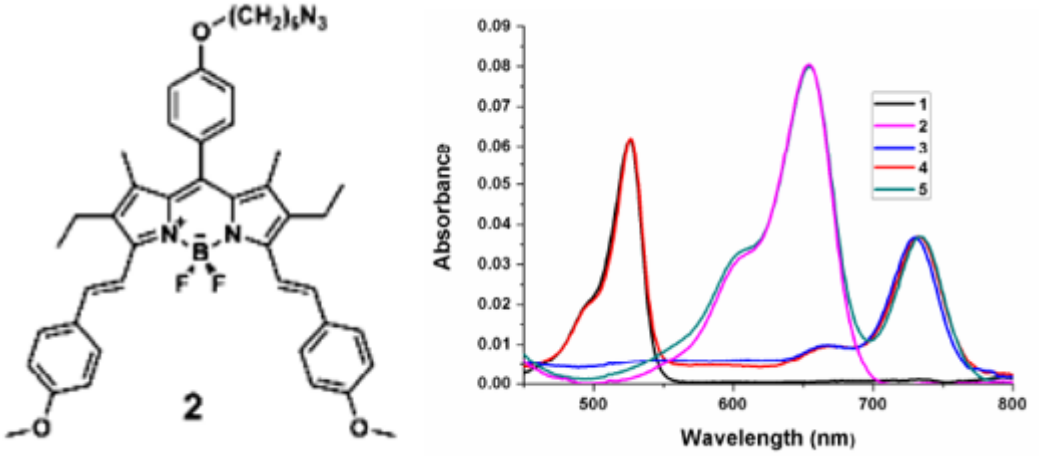

Figure 72. Literature example for FL (Copyright ©, 2012, Elsevier. Reprinted with permission from Ref. 79)